Widespread Impacts of Land-Based Source Pollution on Southwestern Puerto Rican Coral Reefs

Final Report

Submitted to Protectores de Cuencas, Inc. and Ridge to Reefs, Inc.

Edwin A. Hernández-Delgado

Carmen M. González-Ramos, Jeiger L. Medina-Muñiz, Alfredo A. Montañez-Acuña, Abimarie Otaño-Cruz, Bernard J. Rosado-Matías, Gerardo Cabrera-Beauchamp

Sociedad Ambiente Marino and University of Puerto Rico/CATEC

San Juan, Puerto Rico

December 27, 2014

Index

This report was completed thanks to the financial support of

to Protectores de Cuencas, Inc. and Ridge to Reefs, Inc.

With the collaboration and support of the Center for Applied Tropical Ecology and Conservation (CATEC) of the University of Puerto Rico, Río Piedras Campus

HRD #0734826

to Edwin A. Hernández-Delgado

This report should be cited as follows:

Hernández-Delgado, E.A., C.M. González-Ramos, J.L. Medina-Muñiz A.A. Montañez-Acuña, A. Otaño-Cruz, B.J. Rosado-Matías, & G. Beauchamp-Cabrera. 2014. Widespread impacts of land-based source pollution on Sowthwestern Puerto Rican coral reefs. Final Report submitted to Protectores de Cuencas, Inc., Yauco, PR, and Ridge to Reefs, Inc., Baltimore, MD, December 27, 2014. 134 pp.

Further information about coral reef conservation in Puerto Rico can be obtained at:

Dr. Edwin A. Hernández-Delgado
Affiliate Researcher
University of Puerto Rico, Center for Applied Tropical Ecology and Conservation, PO Box 23360, San Juan, PR 00931-3360
edwin.hernandezdelgado@gmail.com
edwin.hernandez13@upr.edu

http://upr.academia.edu/EdwinHernandez
http://www.researchgate.net/profile/Edwin_Hernandez2
http://catec.upr.edu

Mr. Samuel E. Suleimán-Ramos
President
Sociedad Ambiente Marino, PO Box, 22158, San Juan, PR 00931-2158
samuelsuleiman@gmail.com
samprorg@gmail.com

Widespread Impacts of Land-Based Source Pollution on Southwestern Puerto Rican Coral Reefs

Edwin A. Hernández-Delgado[1,2,3]*, Carmen M. González-Ramos[1,2,3], Jeiger L. Medina-Muñiz[4], Alfredo A. Montañez-Acuña[1,2,3], Abimarie Otaño-Cruz[1,2,5], Bernard J. Rosado-Matías[1,2], Gerardo Cabrera-Beauchamp[1]

[1]Sociedad Ambiente Marino, PO Box 22158, San Juan, PR 00931-2158
[2]University of Puerto Rico, Center for Applied Tropical Ecology and Conservation, Coral Reef Research Group, San Juan, Puerto Rico 00931-3360
[3]University of Puerto Rico, Department of Biology, San Juan, Puerto Rico 00931-3360
[4]Protectores de Cuencas, PO Box 1563, Yauco, PR 00698
[5]Dept. of Environmental Sciences, PO Box 70377, University of Puerto Rico, San Juan, Puerto Rico 00936-8377

***Corresponding author:** edwin.hernandezdelgado@gmail.com

December 27, 2014

***Abstract*—** Local coral reef ecosystems across the southwestern Puerto Rico shelf still represent a critical natural resource with invaluable socio-economic significance. However, they were showing unequivocal signs of decline mostly as a result of chronic land-based source pollution (LBSP) impacts. This study showed important evidence suggesting there were signs of a LBSP gradient across the western Puerto Rico shelf and that chronic water quality decline has significantly affected the face of coral reef benthic communities, coral recruit assemblages, and have indirectly affected reef fish communities. A snapshot view of water quality across the shelf showed that particularly turbidity and phosphate (PO_4) and ammonium (NH_4^+) concentrations increased along inshore sites, while dissolved oxygen concentration declined along inshore waters. PO_4 concentrations resulted nearly 11 times above the recommended concentration for healthy coral reefs across inshore sites, almost 8 times across mid-shelf sites, and about 3 times across outer shelf sites. Observed NH_4^+ concentrations across inshore sites exceeded 981 times the recommended concentration for healthy coral reefs. Concentrations also exceeded the recommended limits 590 times across mid-shelf sites, and 155 times across outer shelf sites. Chlorophyll-*a* concentration was up 4 to 7 times higher than recommended limits for healthy coral reefs across inshore sites, 3 to 6 times across mid-shelf sites, and 3 to 6 times across outer shelf sites. Coral reef benthic community structure, coral recruit assemblages and fish community structure showed significant differences across the observed LBSP gradient. Coral species richness, H'n, J'n and percent living cover increased with increasing distance from the shore. Also, coral recruit abundance and the presence of important reef-building species increased with increasing distance. Overall fish species richness, abundance, biomass, and the abundance and biomass of total carnivores, piscivores, omnivores, and of many fishery-targeted species (subfamily Epinephelinae, family Lutjanidae) and indicator species (Chaetodontidae, Pomacentridae) increased with increasing distance from the shore. Nonetheless, inshore coral reef ecosystems still supported critical large populations of juvenile and semi-adult stages of parrotfishes (Scaridae) and other fish taxa. This suggests the critical importance of protecting and restoring inshore and mid-shelf coral reefs. Multiple recommendations are discussed to address LBSP impacts across the shelf, to implement best management practices (BMPs) to reduce impacts, to monitor its impacts on coastal ecosystems, and to rehabilitate reef ecological functions of inshore and mid-shelf coral reefs.

I. INTRODUCTION

Coral reefs across the southwestern shelf of Puerto Rico have shown evidence of significant environmental degradation over the last three to four decades. Loya (1976), and Goenaga and Cintrón (1979) documented signs of degradation across inshore and mid-shelf reefs. Many of these have suffered damage over time due to high terrigenous sediment loads (Goenaga, 1988; Goenaga and Boulon, 1992; Torres and Morelock, 2002), and massive coral bleaching (Goenaga and Canals, 1990). Schärer et al. (2010) documented high densities of threatened Elkhorn coral, *Acropora palmata*, across offshore western mid-shelf reefs and were concerned about their conservation due to potential water quality degradation. Other studies have shown further reef degradation associated to land-based source pollution (LBSP), including sedimentation and turbidity (Morelock et al., 2001; Hernández-Delgado, 2005), and sewage and eutrophication (Bonkosky et al., 2009; Hernández-Delgado et al., 2010; Hernández-Delgado and Sandoz-Vera, 2011). Declining environmental conditions across the shelf have resulted in declining coral growth rates (Goenaga, 1988; García-Urueña, 2004), and in significant declines of *A. palmata* populations across inshore reefs adjacent to areas impacted by LBSP (Hernández-Delgado, 2000, 2005; Weil et al., 2002; Hernández-Delgado et al., 2010, 2012; Méndez-Lázaro et al., 2012; Norat-Ramírez et al., 2013).

Chronic decline in water quality could also have significant negative impacts on fish assemblages as several fish taxa can be sensitive to environmental degradation (Bejarano and Appeldoorn, 2013). These findings imply potential LBSP impacts across very large temporal and spatial scales, with very wide and persistent implications on coral reef benthic communities and on reef-associated fauna. LBSP impacts (i.e., sewage pollution from human and animal sources) were documented across the entire southwestern shelf in Puerto Rico, even in waters complying with existing microbiological quality standards (Bonkosky et al., 2009). This points out at the increasing spatial scale of chronic LBSP impacts across multiple coral reef systems and at the potentially increasing turnover rates of reef communities. The lack of adequate controls of LBSP across the region constitutes one of the most significant concerns regarding the conservation and recovery of declining coral reef ecosystems.

Efforts are being currently developed to implement erosion and sedimentation controls across watershed scales in southwestern Puerto Rico. But so far, these efforts have completely missed a long-term ecological monitoring component to determine if current land-based efforts have had any meaningful impacts on improving adjacent coral reef ecosystems. To obtain a spatial synoptic understanding of coral reef health and the land-based factors affecting it a broad-scale assessment of reef condition is needed.

This project conducted a large-scale assessment across 11 coral reefs located along a LBSP gradient across the southwestern Puerto Rico shelf. Standardized random photo-transect techniques were used across one to four different depth zones when present (5 m, 5-10 m, 10-15 m, 15-20 m), depending on the site, to characterize benthic communities and assess coral recruit density. Fish community structure was also assessed across similar depth zones. In addition, a snapshot characterization of water quality parameters was determined during each visit to study sites to establish a baseline data bank. This approach provided critical baseline information regarding the current status of benthic and fish communities across a LBSP stress gradient. This information will allow designing a long-term ecological monitoring program specifically targeted at addressing impacts from LBSP on reef ecosystems, as well as the impacts of best management practices (BMPs) implemented on selected watersheds.

The objectives of this project were to:

(1) Provide a large-scale spatial characterization over a variety of reef locations and conditions of the health of coral reef benthic communities, coral recruit assemblages, and reef fish communities.

(2) Obtain a snapshot characterization of water quality across each sampling site.

(3) Infer possible causative factors underlying observed spatial patterns in benthic and fish community structure.

This design allowed us testing multiple null hypotheses regarding spatial patterns in benthic community structure, coral recruit assemblages, and reef fish community structure, and in water quality parameters among geographic locations (inshore, mid-shelf, outer shelf), reefs (within each individual geographic region), and among depth zones. This information will be made available to decision-makers at the PR Department of Natural and Environmental Resources (PRDNER) and at the National Oceanic and Atmospheric Administration (NOAA) to help implement future management actions.

II. METHODS

Study sites – A total of eleven coral reefs were studied, subdivided in three different geographic locations (***Figures 1-2***): *Inshore Reefs* (<4 km) – Cayo Ratones (RAT), Punta Ostiones (OST), Punta Lamela (LAM), Punta Guaniquilla (GUA), Arrecife Enmedio (EME); *Mid-Shelf Reefs* (4-8 km) – Bajo Resuello (RES), Arrecife Corona del Norte (CON), Arrecife El Ron (RON); and *Outer Shelf Reefs* (8-15 km) – Arrecife El Negro (NEG); Arrecife Papa San-Tourmaline (PPS), Bajo Gallardo (GAL). Sampling was completed during July 13-30, 2014. Six of the above sites (55%) were located within Natural Reserves managed by PRDNER, including the Marine Extension of Finca Belvedere Natural Reserve, off Puerto Real (OST), the Marine Extension of Punta Guaniquilla Natural Reserve, off Boquerón Bay (GUA), Cayo Ratones Natural Reserve (RAT), and Tourmaline Natural Reserve (RON, CON, PPS). From these, there is a 6 month-seasonal fishing closure at Tourmaline Natural Reserve. Fishing remains open across all other reserves.

Benthic communities – Coral species richness, colony abundance, percentage cover of all major benthic components (i.e., corals, algal functional groups, sponges, other macroinvertebrates), and coral species diversity and evenness indices were documented. When possible, sources of recent mortality in coral colonies were identified. Data was collected from randomly-placed 10 m-long photo-transects from four different depth zones when present (<5 m, 5-10 m, 10-15 m, 15-20 m). Briefly, a total of 5 to 15 replicate transects per depth zone were obtained using 5 non-overlapping, high-resolution digital images from a roughly 1.0 x 0.7 m quadrat per transect at fixed intervals (1, 3, 5, 7, and 9 m along each transect). This provided a total of 25-75 images per

depth zone/reef. A digital grid of 48 regularly-distributed dots was projected over each image for analysis of percent coverage of benthic components. A 3-way permutational analysis of variance (PERMANOVA) design (geographic location, reef site, depth) was used to test hypotheses regarding spatial and variation patterns in benthic community parameters and benthic community structure. Principal component ordination (PCO) was determined in PRIMER-e 6.1.16 + PERMANOVA 1.06 (Plymouth Marine Laboratory, UK) to test for indicator benthic categories of spatial clustering patterns of coral reef benthic communities (Clarke and Warwick, 2001; Anderson et al., 2008).

Coral recruit communities – Coral recruit species richness and colony abundance were documented following a similar sampling design. Data was collected from five replicate, randomly-placed 10 m-long photo-transects from four different depth zones when present (<5 m, 5-10 m, 10-15 m, 15-20 m). Data was obtained using 5 non-overlapping, high-resolution digital images from a roughly 0.40 x 0.27 m quadrat per transect at fixed intervals (1, 3, 5, 7, and 9 m along each transect). This provided a total of 25 images per depth zone/reef. All coral recruits were counted and identified to the lowest taxon possible. A 3-way permutational analysis of variance (PERMANOVA) design (geographic location, reef site, depth) was used to test hypotheses regarding spatial and variation patterns in coral recruit community structure. PCO was determined to test for indicator coral recruit species of spatial clustering patterns of coral recruit communities (Clarke and Warwick, 2001; Anderson et al., 2008).

Fish communities – Fish communities were sampled within 7.5 m-radius circular transects. Sampling was conducted at 10-min time intervals and through similar depth zones, with a total of 4-6 replicate censuses/depth zone. A 3-way factorial design as above (geographic location, reef site, depth) was used to test hypotheses regarding spatial and variation patterns in fish community parameters and fish community structure. Fork lengths (FL) were converted to weight (Bohnsack and Harper 1988, Bohnsack unpub. data). Abundance within large fish schools were estimated by 10s, 20s, 50s or 100s. Fish species richness, species diversity and evenness, abundance and biomass were calculated. Multivariate SIMPER analysis of indicator species (Clarke and Warwick, 2001) and PCO was used to test for indicator species of spatial clustering patterns.

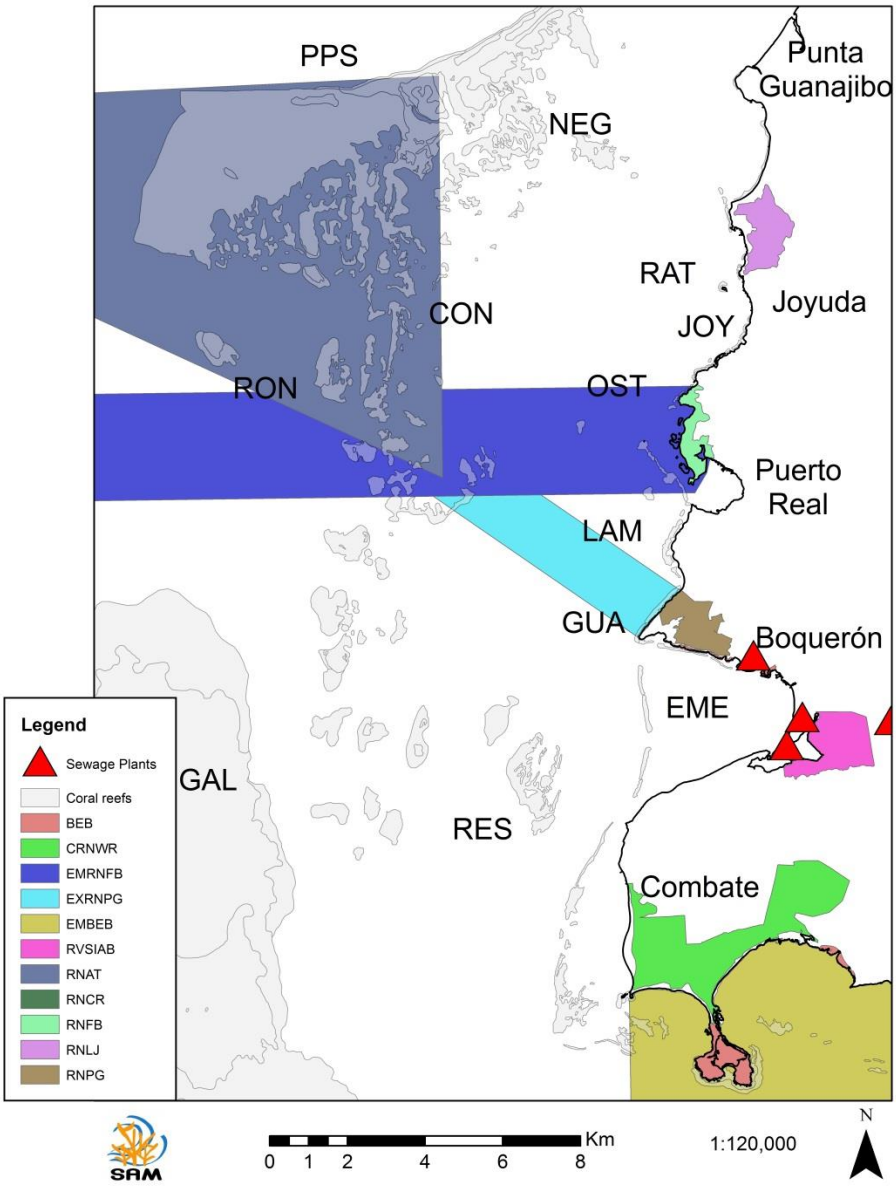

FIGURE 1. Selected sampling sites across the Southwestern PR insular shelf. Sites were subdivided in three different geographic locations: *Inshore Reefs* (<4 km) – Cayo Ratones (RAT), Punta Ostiones (OST), Punta Lamela (LAM), Punta Guaniquilla (GUA), Arrecife Enmedio (EME); *Mid-Shelf Reefs* (4-8 km) – Bajo Resuello (RES), Arrecife Corona del Norte (CON), Arrecife El Ron (RON); and *Outer Shelf Reefs* (8-15 km) – Arrecife El Negro (NEG), Arrecife Papa San (PPS), Bajo Gallardo (GAL). Eleven different protected areas surround the study sites: BEB= Boquerón State Forest; CRNWR= Cabo Rojo National Wildlife Refuge (USFWS), EMRNFB= Finca Belvedere Natural Reserve Marine Extension; EMRNPG= Punta Guaniquilla Natural Reserve Marine Extension; EMBEB= Boquerón State Forest Marine Extension; RVSIAB= Boquerón's Iris Alameda Wildlife Refuge; RNAT= Arrecife Tourmaline Natural Reserve; RNCR= Cayo Ratones Natural Reserve; RNFB= Finca Belvedere Natural Reserve; RNLJ= Laguna Joyuda Natural Reserve; RNPG= Punta Guaniquilla Natural Reserve.

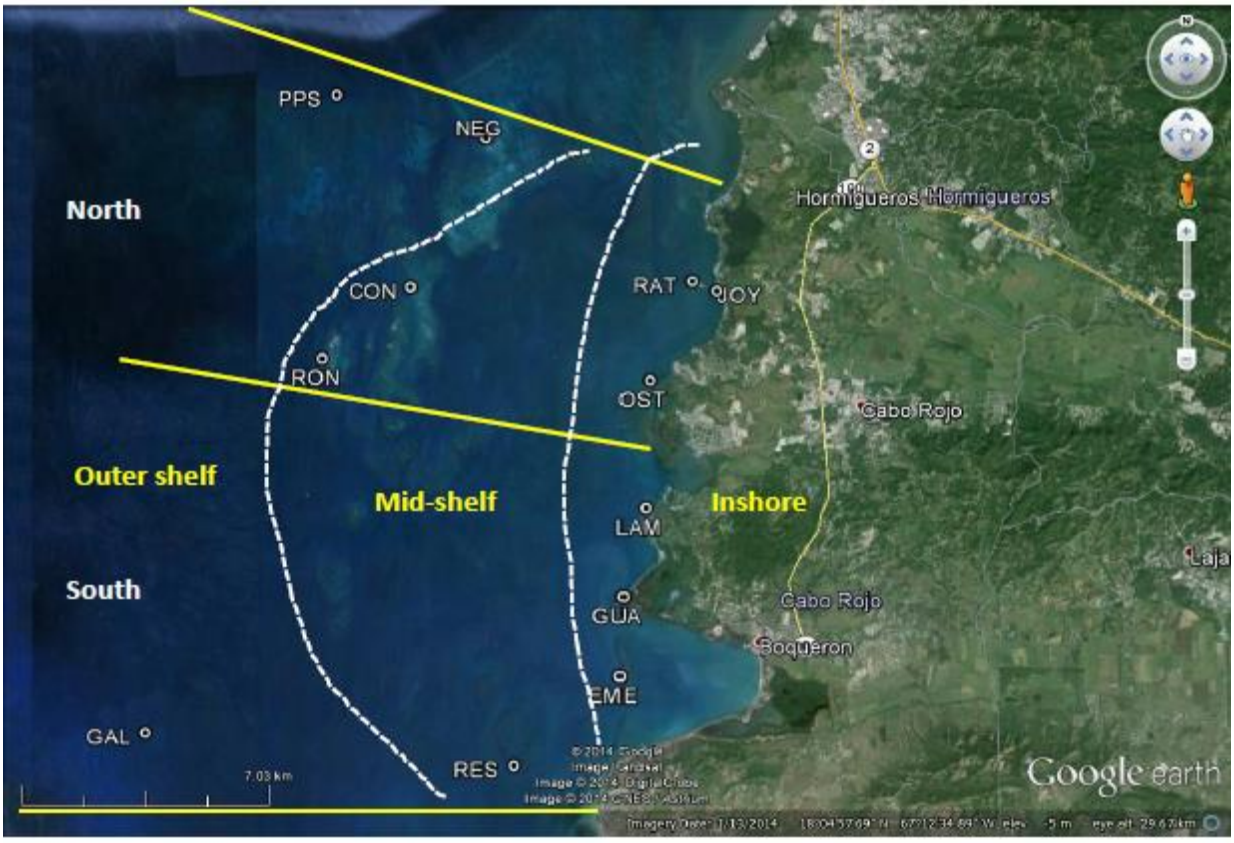

FIGURE 2. Selected sampling sites across the Southwestern PR insular shelf. Sites were subdivided in three different geographic locations: *Inshore Reefs* (<4 km) – Cayo Ratones (RAT), Punta Ostiones (OST), Punta Lamela (LAM), Punta Guaniquilla (GUA), Arrecife Enmedio (EME); *Mid-Shelf Reefs* (4-8 km) – Bajo Resuello (RES), Arrecife Corona del Norte (CON), Arrecife El Ron (RON); and *Outer Shelf Reefs* (8-15 km) – Arrecife El Negro (NEG), Arrecife Papa San (PPS), Bajo Gallardo (GAL).

Water quality parameters – Water quality parameters were documented at each site, including temperature, salinity, conductivity and dissolved oxygen concentration using a YSI85 data logger. Turbidity was measured using a LaMotte turbidimeter. Chlorophyll-*a* concentration and optical brighteners concentration was documented using a Turner fluorometer. Phosphate (PO_4), ammonium (NH_3), and ionized ammonium (NH_4^+) concentrations were determined using a Smart V2 spectrophotometer (LaMotte). Triplicate samples were obtained per site at 30 cm below surface. Water quality data was analyzed following a two-way PERMANOVA with geographic location and reef site as main factors to test null hypotheses regarding spatial

variation patterns in water quality. PCO was determined used to test for indicator water quality parameters of spatial LBSP patterns (Clarke and Warwick, 2001; Anderson et al., 2008).

Multivariate RELATE routine from PRIMER-e 6.1.16 was used to test for correlations of water quality parameters with benthic community structure, coral recruit community structure, and fish community structure. Multivariate LINKTREE test was conducted following BEST routine and independent BIOENV and BVSTEP stepwise regression procedures to determine which individual or combined water quality parameters better explained observed spatial patterns in biological community structure for benthic, coral recruit, and fish communities.

Cross-shelf spatial patterns of LBSP

Arc-View 10.2 (ESRI) was used to address cross-shelf spatial patterns of water quality patterns based on the preliminary sampling of multiple water quality parameters.

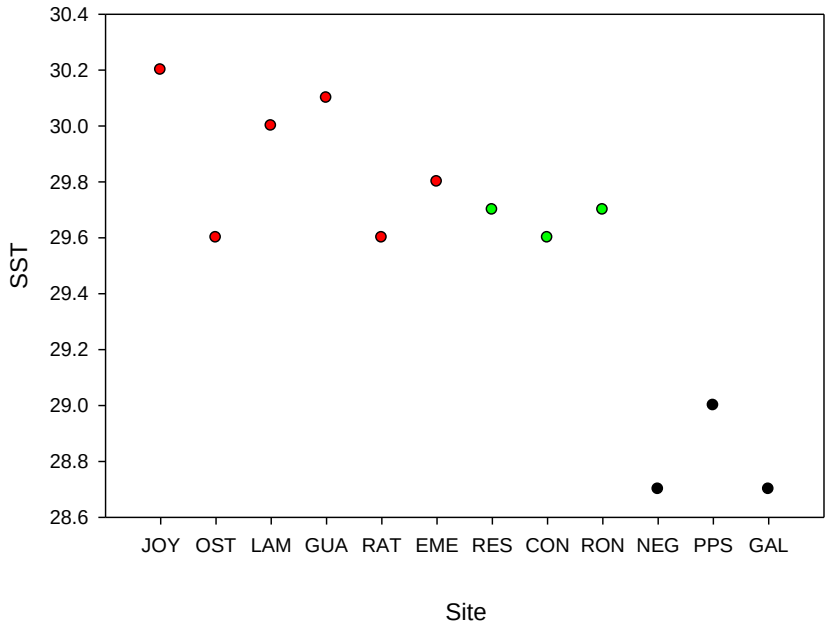

FIGURE 3. Sea surface temperature across sites. Red circles= Inshore sites; Green circles= Mid-shelf sites; Black circles= Outer shelf sites. Mean±95% confidence interval.

III. RESULTS

a. Water quality

Sea surface temperature (SST) was significantly higher and had a higher fluctuation at shallower inshore sites (29.6°C to 30.2°C), than at mid-shelf sites (29.6°C to 29.7°C), and outer shelf sites (28.7°C to 29.0°C) (**Figure 3**). Salinity ranged from 35.4 to 35.7 ppt across inshore sites, from 35.2 to 35.7 ppt across mid-shelf sites, and from 35.1 to 35.7 ppt across outer shelf sites (**Figure 4**). Conductivity showed a spatial gradient with higher mean values across inshore sites (58.0 to 59.4 mS), followed by mid-shelf sites (58.3 to 59.0 mS), and outer shelf sites (57.2 to 58.0 mS) (**Figure 5**). The observed pattern suggest a relationship between warmer SST and higher salinity across inshore sites, in comparison to outer shelf localities. This pattern could be the result of very complex cross-shelf tidal circulation as well as by regional circulation factors.

Dissolved oxygen concentration also showed a significant increase with increased distance from known polluted coastal reef communities (**Figure 6**). Inshore reef sites showed a range from 3.8 to 4.3 mg/L. These values became particularly low under the influence of turbid ebbing tides as previously documented by Bonkosky et al. (2009). Dissolved oxygen concentration fluctuated from 3.8 to 4.5 mg/L across mid-shelf sites, and from 5.5 to 5.8 mg/L across outer shelf sites. Mean turbidity showed an opposite trend, with higher mean values across inshore sites, which showed a range from 1.0 to 3.8 NTU (**Figure 7**). Mid-shelf sites averaged 0.9 to 1.0 NTU, and outer shelf sites 0.4 to 0.9 NTU. Dissolved oxygen and turbidity patterns show often complex spatial and temporal variability across the western shelf due to complex circulation patterns.

Chlorophyll-*a* concentration ranged from 1.50 to 2.69 µg/L across inshore sites, from 1.83 to 2.31 µg/L across mid-shelf sites, and from 1.89 to 2.29 µg/L across outer shelf sites (**Figure 8**). Upper mean values were documented across Punta Ostiones, Cayo Ratones and Bajo Enmedio, all across the inshore sites. Optical brighteners concentration (OABs) ranged from 17 to 32 ppm across inshore sites, from 22 to 28 ppm across mid-shelf sites, and from 17 to 25 ppm across outer shelf sites. OABs concentration showed large fluctuations as a result of complex ocean circulation patterns across the shelf. Nonetheless, higher OABs concentrations were observed at Joyuda and at Bajo Enmedio, off Boquerón Bay mouth. Both sites are known to receive raw sewage and gray water discharges directly to coastal waters. OABs concentrations were also fairly high at Arrecife El Ron and at Corona del Norte mid-shelf sites. These also receive Río

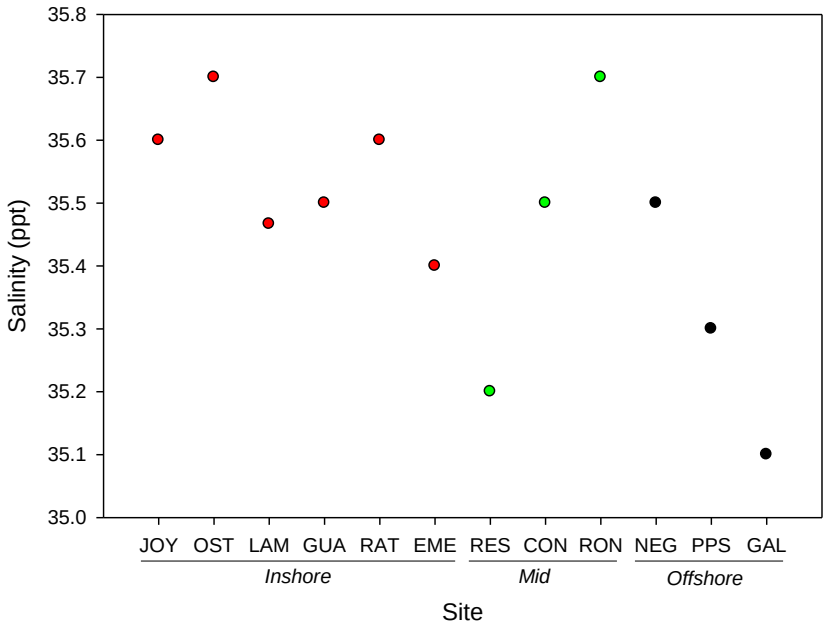

FIGURE 4. Salinity across sites. Red circles= Inshore sites; Green circles= Mid-shelf sites; Black circles= Outer shelf sites. Mean±95% confidence interval.

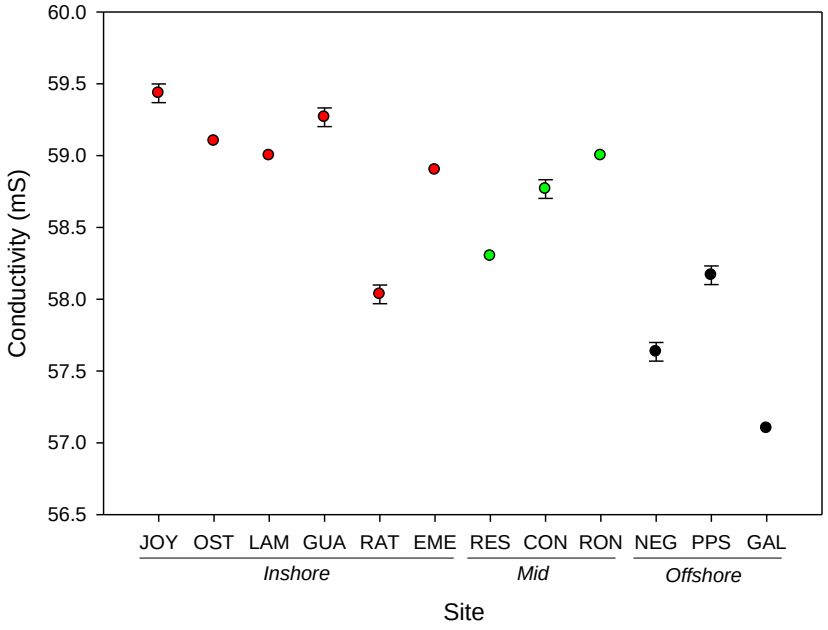

FIGURE 5. Salinity across sites. Red circles= Inshore sites; Green circles= Mid-shelf sites; Black circles= Outer shelf sites. Mean±95% confidence interval.

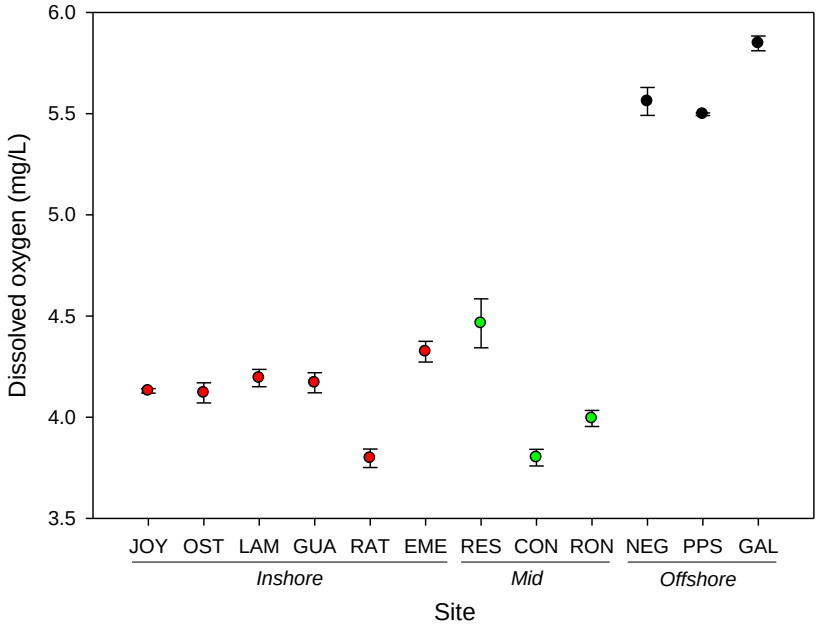

FIGURE 6. Dissolved oxygen across sites. Red circles= Inshore sites; Green circles= Mid-shelf sites; Black circles= Outer shelf sites. Mean±95% confidence interval.

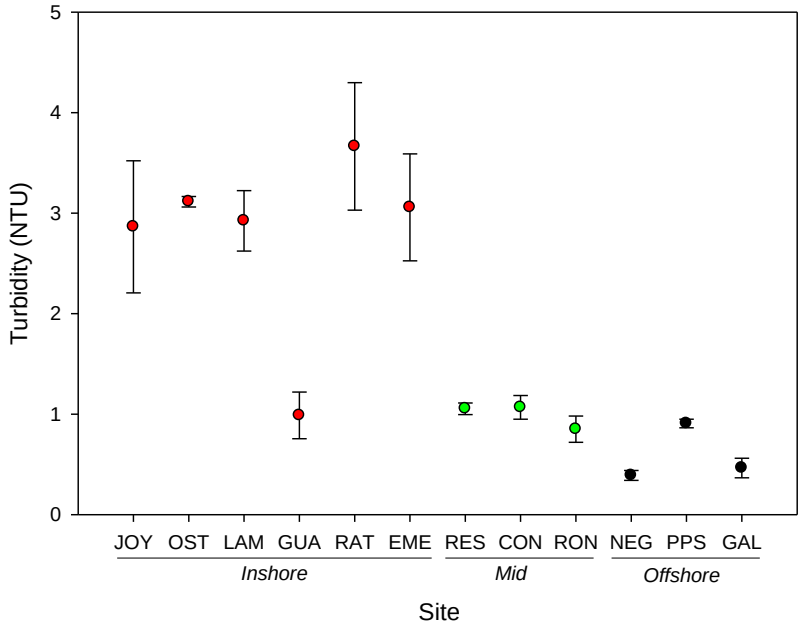

FIGURE 7. Turbidity across sites. Red circles= Inshore sites; Green circles= Mid-shelf sites; Black circles= Outer shelf sites. Mean±95% confidence interval.

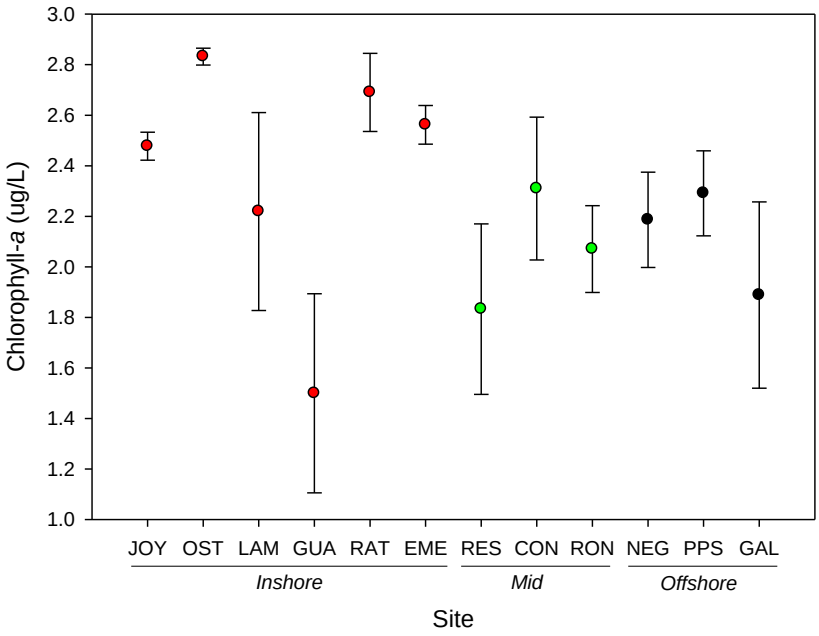

FIGURE 8. Chlorophyll-*a* concentration across sites. Red circles= Inshore sites; Green circles= Mid-shelf sites; Black circles= Outer shelf sites. Mean±95% confidence interval.

Guanajibo effluents during ebbing tides through the Guanajibo Channel.

Phosphate (PO_4) concentrations resulted higher within inshore sites, ranging from 2.2 to 4.4 µM (***Figure 10***). PO_4 concentrations ranged from 2.5 to 3.0 µM across inshore sites, and from 0.8 to 1.9 µM across outer shelf sites. This reflects a concentration gradient with increasing distance. Ammonium concentration (NH_3) showed large spatial variability, with inshore sites ranging from 25 to 264 µM (***Figure 11***). Mid-shelf sites ranged from 22 to 133 µM, and outer shelf sites ranged from 15 to 16 µM. Bajo Enmedio (264 µM), Punta Guaniquilla (136 µM), and Bajo Resuello (133 µM), which are located just off Boquerón Bay and are known to receive recurrent raw sewage illegal discharges and poorly-treated sewage effluents from a malfunctioning treatment facility from Boquerón Bay, showed the highest NH_3 concentrations. NH_3 concentration at Punta Lamela, located just off Puerto Real, showed also a concentration of 94 µM, which is also considered very high.

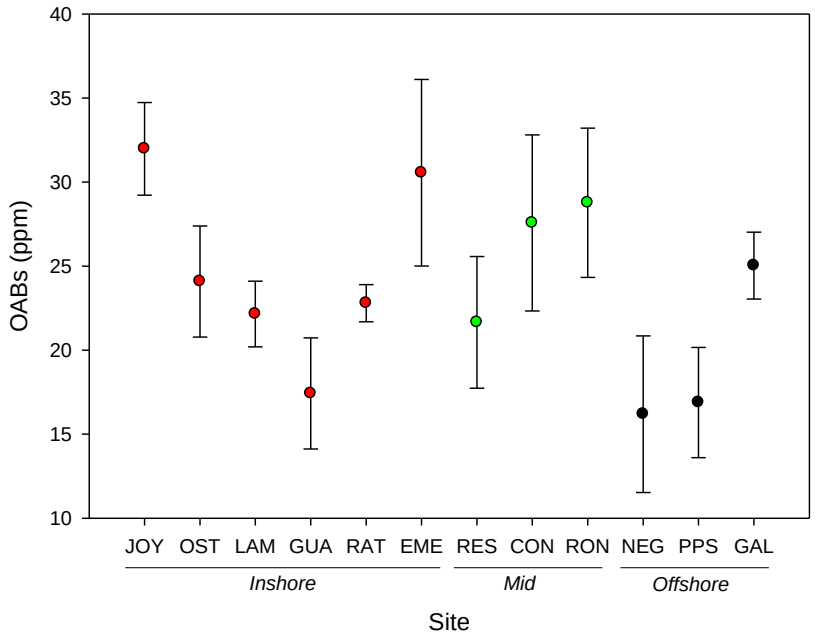

FIGURE 9. Optical brighteners (OABs) concentration across sites. Red circles= Inshore sites; Green circles= Mid-shelf sites; Black circles= Outer shelf sites. Mean±95% confidence interval.

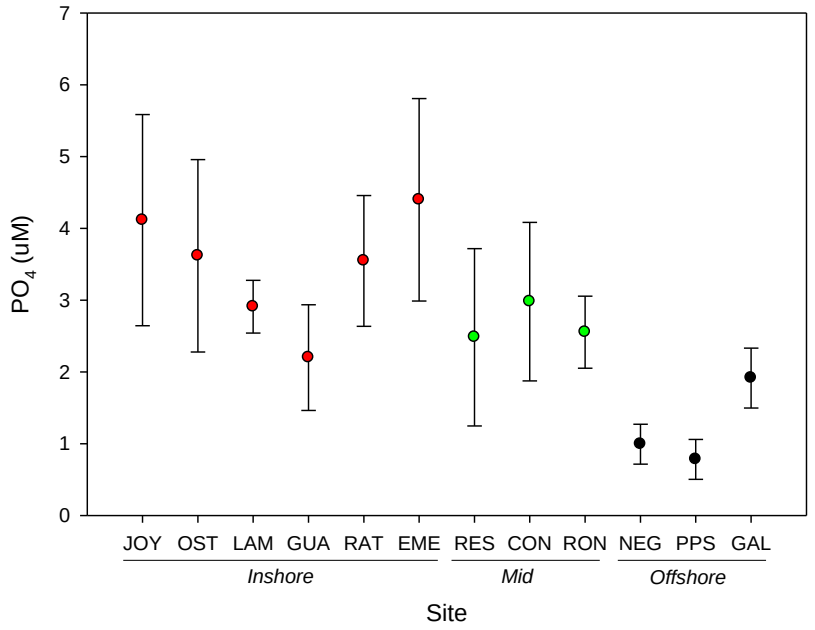

FIGURE 10. Phosphate (PO_4) concentration across sites. Red circles= Inshore sites; Green circles= Mid-shelf sites; Black circles= Outer shelf sites. Mean±95% confidence interval.

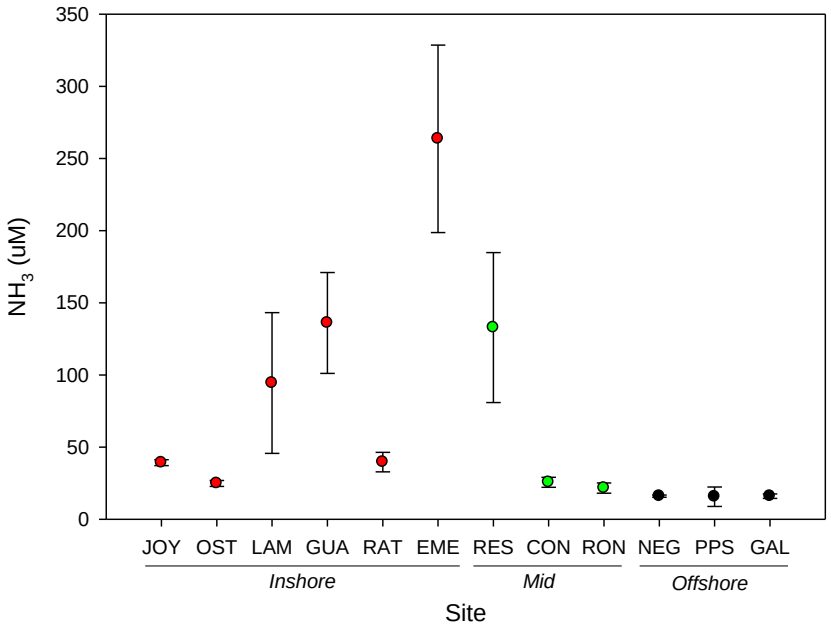

FIGURE 11. Ammonium (NH_3) concentration across sites. Red circles= Inshore sites; Green circles= Mid-shelf sites; Black circles= Outer shelf sites. Mean±95% confidence interval.

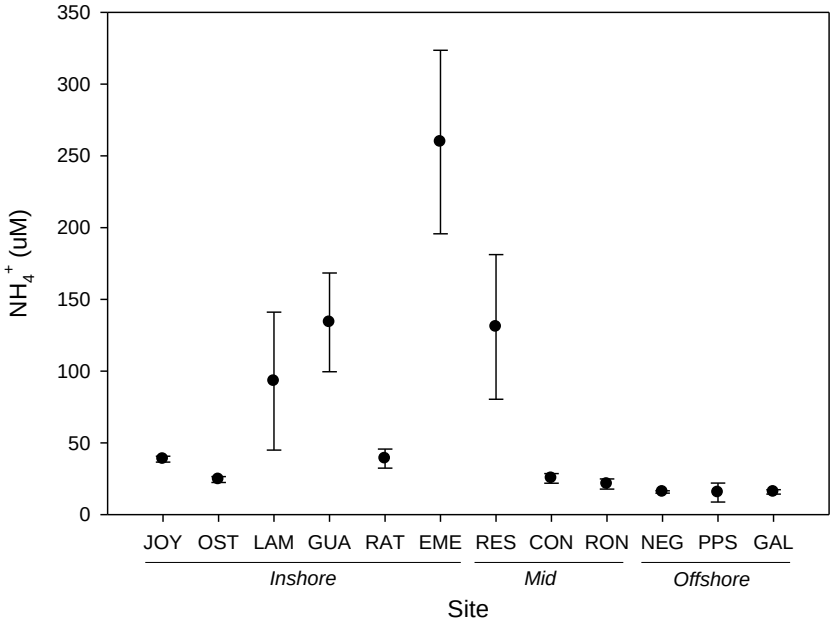

FIGURE 12. Ionized ammonium (NH_4^+) concentration across sites. Red circles= Inshore sites; Green circles= Mid-shelf sites; Black circles= Outer shelf sites. Mean±95% confidence interval.

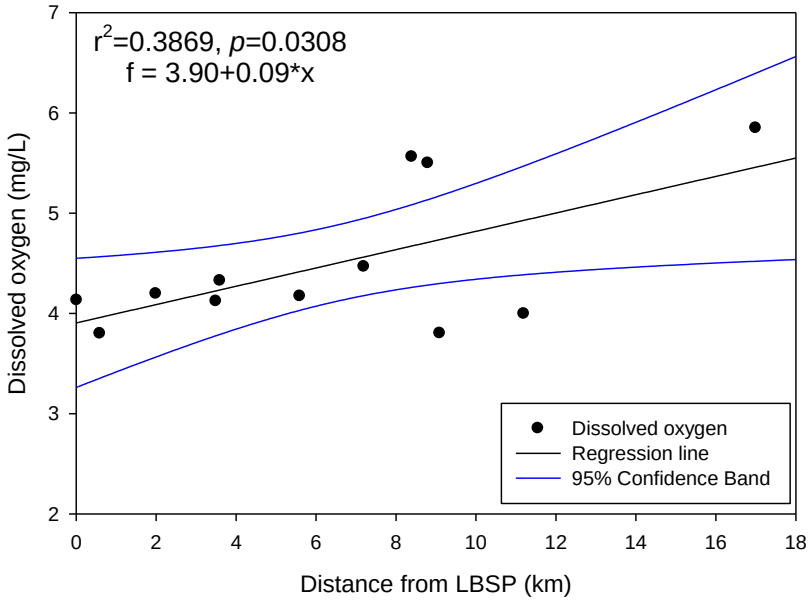

FIGURE 13. Linear regression analysis between dissolved oxygen concentration and distance from the known pollution centers along the coast.

Ionized ammonium concentration (NH_4^+) followed similar spatial patterns, with inshore sites ranging from 24 to 260 µM (***Figure 12***). Mid-shelf sites ranged from 21 to 131 µM, and outer shelf sites ranged from 15 to 16 µM. Bajo Enmedio (260 µM), Punta Guaniquilla (134 µM), and Bajo Resuello (131 µM) also showed the highest NH_4^+ concentrations. NH_4^+ concentration at Punta Lamela, located just off Puerto Real, showed also a concentration of 93 µM, which is also considered very high. These observations are highly consistent with previous observations of significant sewage pollution impacts across the western Puerto Rican shelf (Bonkosky et al., 2009; Hernández-Delgado et al., 2010).

A linear regression analysis showed a significant (r^2=0.3869; *p*=0.0308) increase in dissolved oxygen concentration with increasing distance from known pollution centers along the coast (***Figure 13***). Also, water turbidity showed a highly significant decline (r^2=0.7119; *p*=0.0006) with increasing distance from the coast (***Figure 14***). No significant spatial gradient was found with the chlorophyll-*a* concentration (***Figure 15***) and OABs concentration (***Figure 16***) and increasing distance from LBSP. Phosphate (PO_4) showed a significant decline (r^2=0.3952; *p*=0.0286) with increasing distance from LBSP (***Figure 17***). There was a significant (r^2=0.4961;

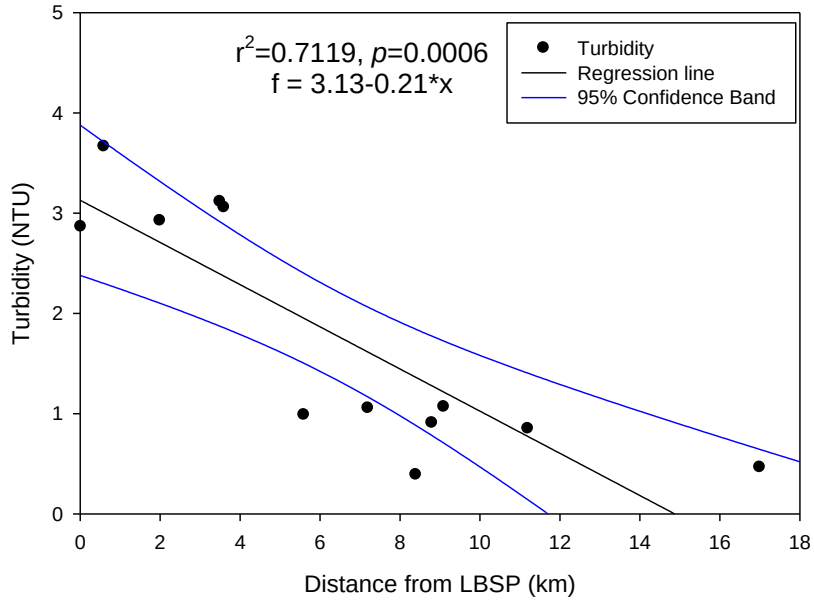

FIGURE 14. Linear regression analysis between turbidity and distance from the known pollution centers along the coast.

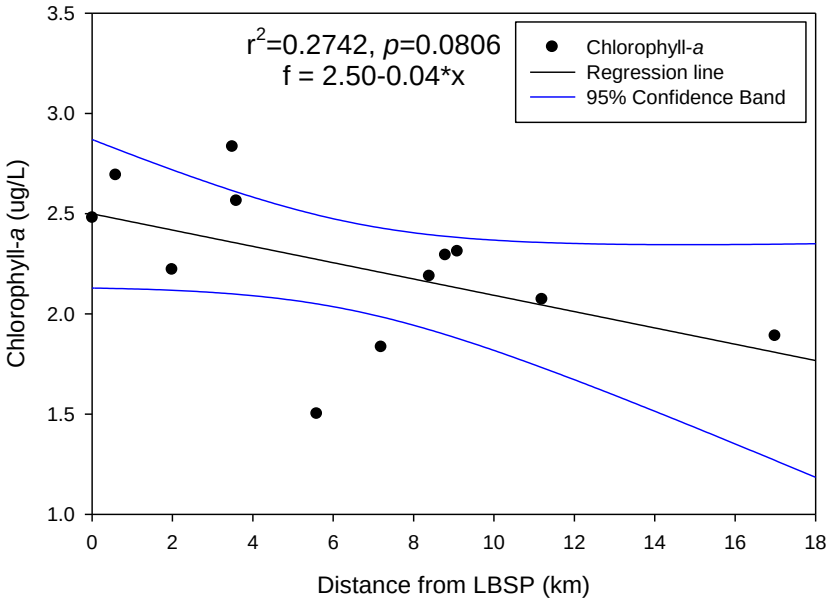

FIGURE 15. Linear regression analysis between chlorophyll-*a* concentration and distance from the known pollution centers along the coast.

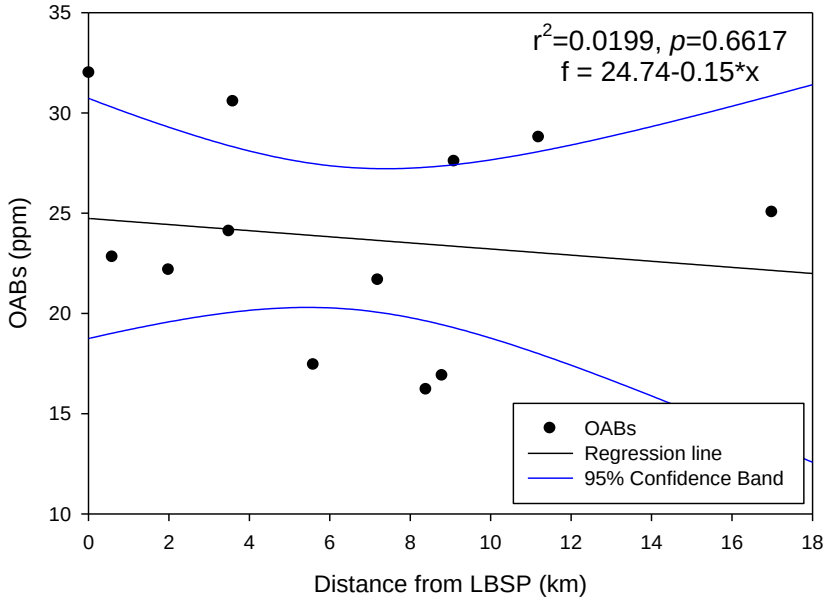

FIGURE 16. Linear regression analysis between optical brighteners (OABs) concentration and distance from the known pollution centers along the coast.

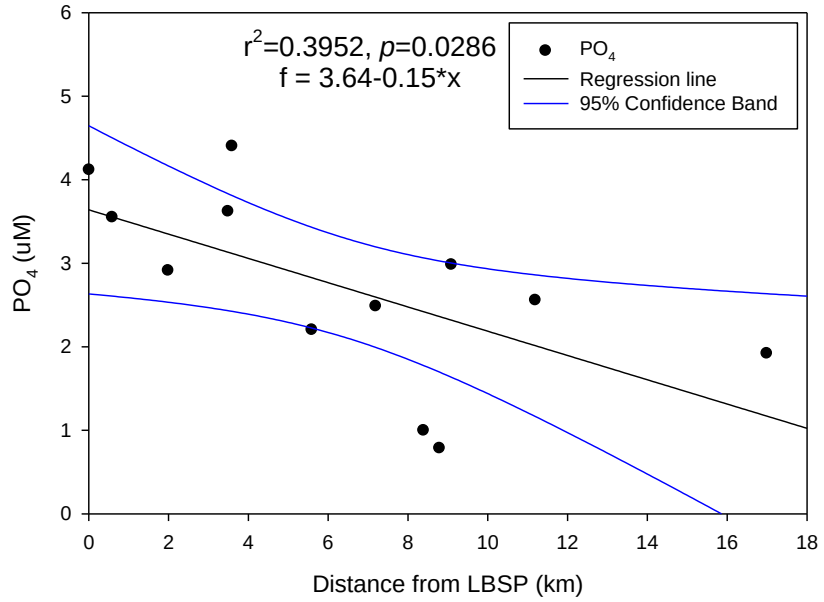

FIGURE 17. Linear regression analysis between phosphate (PO_4) concentration and distance from the known pollution centers along the coast.

p=0.0458) non-linear relationship between NH_3 (***Figure 18***) and NH_4^+ (***Figure 19***) with increasing distance from LBSP. There was a significant non-linear decline (r^2=0.6174; *p*=0.0133) in dissolved oxygen concentration with increasing turbidity (***Figure 20***). Chlorophyll-*a* concentration showed a significant linear increase (r^2=0.5440; *p*=0.0062) with increasing turbidity (***Figure 21***).

There was also a significant linear increase (r^2=0.6579; *p*=0.0014) in PO_4 concentration with increasing turbidity (***Figure 22***), and a significant non-linear increase (r^2=0.5121; *p*=0.0396) in chlorophyll-*a* concentration with increasing PO_4 concentration (***Figure 23***). In addition, there was a significant linear decline (r^2=0.5364; *p*=0.0068) in dissolved oxygen concentration with increasing PO_4 concentration (***Figure 24***).

There was a highly significant (*p*<0.0001) spatial gradient of LBSP (***Table 1***) which produced four different clusters. A first large cluster was composed of inshore sites JOY, OST, RAT, LAM, and mid-shelf sites CON, RON (***Figure 25***). OST and RAT were largely explained by high chlorophyll-*a* concentration. JOY was largely explained by high NTU and OABs. LAM and EME were explained by high PO_4, sea surface temperature (SST) and conductivity. CON and RON were explained by high salinity. EME constituted a second individual cluster. A third cluster was composed of GUA and RES and was explained by high NH_4^+. A final cluster was composed by NEG, PPS, GAL and was explained by higher dissolved oxygen concentration. This model explained 74.3% of the spatial variation observed in water quality parameters across the entire shelf.

Cross-shelf spatial patterns of LBSP

GIS-based analysis was used to determine cross-shelf spatial patterns in selected water quality parameters. Salinity showed slightly higher values across northern inshore and mid-shelf sites (***Figure 26***). Dissolved oxygen concentration showed lower values across inshore RAT site and mid-shelf sites CON, RON (***Figure 27***). All other inshore sites showed moderately low values. Higher values were observed at outer shelf sites. With exception of inshore site GUA, turbidity was higher across all inshore sites and moderate across mid-shelf sites (***Figure 28***). Turbidity was lower across outer shelf sites. Chlorophyll-*a* was higher across inshore sites, and moderate

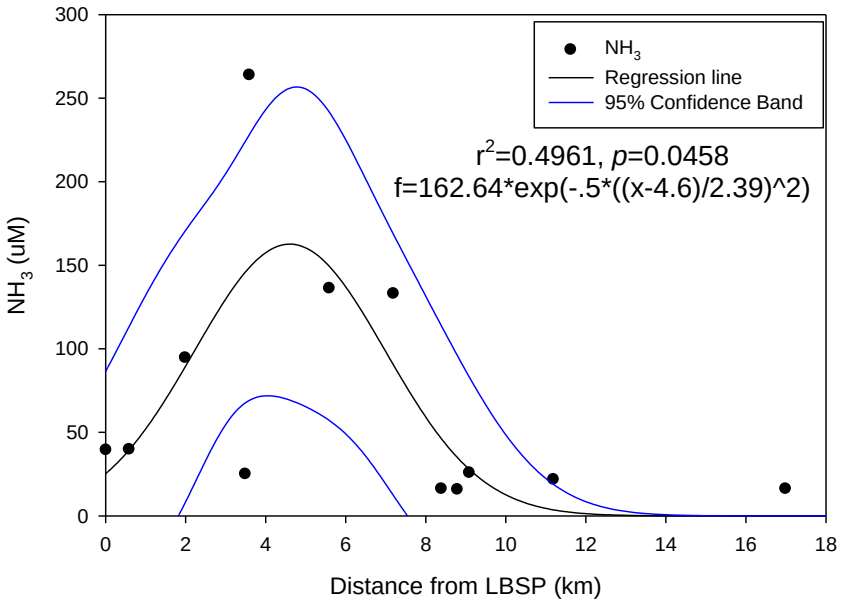

FIGURE 18. Non-linear regression analysis between ammonium (NH_3) concentration and distance from the known pollution centers along the coast.

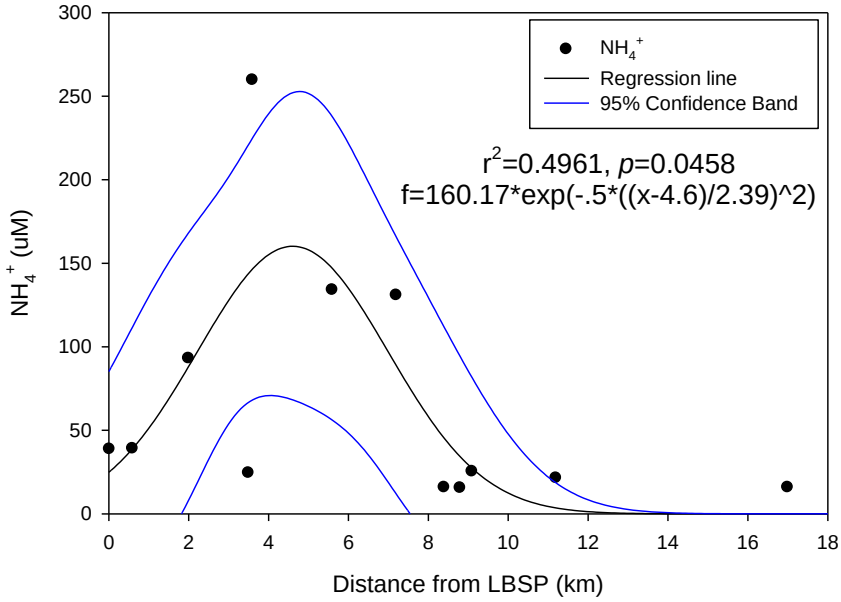

FIGURE 19. Non-linear regression analysis between ionized ammonium (NH_4^+) concentration and distance from the known pollution centers along the coast.

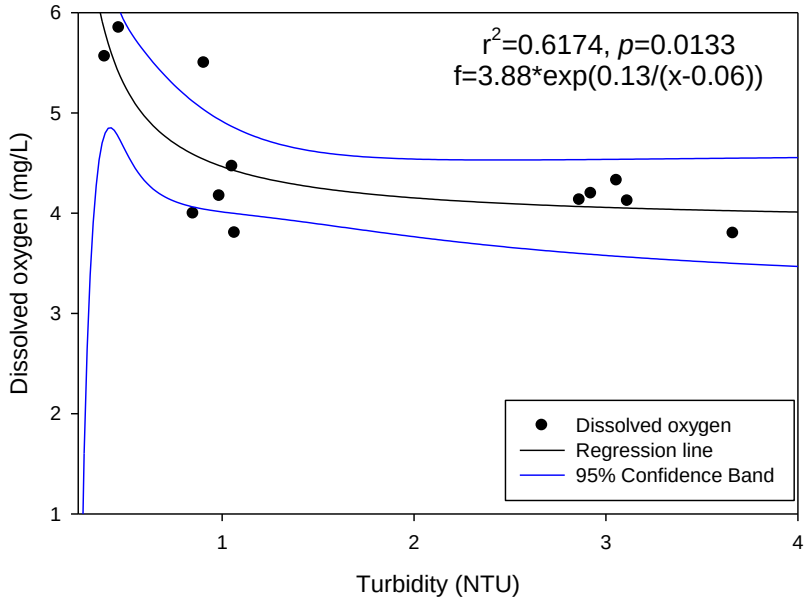

FIGURE 20. Non-linear regression analysis between dissolved oxygen concentration and turbidity.

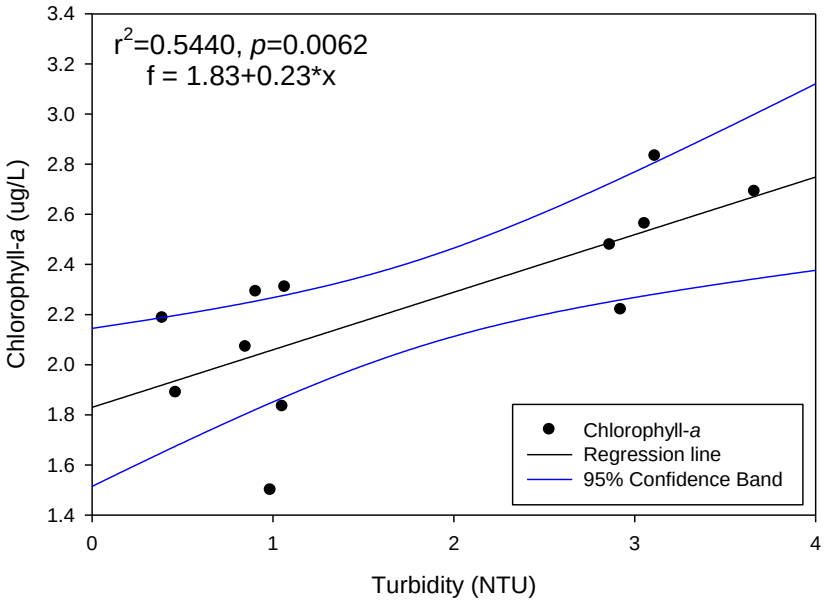

FIGURE 21. Linear regression analysis between chlorophyll-*a* concentration and turbidity.

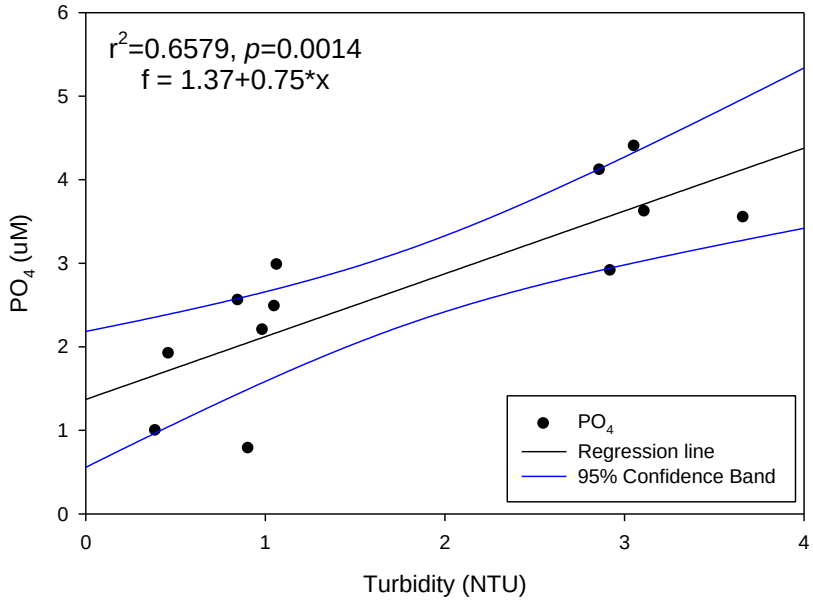

FIGURE 22. Linear regression analysis between phosphate (PO_4) concentration and turbidity.

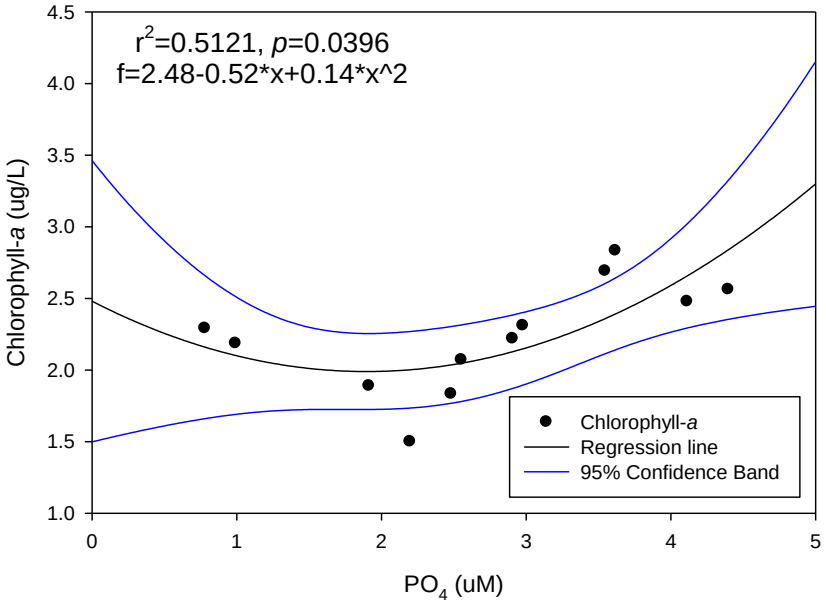

FIGURE 23. Non-linear regression analysis between cholorphyll-*a* concentration and phosphate (PO_4) concentration.

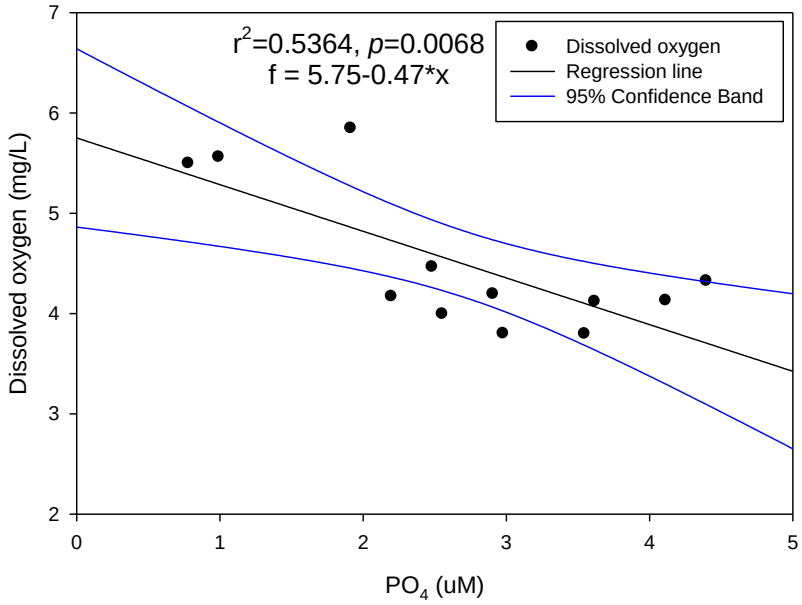

FIGURE 24. Linear regression analysis between dissolved oxygen concentration and phosphate (PO_4) concentration.

TABLE 1. Summary of a two-way PERMANOVA test of sampling sites clustering patterns based on water quality parameters.

Variable	d.f.	Pseudo-F	*p*
Geographic location	2,33	13.67	<0.0001
Site	11,24	13.66	<0.0001
Location x Site	11,24	13.66	<0.0001

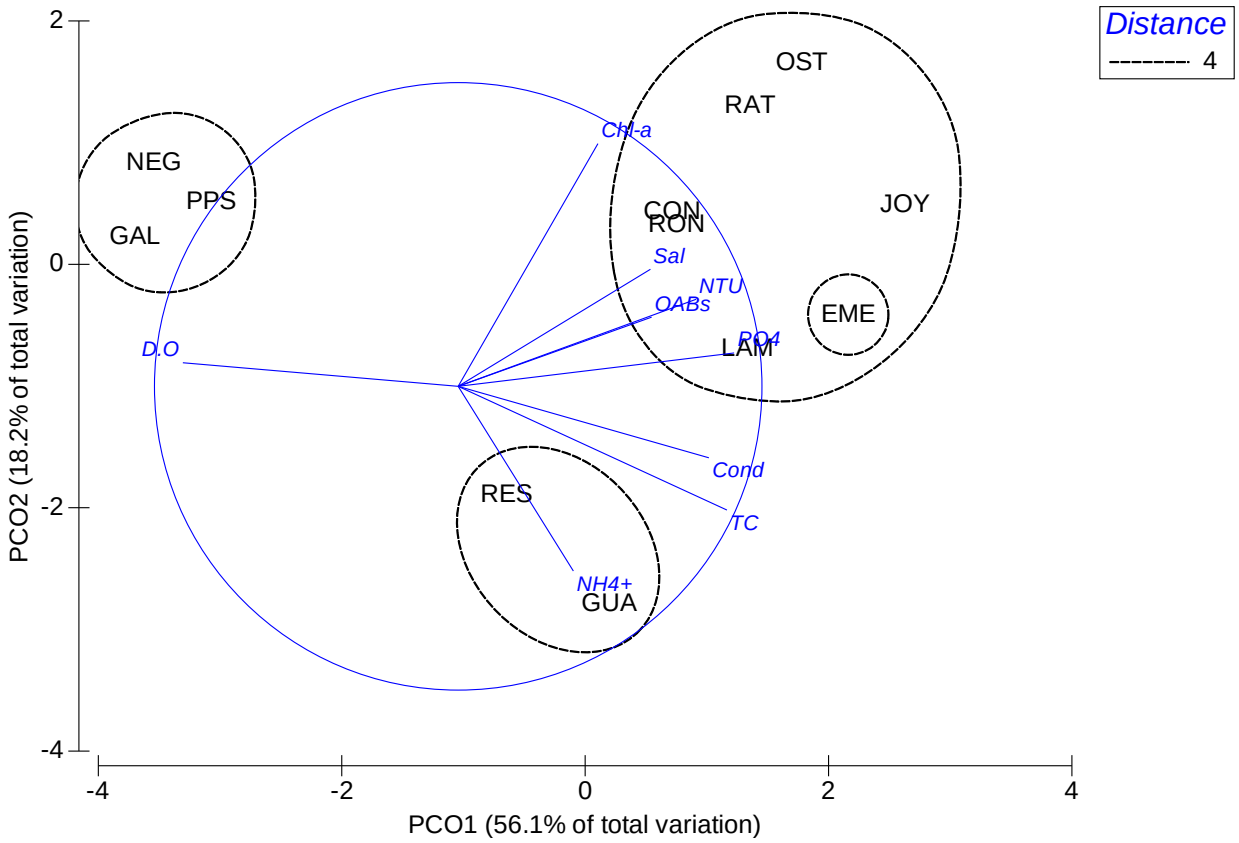

FIGURE 25. Principal component ordination (PCO) plot of the LBSP stress gradient across study sites. Based on Euclidean distance of Log_{10}-transformed water quality parameters. NH_3 data was removed from the matrix due to co-linearity with NH_4^+ data. Total variation= 74.3%.

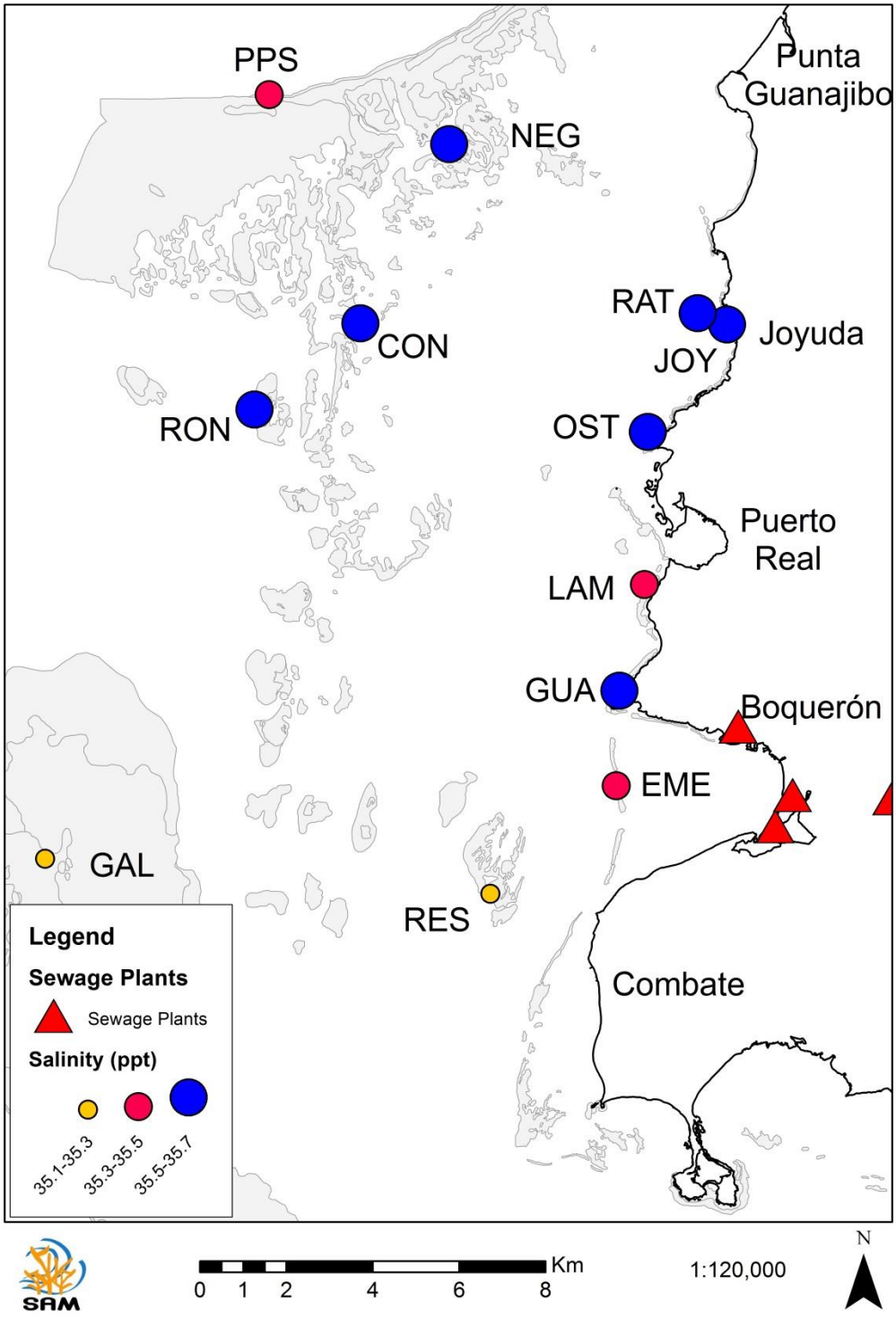

FIGURE 26. Cross-shelf spatial patterns of salinity.

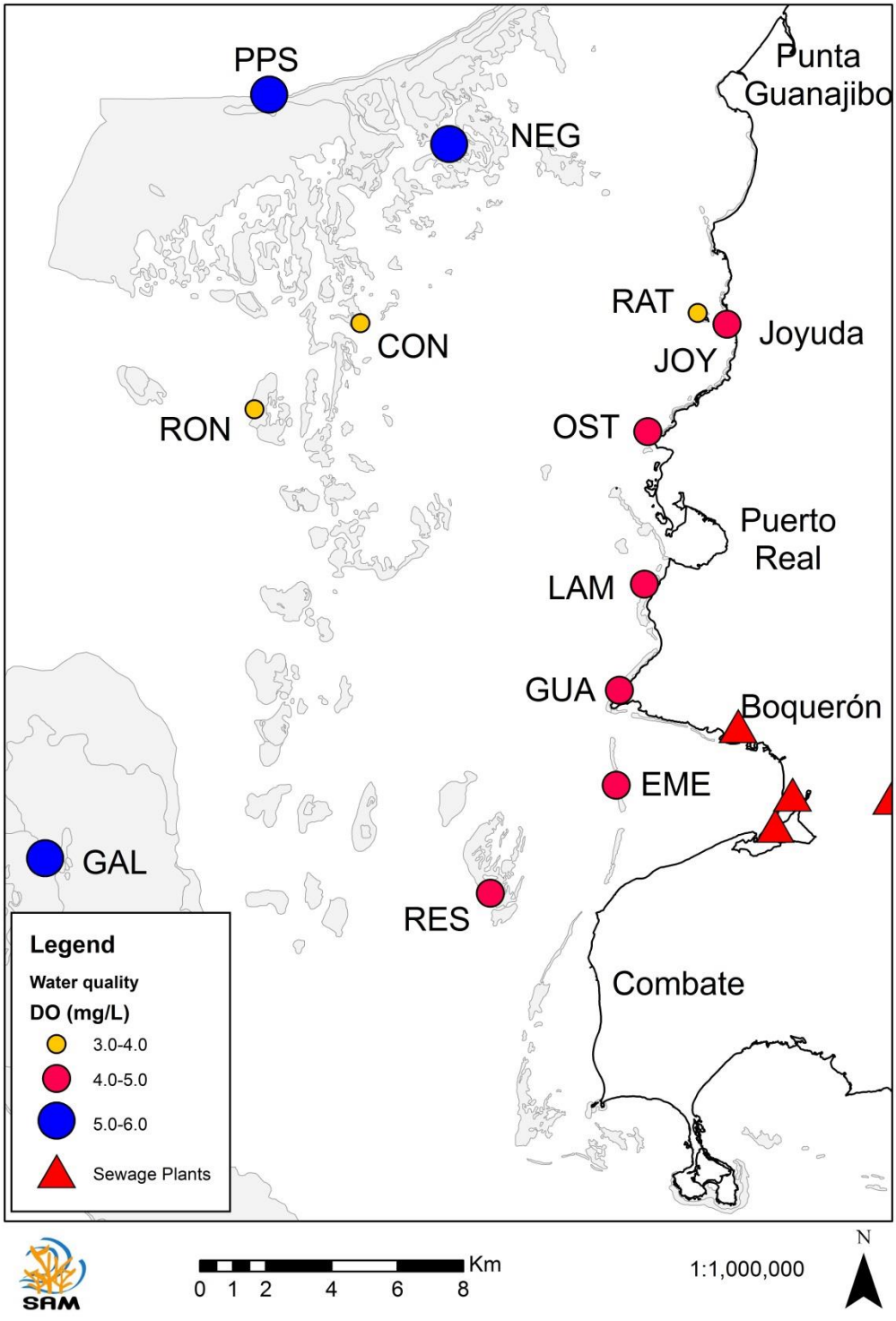

FIGURE x. Cross-shelf spatial patterns of dissolved oxygen.

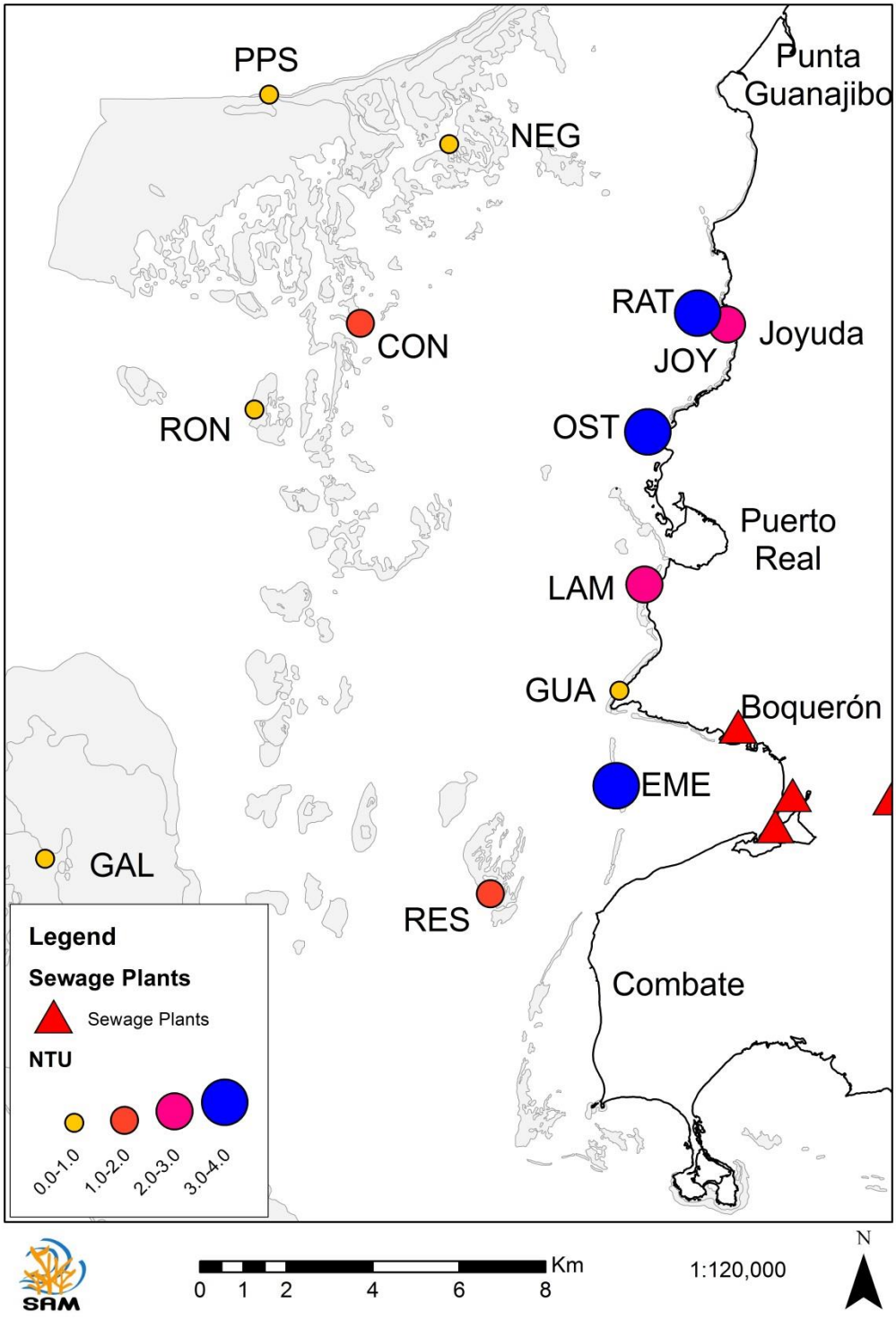

FIGURE 28. Cross-shelf spatial patterns of turbidity.

across northern inshore, mid-shelf and offshore sites, suggesting potential influences from north south surface circulation from Mayagüez Bay (***Figure 29***). OABs concentrations showed higher and moderate concentrations across inshore reef sites, particularly adjacent to Boquerón Bay and Playa Joyuda (***Figure 30***).

PO_4 concentrations were significantly higher across all inshore sites in comparison to mid-shelf and outer sites, suggesting a direct linear relationship with proximity to LBSP (***Figure 31***). NH_4^+ concentrations were also concerning and higher across inshore sites, particularly in those adjacent to Boquerón Bay and Puerto Real Bay (***Figure 32***). Observed spatial trends suggest five possible terrestrial influences of pollution. The most critical one appears to be raw sewage effluents and septic tank infiltration from multiple non-point sources across Boquerón Bay, plus poorly-treated discharges from four different package sewage treatment plants. The second source of LBSP is raw sewage pollution from Puerto Real Bay and septic tank infiltration from private houses from Puerto Real and Punta Lamela. A third potential source of human-borne pollution is the multiple non-point sources of raw sewage, gray waters, and septic tank infiltration from Playa Joyuda. A fourth significant source of pollution can come from the Río Guanajibo outlet. Its effluents move to the west, south-west, across Las Coronas coral reef system across the Guanajibo Channel. A final potential source of LBSP is Mayagüez Bay. These findings are very consistent with Bonkosky et al. (2009) and suggest the complex nature of water circulation pattern and the network of terrestrial-marine connectivity across the southwestern region.

Discussion of water quality observations

This study had the limitation that sampling was conducted only once, so it must be interpreted with caution. However, a key concern associated to sewage and eutrophication impacts from LBSP across the western Puerto Rican shelf in this study was the elevated mean chlorophyll-*a* concentration range found in this study across the shelf (1.50-2.69 μg/L). These values were up to 4-8 times higher than the recommended concentration for coral reef waters (0.3-0.5 μg/L) (Lapointe and Clark, 1992; Otero, 2009). Recent studies conducted at severely eutrophied Vega Baja beach, in northern Puerto Rico, showed chlorophyll-*a* concentrations of up to 17-83 times higher than recommended limits (Díaz-Ortega and Hernández-Delgado, 2014).

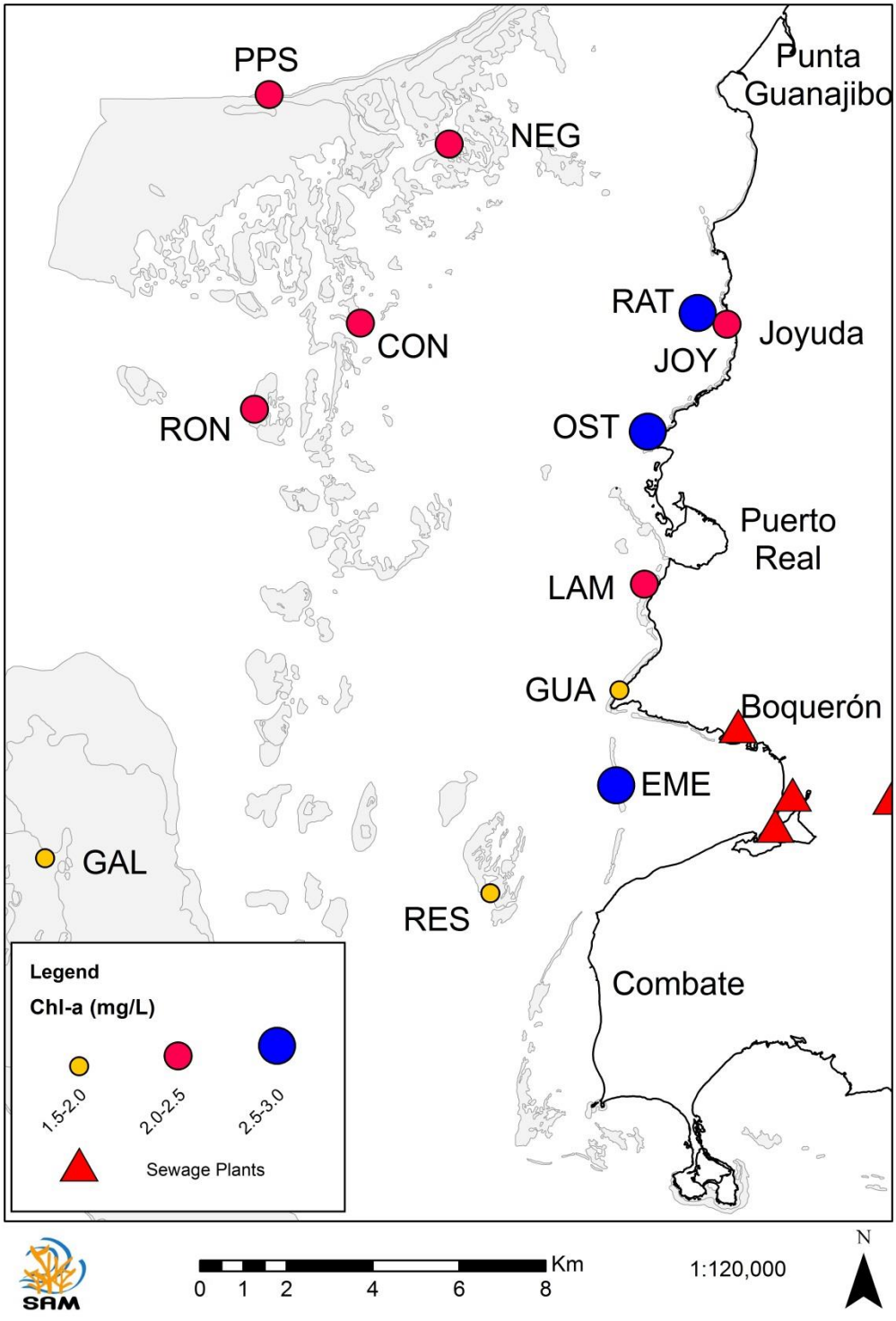

FIGURE 29. Cross-shelf spatial patterns of chlorophyll-*a* concentration.

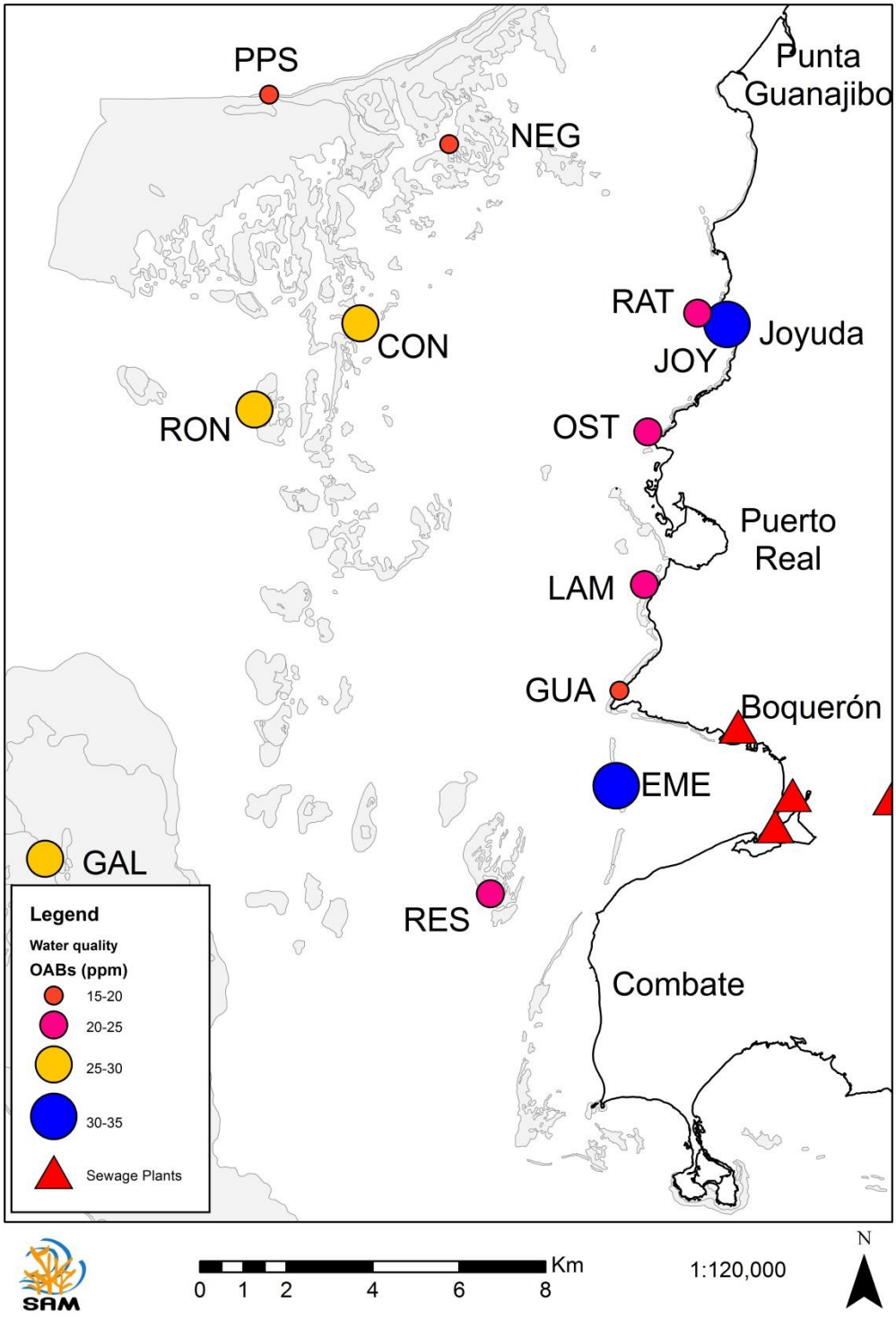

FIGURE 30. Cross-shelf spatial patterns of optical brighteners (OABs) concentration.

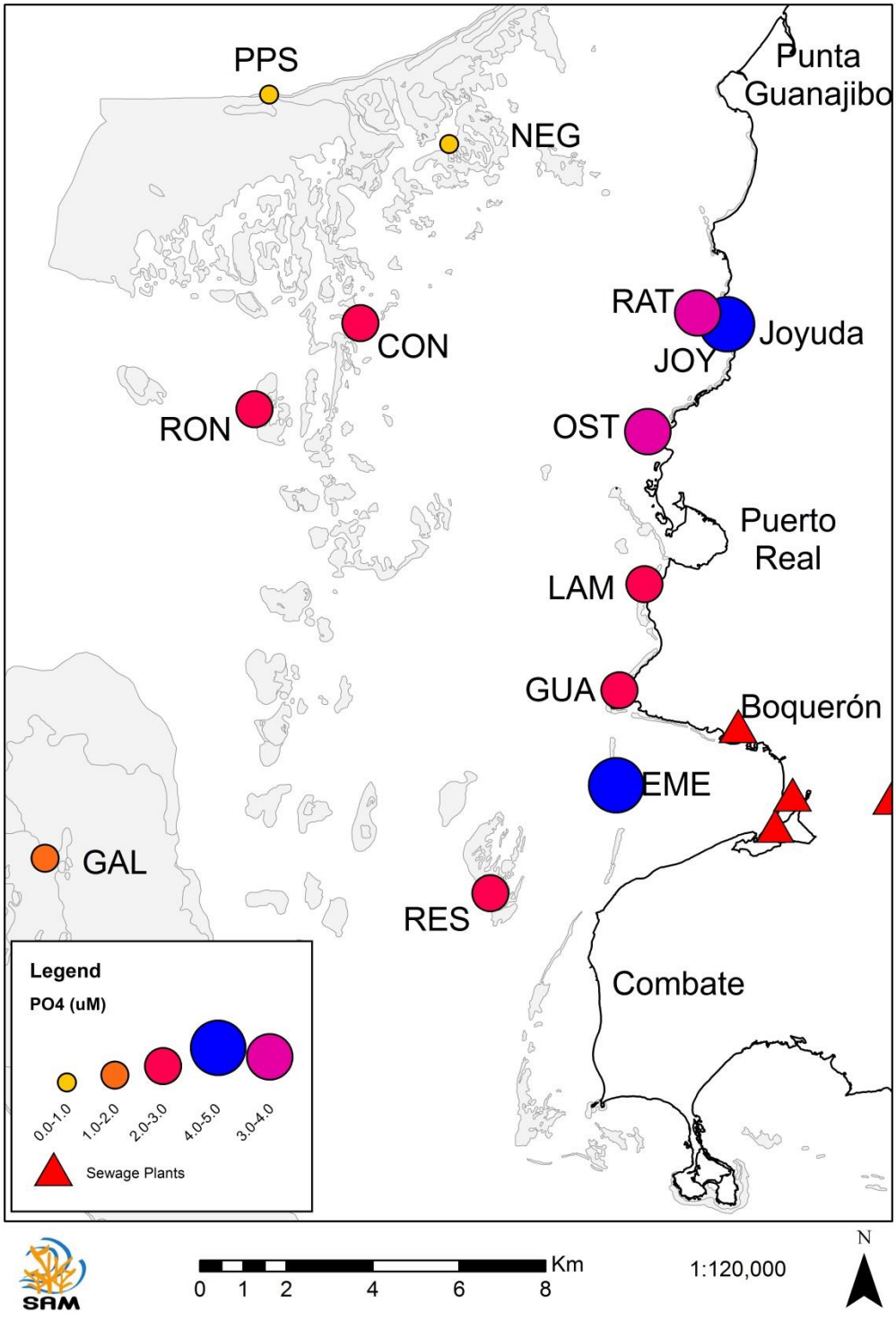

FIGURE 31. Cross-shelf spatial patterns of phosphate (PO_4) concentration.

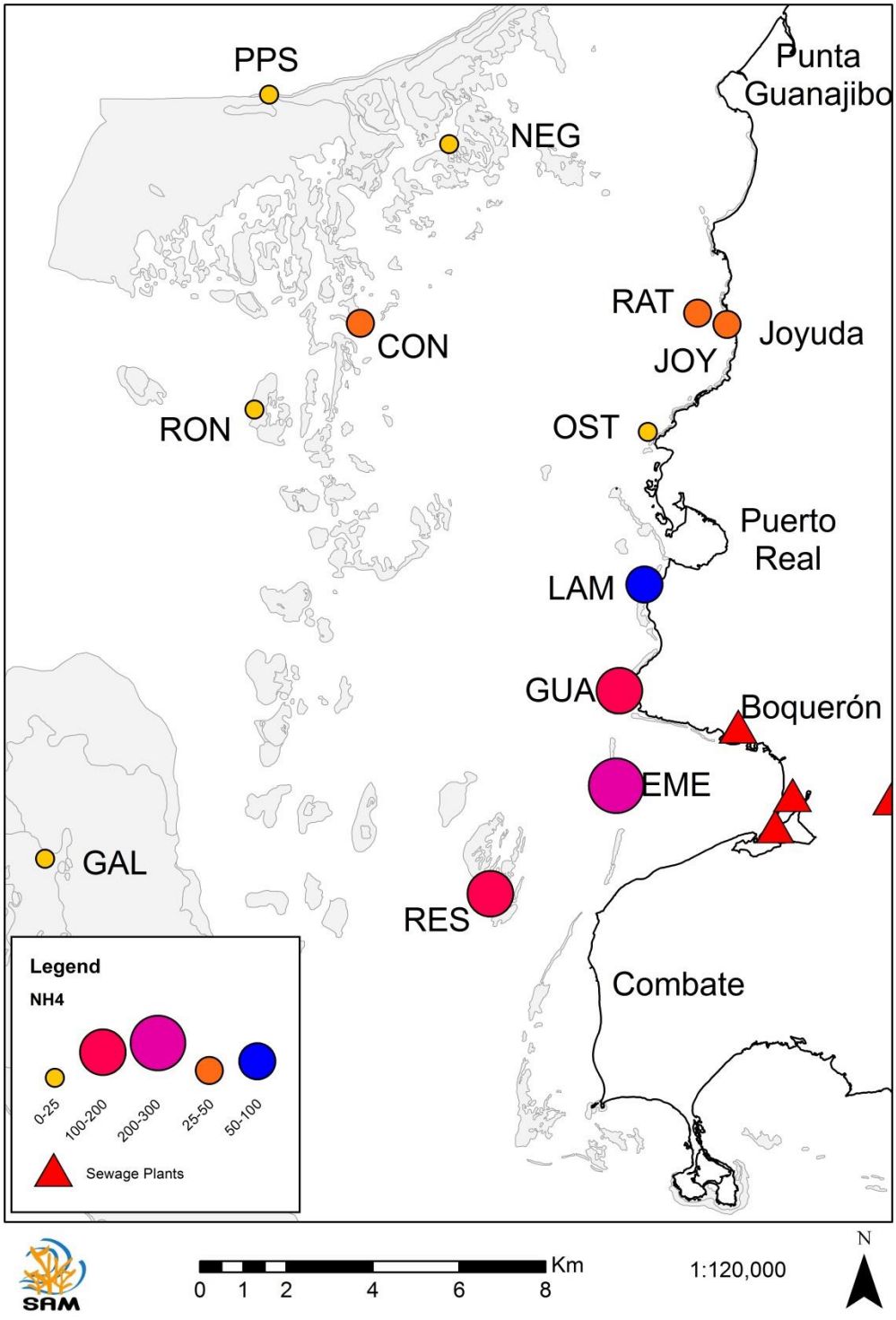

FIGURE 32. Cross-shelf spatial patterns of ionized ammonium (NH_4^+) concentration.

OABs ranged in this study from 16 to 32 ppm across the shelf. These values were similar to those obtained by Díaz-Ortega and Hernández-Delgado (2014) under moderately polluted reef zones, where highly polluted areas showed OAB concentrations ranging from 50 to 200 ppm. Our findings indicated potentially moderate human pollution across shelf-wide scales in western Puerto Rico. PO_4 concentrations ranged from 0.8 to 4.4 μM across the shelf in this study. Lapointe and Clark (1992) suggested that PO_4 concentration on coral reef habitats should not exceed 0.3 μM. Lapointe and Matzie (1996) suggested that any concentration above 1.5 μM would be too high for coral reefs. Our findings suggest that concentrations observed were from 1.7 to 13.7 times higher than the recommended limits for coral reefs. Further, 10 out of the 12 sampled sites (83%) showed PO_4 concentrations that were from 0.3 to 1.9 times higher than the concentration considered unsustainable for coral reefs.

NH_4^+ concentrations in this study ranged from 15 to 260 μM. Lapointe and Clark (1992) suggested that NH_4+ concentrations for coral reefs should not exceed 0.1 μM, and that any concentration above 24 μM were deemed as too high. Our findings are highly concerning as observed NH_4^+ concentrations were from 149 to 2,590 times higher than recommended limits for coral reefs. Eight out the twelve sampled sites (75%) showed NH_4+ concentrations exceeding dangerous NH_4^+ concentrations for coral reefs from 0.02 to 9.8 times.

Regression analyses showed that several water quality indicator parameters showed significant gradients with increasing distance from LBSP. Also, there was a significant relationship among turbidity, PO_4, chlorophyll-a, and dissolved oxygen concentration, implying that increasing water quality degradation significantly affects multiple water quality parameters, therefore adversely impacting coral reefs. In addition, PCO analysis showed a definite shelf-wide LBSP spatial gradient. Although this study just provided a snapshot view of water quality across the western Puerto Rico shelf, results were concerning as critical water quality parameters resulted significantly higher than recommended limits for sustaining coral reef health. These results suggest that human-driven LBSP across the western Puerto Rico shelf is highly significant, it is a large-scale, chronic phenomenon, and deserves full long-term monitoring across large spatial and temporal scales.

B. Coral reef benthic communities

Coral reef benthic community structure showed a highly significant variation among all geographic zones, sites and depth zones, suggesting a strong effect associated to the LBSP gradient and to depth (***Table 2***). A PCO analysis showed that coral reef benthic communities along the western Puerto Rican shelf were clustered in three different groups characterized by different dominant coral taxa (***Figure 33***). A first group was entirely composed of inshore reef sites RAT, OST, LAM and GUA, and was explained by a combination of green and red macroalgae. The second cluster was composed by EME and RES. The former was the farthest offshore coral reef among all inshore sites and the latter was the closest mid-shelf site. Both are located offshore Boquerón Bay (***Figures 1-2***). EME was dominated by octocorals *Pseudoplexaura* spp. and by *Eunicea laxispica*. The third cluster was composed by mid-shelf CON, RON sites and by outer shelf sites NEG, PPS, GAL. PPS was explained by scleractinian coral *Montastraea cavernosa* and octocoral *Gorgonia ventalina*. RON was explained by *Orbicella franksi* and by dominant cyanobacteria *Lyngbya* spp. The remaining sites were explained by scleractinian *Undaria agaricites*. Percent live coral cover showed a significant increase with increasing distance from LBSP (***Figures 34-35***).

TABLE 2. Summary of a three-way PERMANOVA test of benthic community structure

Variable	d.f.	Pseudo-F	*p*
Geographic location	2,254	22.15	<0.0001
Site	10,246	14.04	<0.0001
Depth	3,253	8.02	<0.0001
Location x Site	10,246	14.04	<0.0001
Location x Depth	8,248	9.97	<0.0001
Site x Depth	22,234	8.78	<0.0001
Location x Site x Depth	22,234	8.78	<0.0001

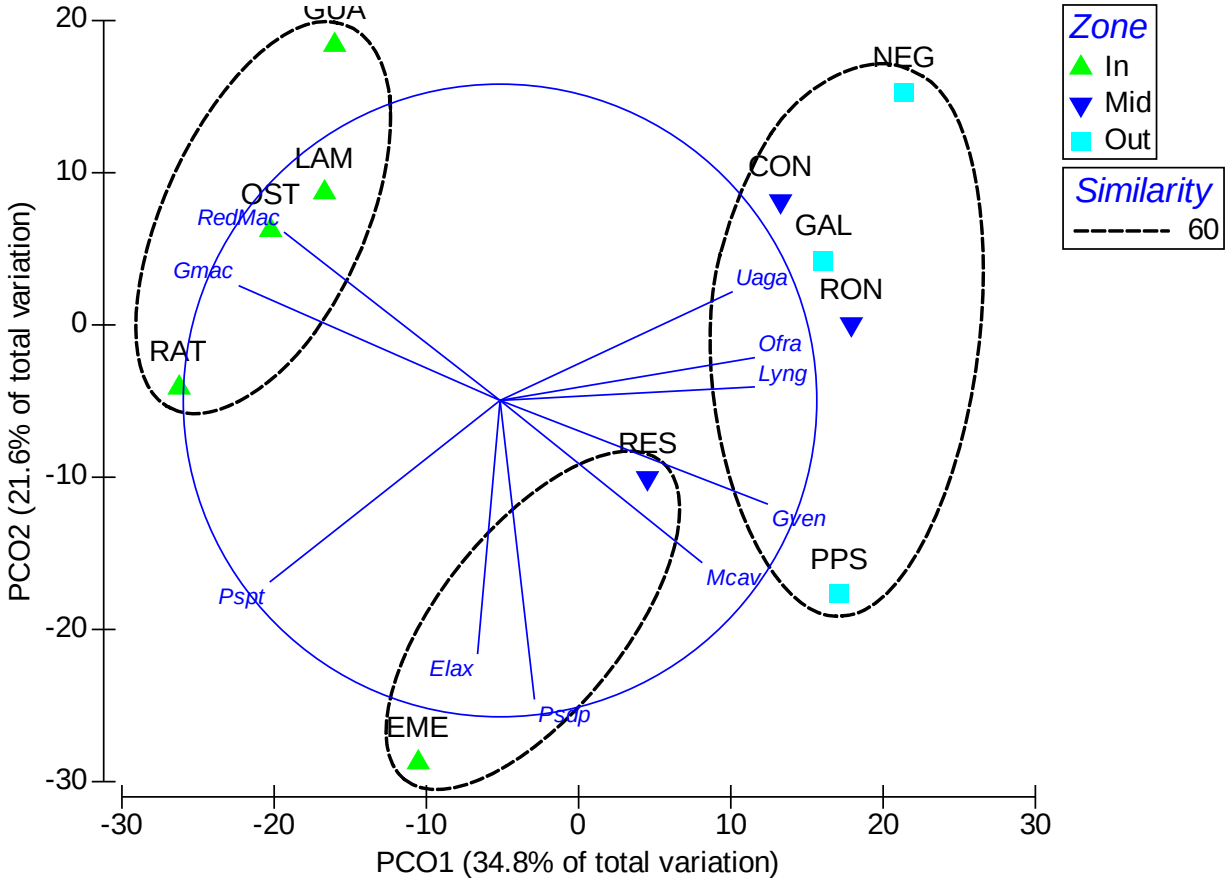

FIGURE 33. Principal component ordination (PCO) of benthic community structure among study sites. Clusters based on a 60% similarity cutoff level. Vectors based on a 0.60 correlation. This model explained 56.4% of the observed variation.

Mean Scleractinian + Hydrocoral species richness increased with increasing distance from the shore, and averaged 2.96/transect across inshore sites, with the lowest value across the 5-10 m depth zone of EME (0.9/transect) and the highest at the <5 m depth zone of GUA (4.0/transect) (***Figure 34***). Mean species richness across mid-shelf sites averaged 6.26/transect, with the lowest value across the <5 m depth zone of CON (3.6/transect) and the highest at the 10-15 m depth zone of RON (9.5/transect). Mean species richness across outer shelf sites averaged 7.13/transect, with the lowest value across the <5 m depth zone of GAL (4.3/transect) and the highest at the 10-15 m depth zone of PPS (8.73/transect).

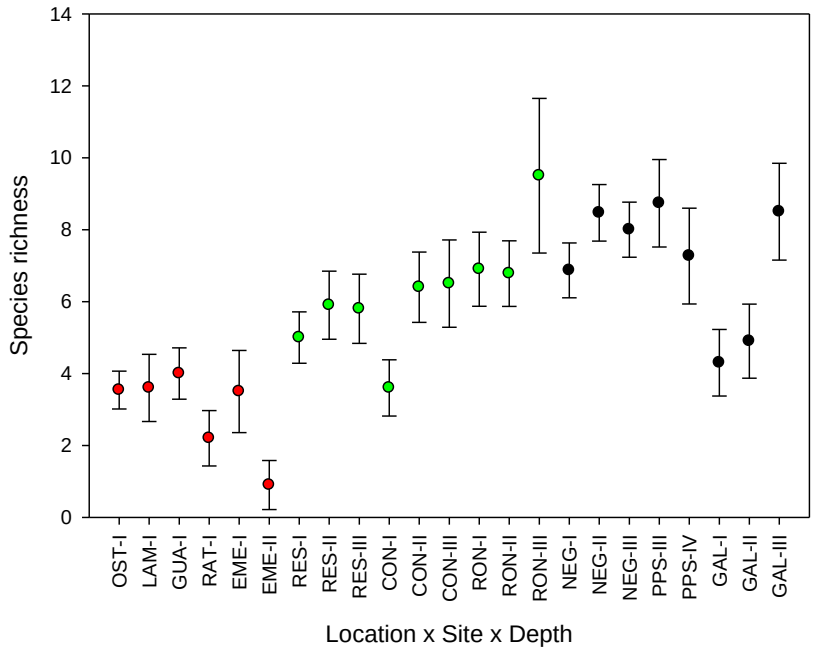

FIGURE 34. Sleractinian + Hydrocoral species richness across sites. Red circles= Inshore sites; Green circles= Mid-shelf sites; Black circles= Outer shelf sites. Mean±95% confidence interval.

Mean coral species diversity (H'n) also increased with increasing distance from the shore, and averaged 0.9156/transect across inshore sites, with the lowest value across the 5-10 m depth zone of EME (0.2367) and the highest at the <5 m depth zone of GUA (1.2648) (***Figure 35***). H'n across mid-shelf sites averaged 1.6626/transect, with the lowest value across the <5 m depth zone of CON (1.1087) and the highest at the 10-15 m depth zone of RON (2.0741). H'n across outer shelf sites averaged 1.7829/transect, with the lowest value across the <5 m depth zone of GAL (1.2519) and the highest at the 10-15 m depth zone of PPS (2.0595).

Mean coral species evenness (J'n) also increased with increasing distance from the shore, and averaged 0.7543/transect across inshore sites, with the lowest value across the 5-10 m depth zone of EME (0.2843) and the highest at the <5 m depth zone of LAM (0.9531) (***Figure 36***). J'n across mid-shelf sites averaged 0.9302/transect, with the lowest value across the <5 m depth zone of CON (0.8302) and the highest at the 10-15 m depth zone of CON (0.9641). J'n across outer shelf sites averaged 0.9345/transect, with the lowest value across the <5 m depth zone of GAL (0.8686) and the highest at the 10-15 m depth zone of PPS (0.9707).

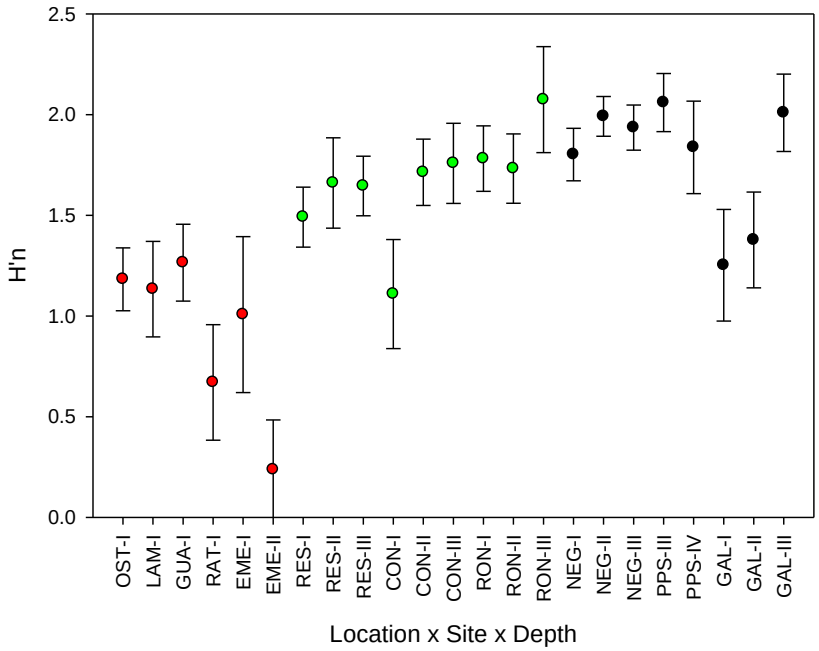

FIGURE 35. Sleractinian + Hydrocoral species diversity index (H'n) across sites. Red circles= Inshore sites; Green circles= Mid-shelf sites; Black circles= Outer shelf sites. Mean±95% confidence interval.

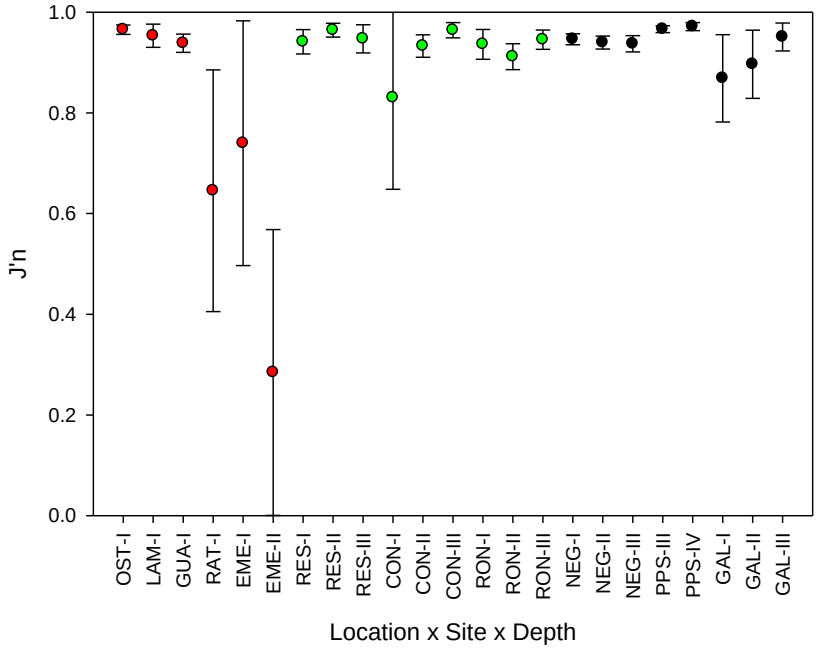

FIGURE 36. Sleractinian + Hydrocoral species diversity index (H'n) across sites. Red circles= Inshore sites; Green circles= Mid-shelf sites; Black circles= Outer shelf sites. Mean±95% confidence interval.

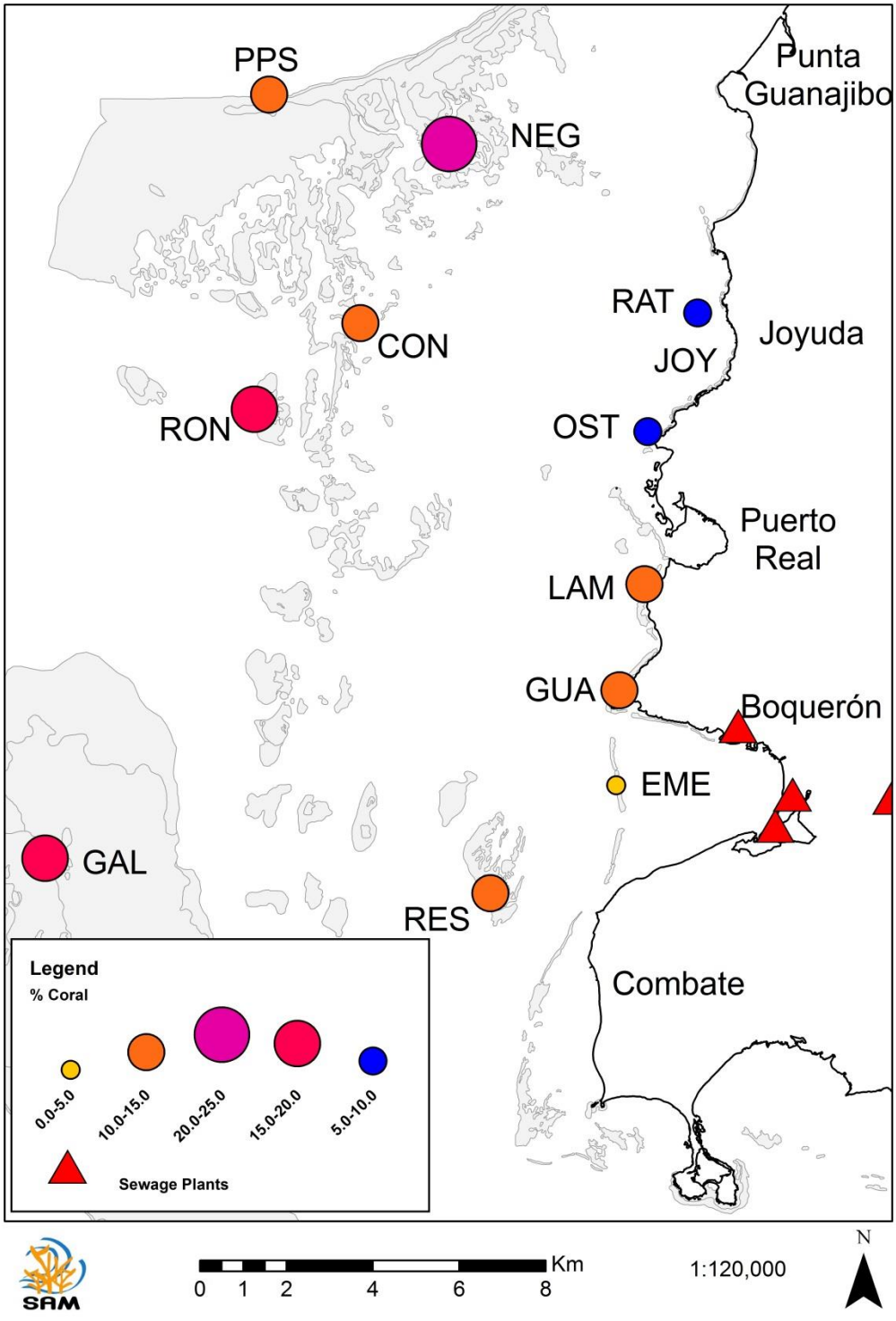

FIGURE 37. Cross-shelf spatial patterns of percent living coral cover.

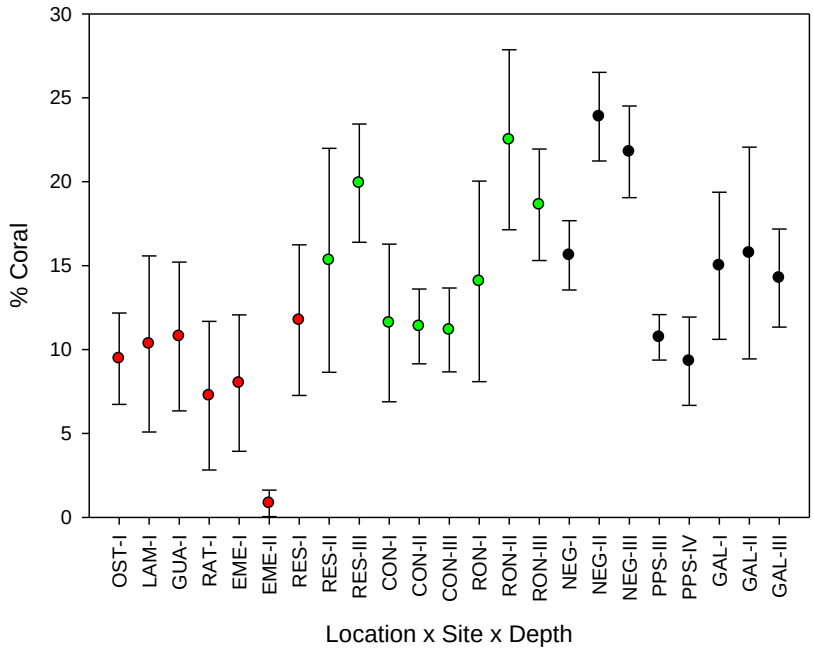

FIGURE 38. Percent living coral cover across sites. Red circles= Inshore sites; Green circles= Mid-shelf sites; Black circles= Outer shelf sites. Mean±95% confidence interval.

Mean percent coral cover increased with increasing distance from the shore (***Figure*** 37), and averaged 7.8% across inshore sites, with the lowest value across the 5-10 m depth zone of EME (0.8%) and the highest at GUA (10.8%) (***Figure 38***). Mean percent cover across mid-shelf sites averaged 15.1%, with the lowest value across the 10-15 m depth zone of CON (11.2%) and the highest at the 5-10 m depth zone of RON (22.5%). Mean percent cover across outer shelf sites averaged 15.8%, with the lowest value across the 15-20 m depth zone of PPS (11.2%) and the highest at the 5-10 m depth zone of NEG (23.9%).

The dominant scleractinian coral at OST was *Siderastrea sidera*, while *Porites porites* was the dominant coral at LAM, *P. astreoides* at GUA, and *Orbicella faveolata* at RAT and the shallow zone of EME (***Figure 39***). The dominant coral at EME deeper zone was also *O. faveolata*, while *P. astreoides* was dominant at RES shallow and middle depth zones. *Orbicella faveolata* was the most common coral across the deeper zone at RES. *Porites astreoides* was the most common coral across all depth zones at CON, while *O. faveolata* was the most abundant at the shallow and middle depth zones a RON.

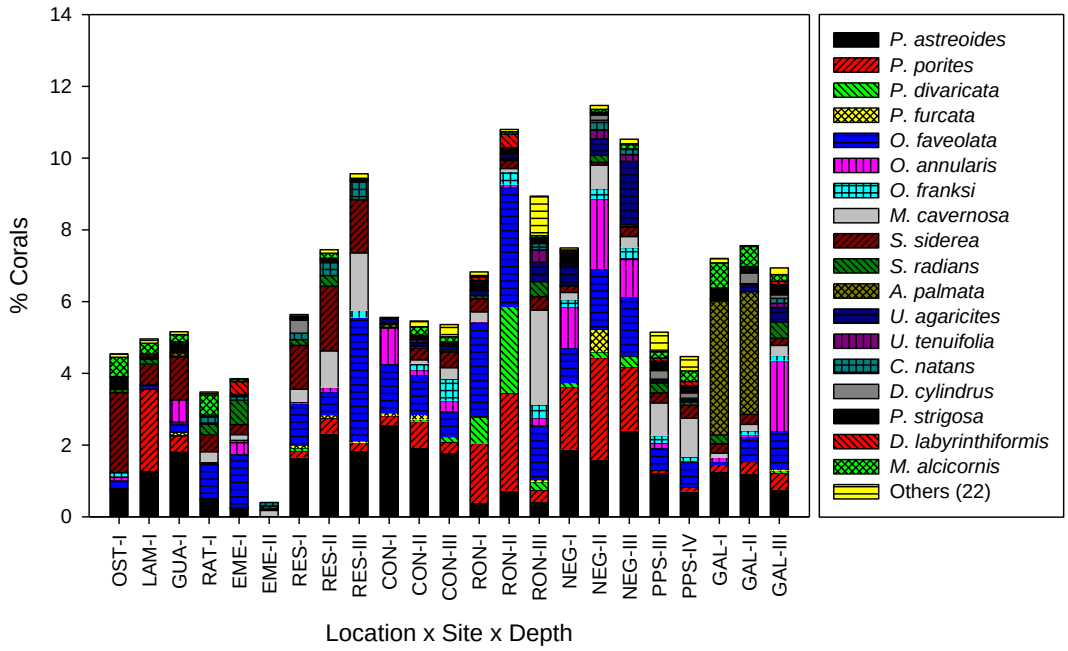

FIGURE 39. Percent relative cover of the most abundant Scleractinian corals + Hydrocorals.

Montastraea cavernosa was dominant across deeper zones at RON. *Porites astreoides* was the most abundant species across the shallower and deeper zones at NEG, while *P. porites* was the dominant scleractinian at the middle depth zones at NEG. *Porites astreoides* was the most common species at the 10-15 m zone and *M. cavernosa* at the 15-20 m depth zone at PPS. *Acropora palmata* was the most common species at the shallower and middle depth zone at GAL, while *O. annularis* was the dominant scleractinian species across the deeper zone at GAL.

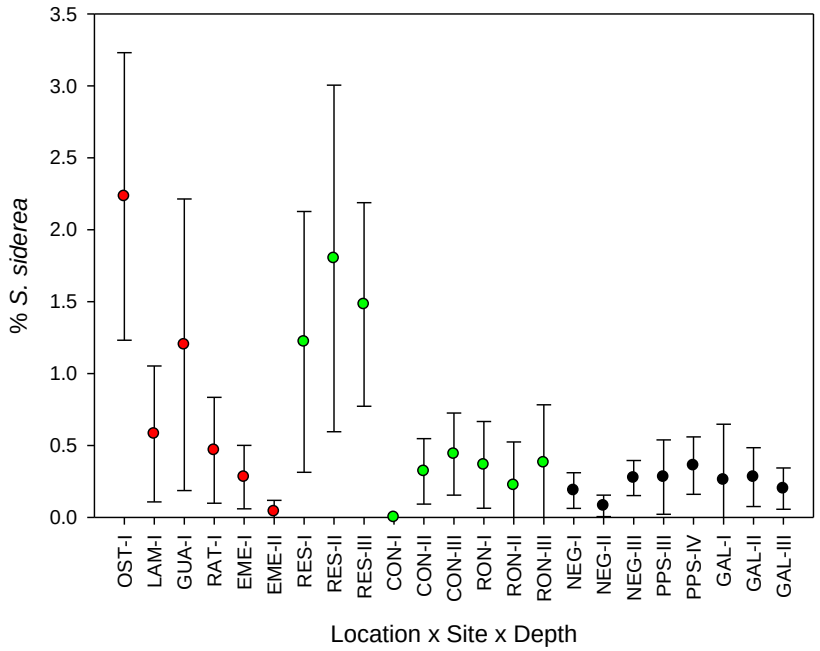

FIGURE 40. Percent cover of *Siderastrea siderea* across sites. Red circles= Inshore sites; Green circles= Mid-shelf sites; Black circles= Outer shelf sites. Mean±95% confidence interval.

Several scleractian coral species show particular spatial patterns that may evidence chronic impacts by LBSP, including high turbidity, high sedimentation rates and eutrophication. For instance, *Siderastrea siderea*, which is a coral commonly found across turbid conditions, was more frequently documented across some of the inshore sites and across RES, which was the most adjacent to shore of the mid-shelf sites (***Figure 40***). These sites resulted with higher turbidity and dissolved nutrient levels. *Montastraea cavernosa* was more abundant at the deeper zone of RON and at the middle depth and deeper zone of RES (***Figure 41***). It was also abundant at PPS. *Undaria* agaricites, in contrast, was absent from inshore sites and was more abundant at NEG, particularly on deeper zones (***Figure 42***). Threatened Elkhorn coral, *Acropora palmata*, was nearly absent across all sites, with the exception of the shallower and mid-shelf zones of Arrecife Gallardo (***Figure 43***). Threatened *Orbicella annularis* was overall more abundant across outer shelf reefs, particularly at NEG and at the deeper zone of GAL (***Figure 44***). Threatened *O. faveolata* was more abundant across mid-shelf reefs, particularly at the deeper zone of RES and at the shallow and middle zones of RON (***Figure 45***). Threatened *Dendrogyra cylindrus* was overall rare across range, but more common across outer shelf reefs (***Figure 46***).

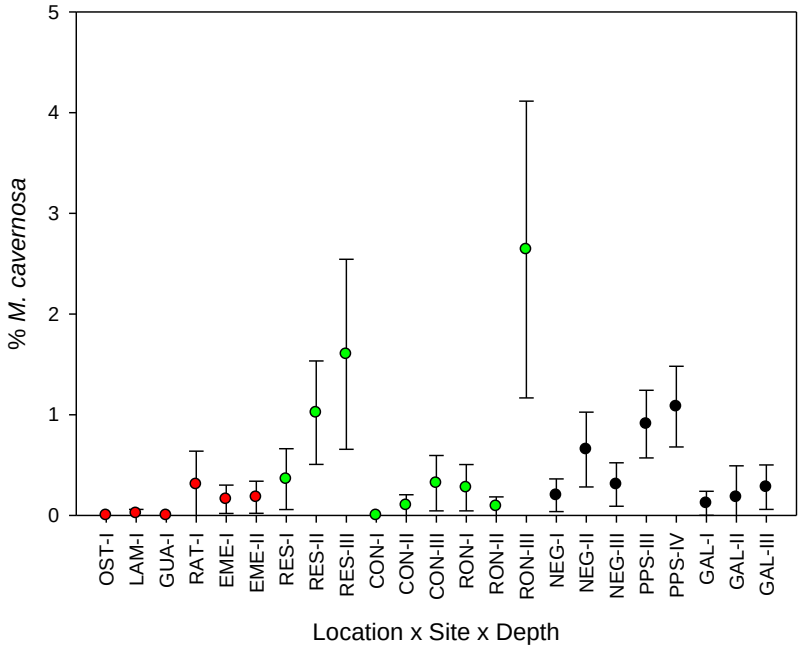

FIGURE 41. Percent cover of *Montastraea cavernosa* across sites. Red circles= Inshore sites; Green circles= Mid-shelf sites; Black circles= Outer shelf sites. Mean±95% confidence interval.

Several scleractian coral species show particular spatial patterns that may evidence chronic impacts by LBSP, including high turbidity, high sedimentation rates and eutrophication. For instance, *Siderastrea siderea*, which is a coral commonly found across turbid conditions, was more frequently documented across some of the inshore sites and across RES, which was the most adjacent to shore of the mid-shelf sites (***Figure 37***). These sites resulted with higher turbidity and dissolved nutrient levels. *Montastraea cavernosa* was more abundant at the deeper zone of RON and at the middle depth and deeper zone of RES (***Figure 38***). It was also abundant at PPS. *Undaria* agaricites, in contrast, was absent from inshore sites and was more abundant at NEG, particularly on deeper zones (***Figure 39***). Threatened Elkhorn coral, *Acropora palmata*, was nearly absent across all sites, with the exception of the shallower and mid-shelf zones of Arrecife Gallardo (***Figure 40***). Threatened *Orbicella annularis* was overall more abundant across outer shelf reefs, particularly at NEG and at the deeper zone of GAL (***Figure 41***). Threatened *O. faveolata* was more abundant across mid-shelf reefs, particularly at the deeper zone of RES and at the shallow and middle zones of RON (***Figure 42***). Threatened *Dendrogyra cylindrus* was overall rare across range, but more common across outer shelf reefs (***Figure 43***).

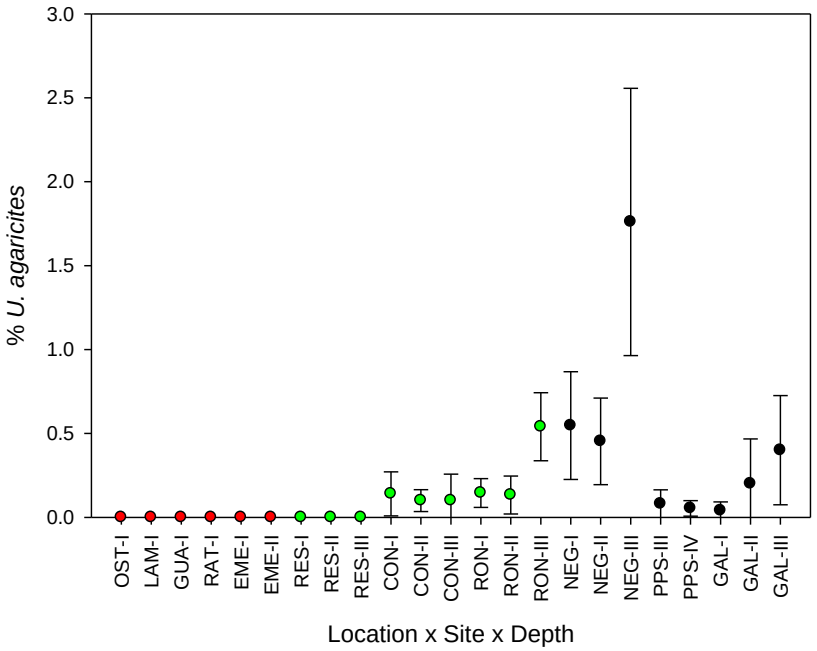

FIGURE 42. Percent cover of *Undaria agaricites* across sites. Red circles= Inshore sites; Green circles= Mid-shelf sites; Black circles= Outer shelf sites. Mean±95% confidence interval.

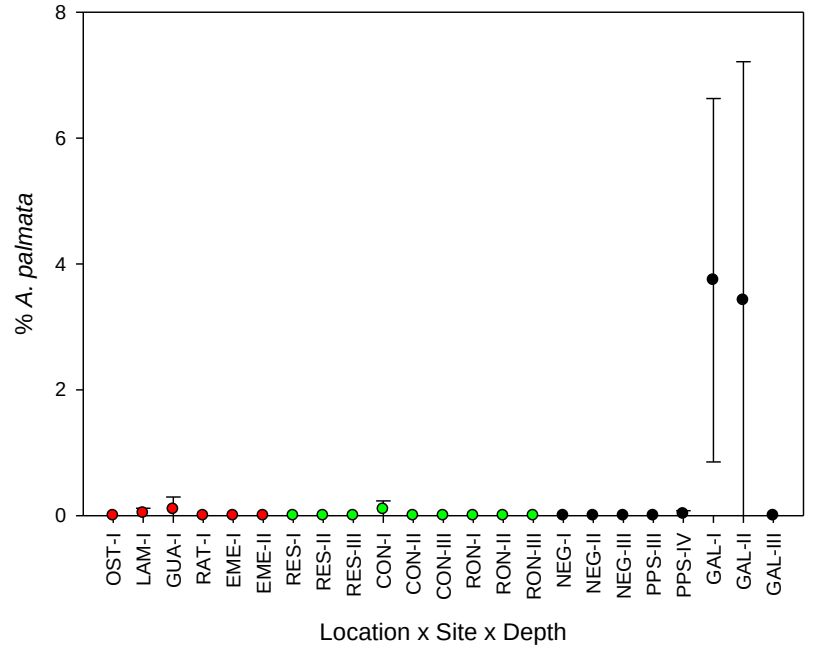

FIGURE 43. Percent cover of E.S.A.-listed *Acropora palmata* across sites. Red circles= Inshore sites; Green circles= Mid-shelf sites; Black circles= Outer shelf sites. Mean±95% confidence interval.

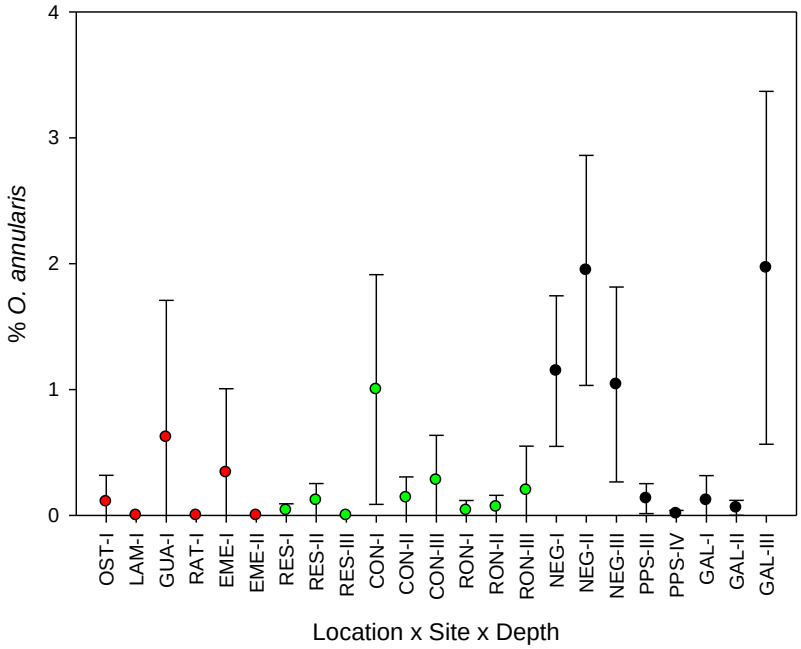

FIGURE 44. Percent cover of E.S.A.-listed *Orbicella annularis* across sites. Red circles= Inshore sites; Green circles= Mid-shelf sites; Black circles= Outer shelf sites. Mean±95% confidence interval.

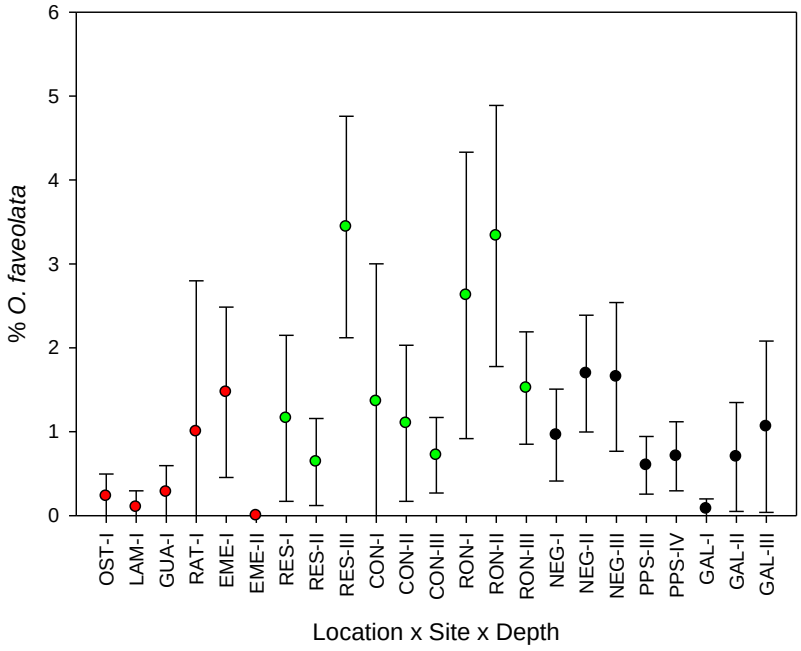

FIGURE 45. Percent cover of E.S.A.-listed *Orbicella faveolata* across sites. Red circles= Inshore sites; Green circles= Mid-shelf sites; Black circles= Outer shelf sites. Mean±95% confidence interval.

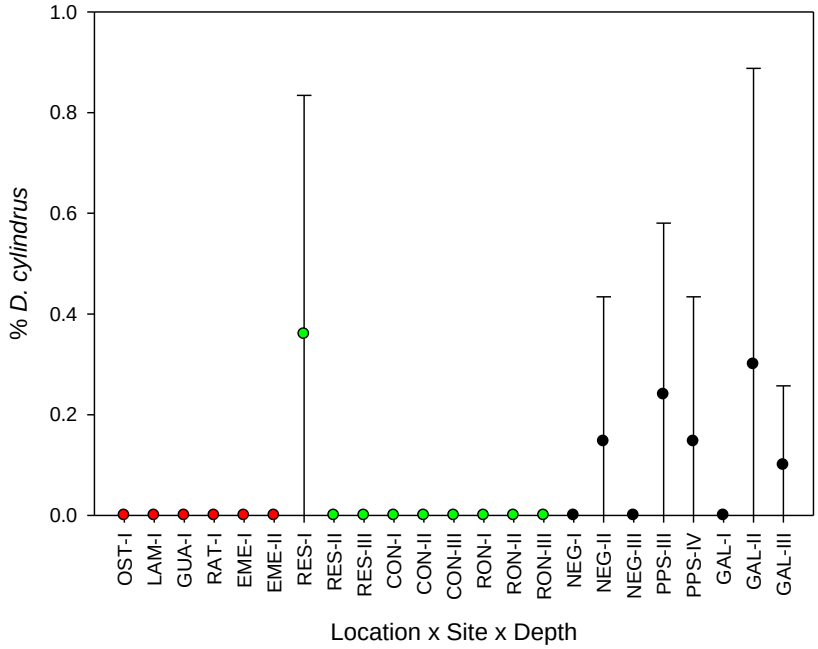

FIGURE 46. Percent cover of E.S.A.-listed *Dendrogyra cylindrus* across sites. Red circles= Inshore sites; Green circles= Mid-shelf sites; Black circles= Outer shelf sites. Mean±95% confidence interval.

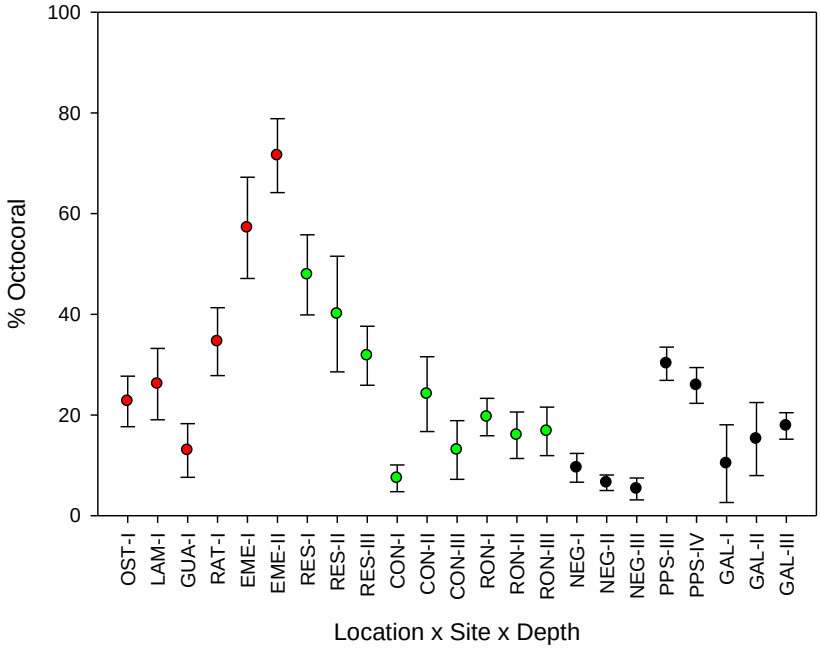

FIGURE 47. Percent octocoral cover across sites. Red circles= Inshore sites; Green circles= Mid-shelf sites; Black circles= Outer shelf sites. Mean±95% confidence interval.

Percent octocoral cover was significantly higher within shallower inshore sites subjected to stronger influences by LBSP (***Figure 47***). Mean percent cover across inshore sites averaged 37.5%, with the lowest value across the 5-10 m depth zone of GUA (13.0%) and the two highest values at the EME <5 m zone (57.1%) and its 5-10 m zone (71.5%). Highly degraded coral reefs show a massive loss of living Scleractinian corals. Substrates were then largely occupied by opportunist octocoral taxa. Mean percent octocoral cover across mid-shelf sites averaged 24.0%, with the lowest value across the <5 m depth zone of CON (7.4%), the farthest mid-shelf site, and the highest two values at the 5-10 m depth zone of RES (40.0%) and its 5-10 m depth zone (47.8%). RES was the closest mid-shelf site, adjacent to polluted Boquerón Bay. Mean percent cover across outer shelf sites averaged 15.1%, with the lowest value across the 5-10 m depth zone of GAL (10.3%) and the highest at the 10-15 m depth zone of PPS (30.1%), followed by its 15-20 m depth zone across the upper vertical wall (25.6%). These results point out at the natural dominance of octocoral communities at shallower inshore sites, as well as across deeper shelf edge PPS site subjected to strong circulation. But also highlight the natural dominance of octocorals on largely degraded habitats.

The most dominant octocoral species across the inshore sites was *Pseudopterogorgia* spp., followed by *P. americana* (***Figure 48***). These sites were highly influenced by LBSP. *Pseudopterogorgia* spp. was also common across the mid-shelf RES mid-shelf site. They were also common across other mid-shelf sites, but other species were also common, including *Gorgonia ventalina*, *Pseudoplexaura* spp., *Eunicea* spp. *Briareum asbestinum*, and the opportunist species *Erythropodium caribbaeorum*. These species were also common at the outer shelf sites, but deeper habitats at mid-shelf NEG and wall habitats at PPS also showed abundant red octocoral *Icilligorgia shrammi*. Black corals were also abundant at the PPS deeper wall (20-30 m), but colonies were located just below surveyed transects. But *Pseudopterogorgia* spp. (***Figure 49***), *P. americana* (***Figure 50***), and *E. caribbaeorum* (***Figure 51***) showed a significant increase in abundance across highly disturbed sites, most of them inshore and adjacent to LBSP.

Percent sponge cover averaged 1.4% across inshore sites, with the lowest value at OST (0.06%) and the highest at the EME 5-10 m zone (3.3%) (***Figure 52***). Mean percent sponge cover across mid-shelf sites was 2.9%, with the lowest value at the <5 m depth zone of RON (0.6%), and the highest at the 5-10 m depth zone of RES (6.2%). Mean percent sponge cover across the outer shelf site was 2.2%, with the lowest value at the <5 m depth zone of GAL (0.5%), and the

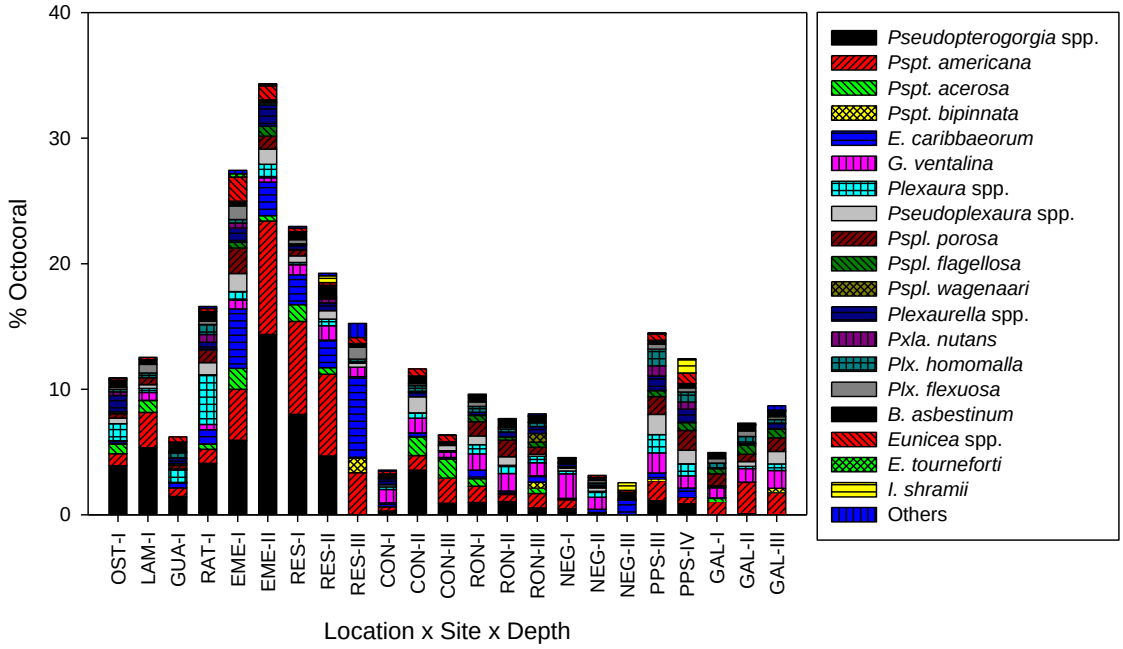

FIGURE 48. Percent relative cover of the most abundant octocorals.

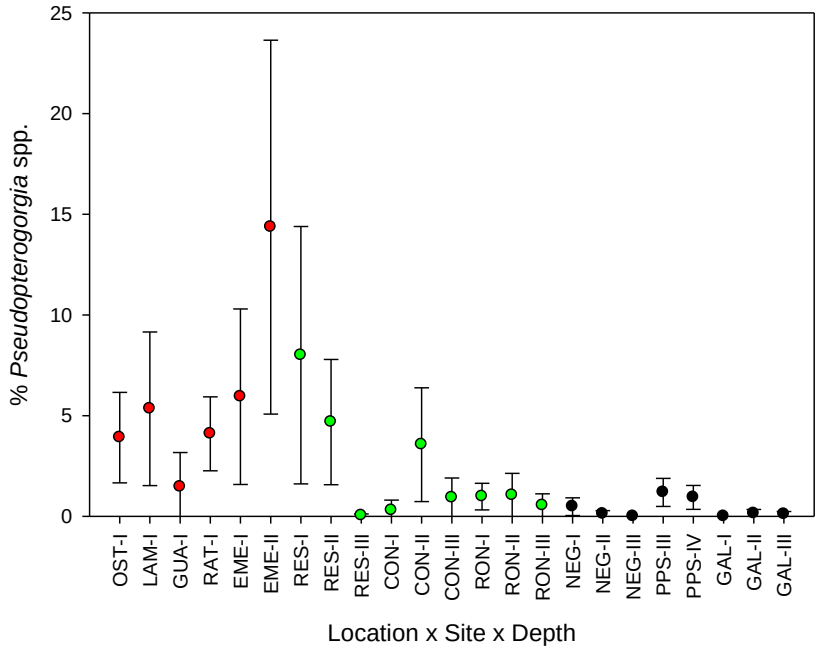

FIGURE 49. Percent cover of *Pseudopterogorgia* spp. across sites. Red circles= Inshore sites; Green circles= Mid-shelf sites; Black circles= Outer shelf sites. Mean±95% confidence interval.

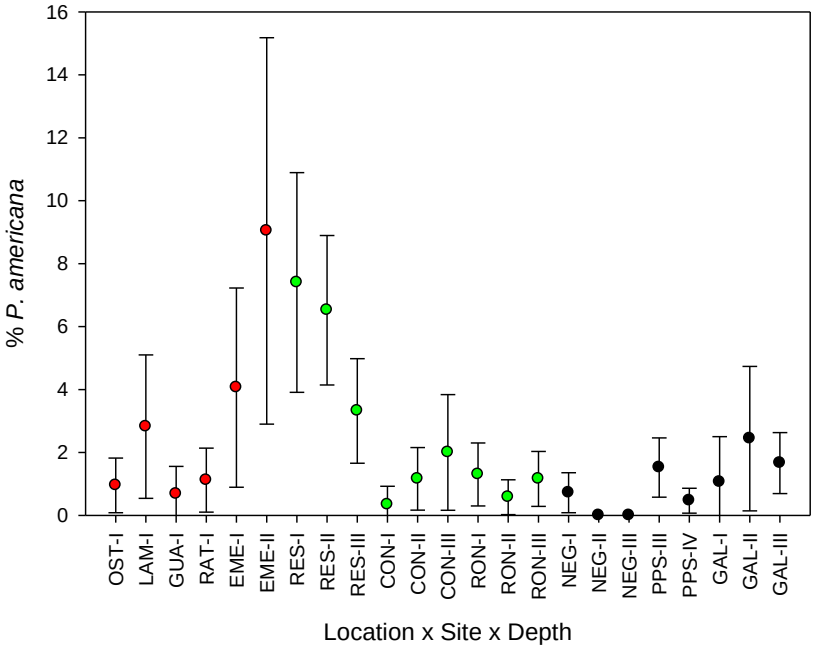

FIGURE 50. Percent cover of *Pseudopterogorgia americana* across sites. Red circles= Inshore sites; Green circles= Mid-shelf sites; Black circles= Outer shelf sites. Mean±95% confidence interval

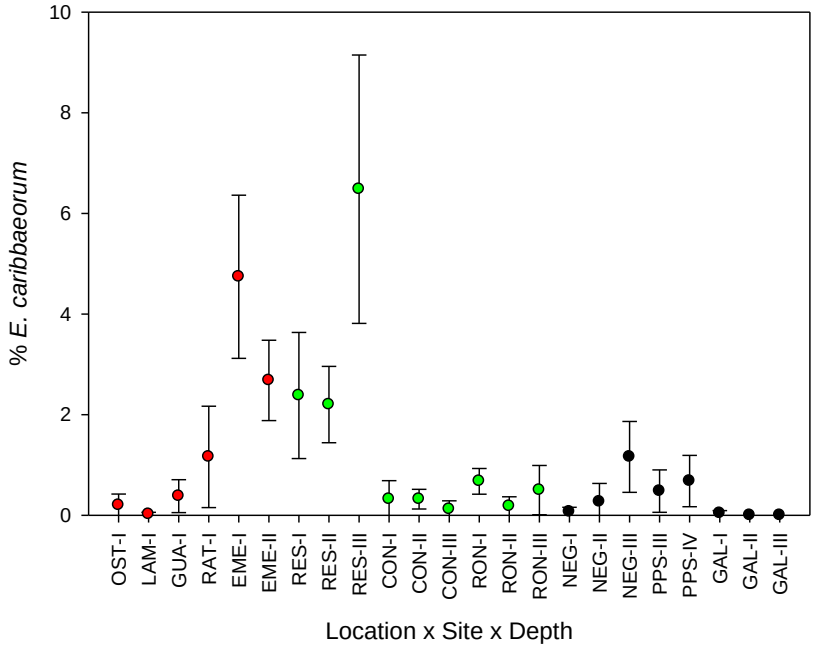

FIGURE 51. Percent cover of *Erythropodium caribbaeorum* across sites. Red circles= Inshore sites; Green circles= Mid-shelf sites; Black circles= Outer shelf sites. Mean±95% confidence interval.

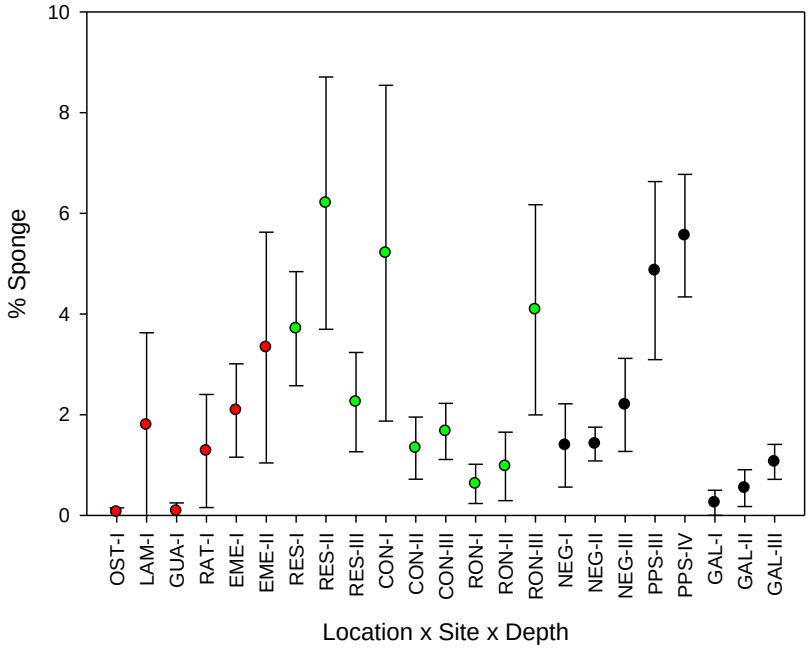

FIGURE 52. Percent sponge cover across sites. Red circles= Inshore sites; Green circles= Mid-shelf sites; Black circles= Outer shelf sites. Mean±95% confidence interval.

highest value at the 15-20 m deep upper wall segment of PPS (5.6%). This site in particular showed also a very high abundance of the giant Barrel sponge, *Xestospongia muta*.

Percent macroalgal cover showed marked differences in cover and species composition across the shelf (***Figures 53-54***). Mean % macroalgal cover was 14.7% across inshore sites, with a minimum value of 1.7% at the 5-10 m depth zone of EME (in the understory below a huge % gorgonian cover) and a highest value at the <5 m depth zone of OST with 32.7%. Mean % macroalgal cover was 4.4% across mid-shelf sites, with a minimum value of 0.5% at the 10-15 m depth zone of CON and a highest value at the 10-15 m zone of RES with 10.3%. Mean % macroalgal cover was 18.5% across outer shelf sites, with a minimum value of 8.5% at the <5 m depth zone of GAL and a highest value at the 10-15 m zone of GAL with 29.1%. Macroalgal species composition varied from site to site (***Figure 55***). Brown and green macroalgae of multiple mixed species were dominant across inshore sites. Brown macroalgae *Dictyota* spp. were dominant across mid-shelf and outer shelf sites. Brown macroalgae *Lobophora variegate* was also dominant, particularly at deeper outer shelf sites.

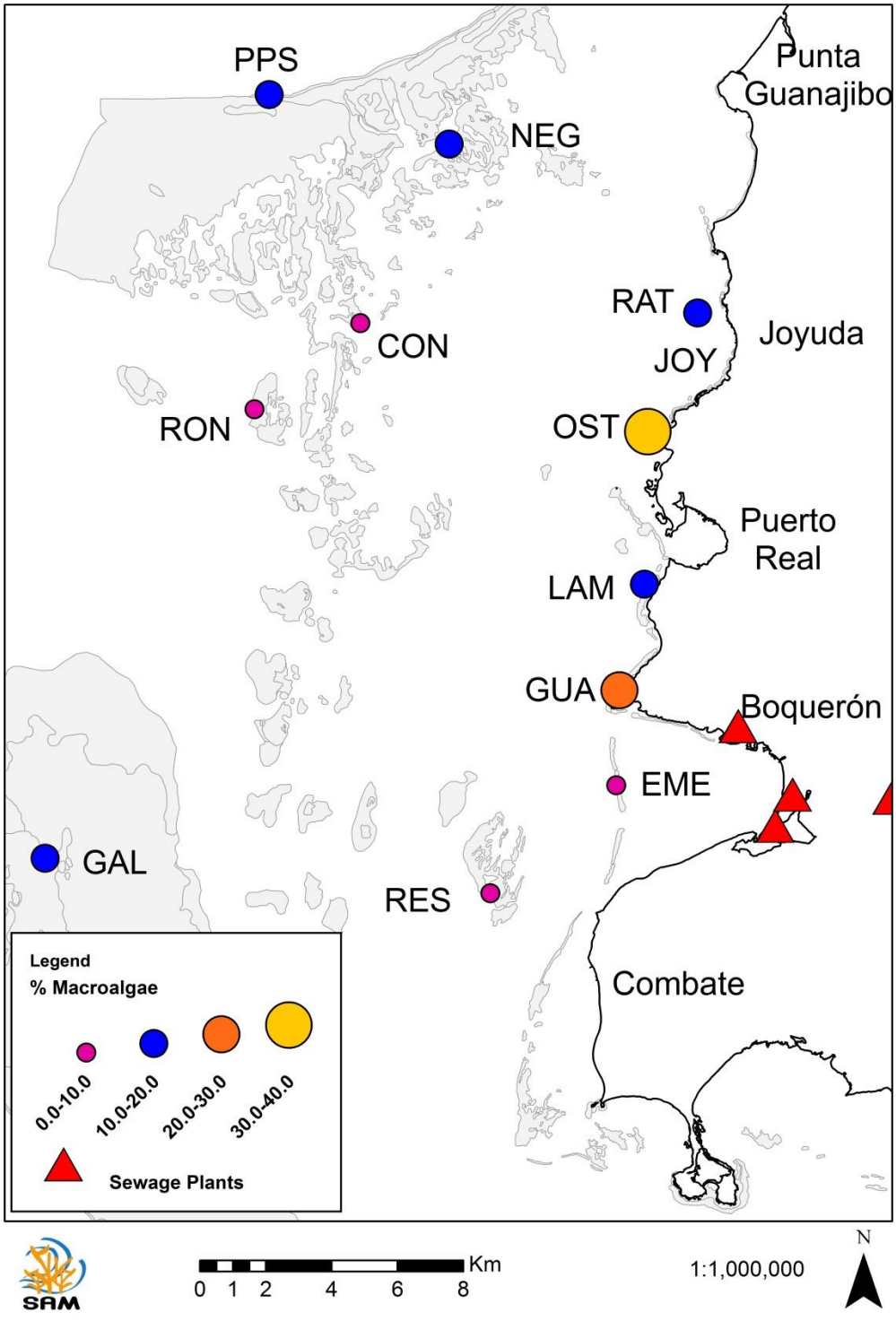

FIGURE 53. Cross-shelf spatial patterns of percent macroalgal cover.

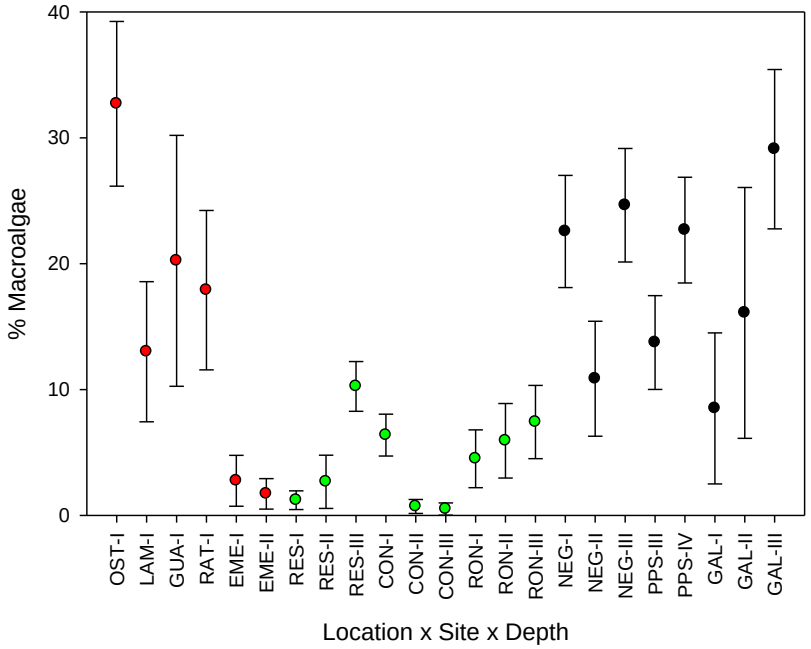

FIGURE 54. Percent macroalgal cover across sites. Red circles= Inshore sites; Green circles= Mid-shelf sites; Black circles= Outer shelf sites. Mean±95% confidence interval.

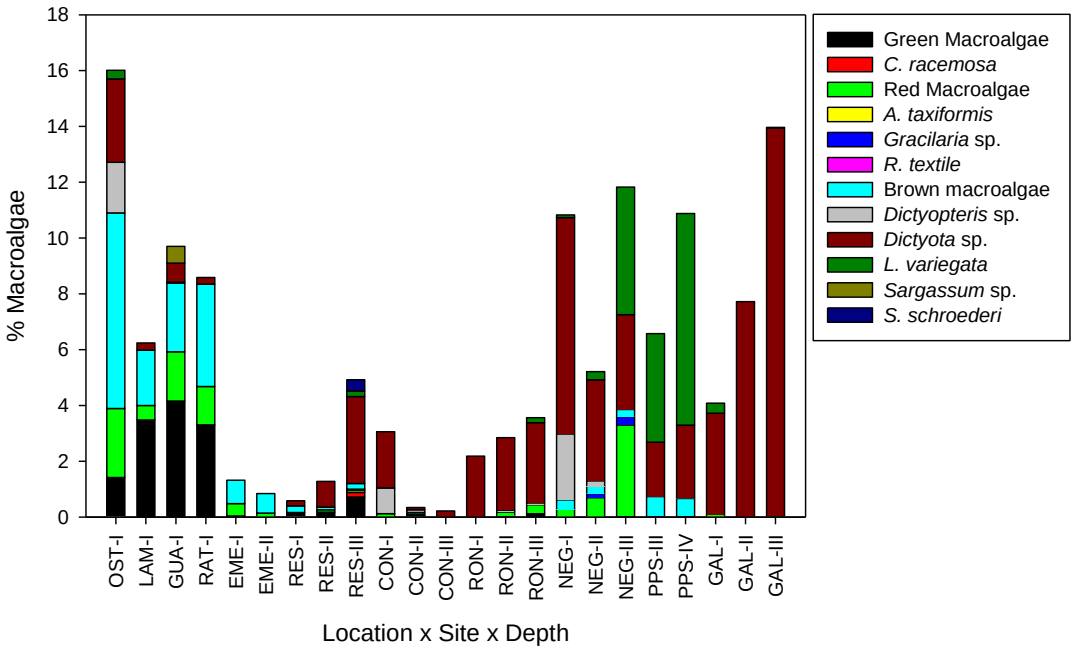

FIGURE 55. Percent relative macroalgal cover across sites. Red circles= Inshore sites; Green circles= Mid-shelf sites; Black circles= Outer shelf sites. Mean±95% confidence interval.

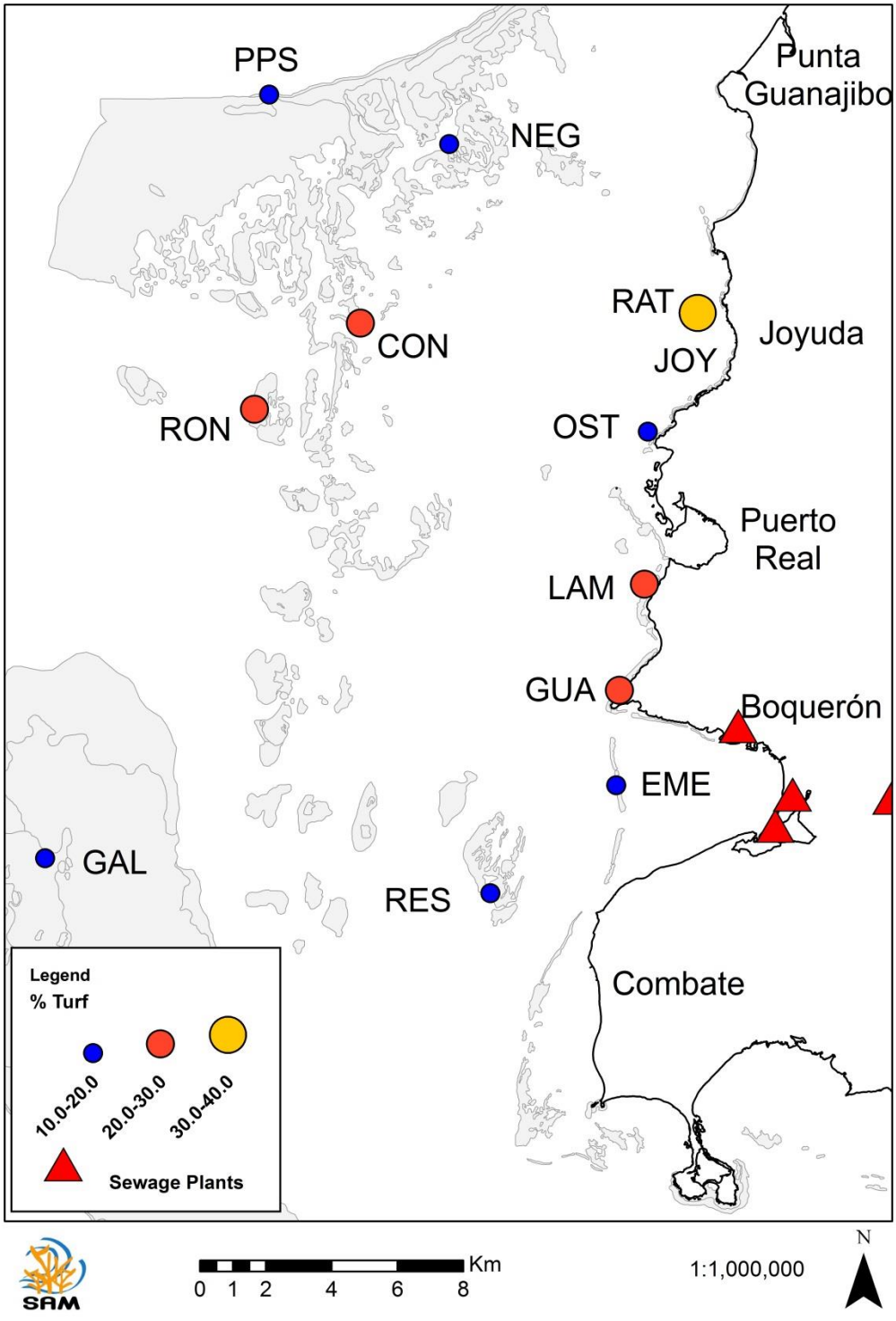

FIGURE 56. Cross-shelf spatial patterns of percent algal turf cover.

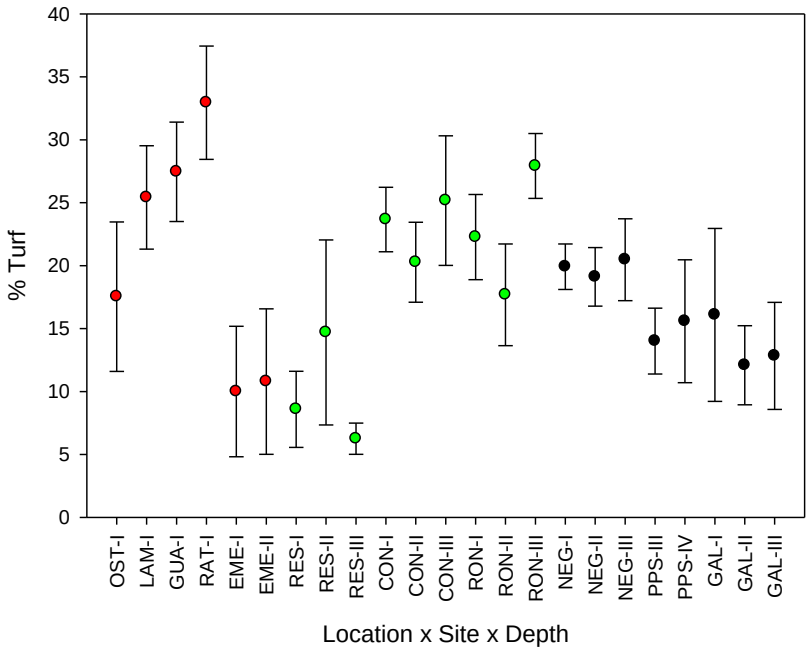

FIGURE 57. Percent algal turf cover across sites. Red circles= Inshore sites; Green circles= Mid-shelf sites; Black circles= Outer shelf sites. Mean±95% confidence interval.

Percent algal turf cover showed also marked differences in cover across the shelf (***Figures 56-57***). Mean % algal turf cover was 20.7% across inshore sites, with a minimum value of 10.0% at the <5 m depth zone of EME and a highest value at the <5 m depth zone of RAT with 32.9%. Mean % algal turf cover was 18.5% across mid-shelf sites, with a minimum value of 6.3% at the 10-15 m depth zone of RES and a highest value at the 10-15 m zone of RON with 27.9%. Mean % algal turf cover was 16.3% across outer shelf sites, with a minimum value of 12.1% at the 10-15 m depth zone of PPS and a highest value at the 5-10 m zone of NEG with 20.5%.

Percent *Halimeda* spp. cover showed also high variation among sites (***Figures 58-59***). Mean % *Halimeda* spp. cover was 5.5% across inshore sites, with a minimum value of 0.04% at the <5 m depth zone of EME and a highest value at the <5 m depth zone of GUA with 8.9%. Mean % *Halimeda* spp. cover was 10.0% across mid-shelf sites, with a minimum value of 0.5% at the 10-15 m depth zone of RON and a highest value at the <5 m zone of CON with 19.6%. Mean % *Halimeda* spp. cover was 3.0% across outer shelf sites, with a minimum value below 0.2% at the 15-20 m depth zone of PPS and a highest value at the 5-10 m zone of NEG with 7.1%.

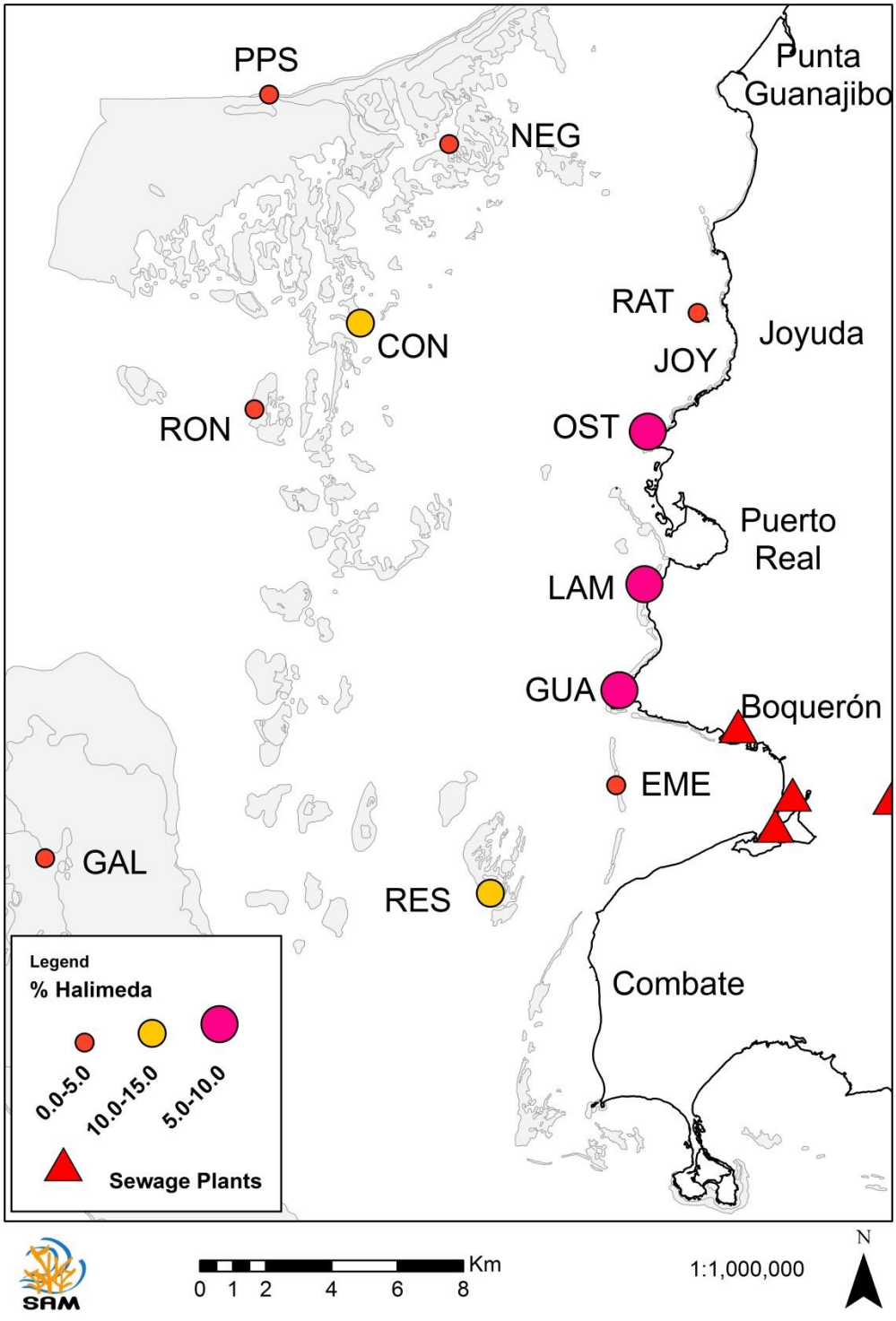

FIGURE 58. Cross-shelf spatial patterns of percent *Halimeda* spp. cover.

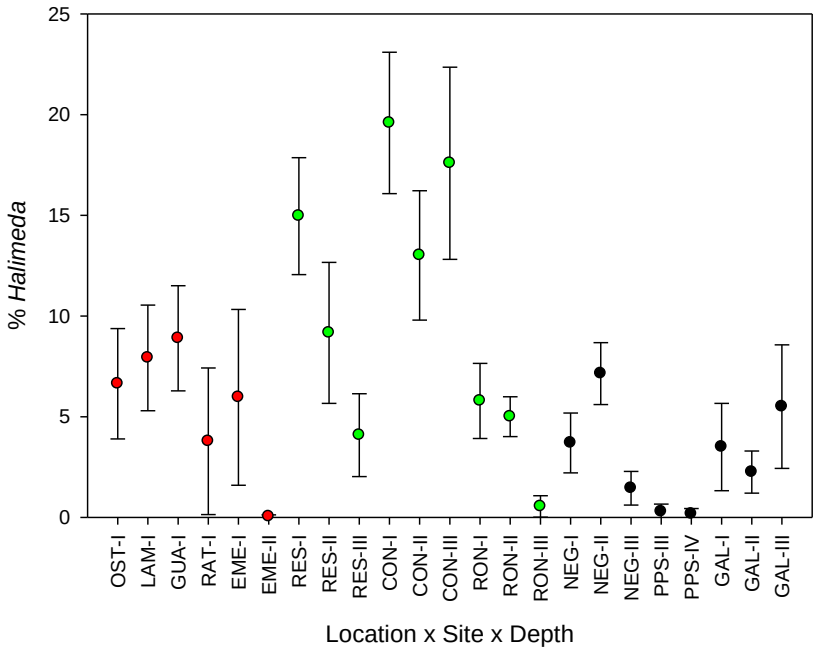

FIGURE 59. Percent *Halimeda* spp. cover across sites. Red circles= Inshore sites; Green circles= Mid-shelf sites; Black circles= Outer shelf sites. Mean±95% confidence interval.

Percent crustose coralline algae (CCA) cover increased with distance from LBSP (***Figures 60-61***). Mean % CCA cover was 0.7% across inshore sites, with a highest value of only 1.6% at the <5 m depth zone of GUA and absent at the <5 m depth zone of both, EME and RAT. Mean % CCA cover was 1.6% across mid-shelf sites, with a minimum value of 0.1% at the 10-15 m depth zone of CON and a highest value at the <5 m zone of CON with 6.8%. Mean % CCA cover was 5.7% across outer shelf sites, with a minimum value below 1.1% at the 10-15 m depth zone of PPS and a highest value at the <5 m zone of GAL with 15.7%. *Porolithon pachydermum* was the most dominant CCA species across the entire shelf among at least five identified species (***Figure 62***). Erect calcareous algae (ECA), particularly *Jania*, showed a limited distribution.

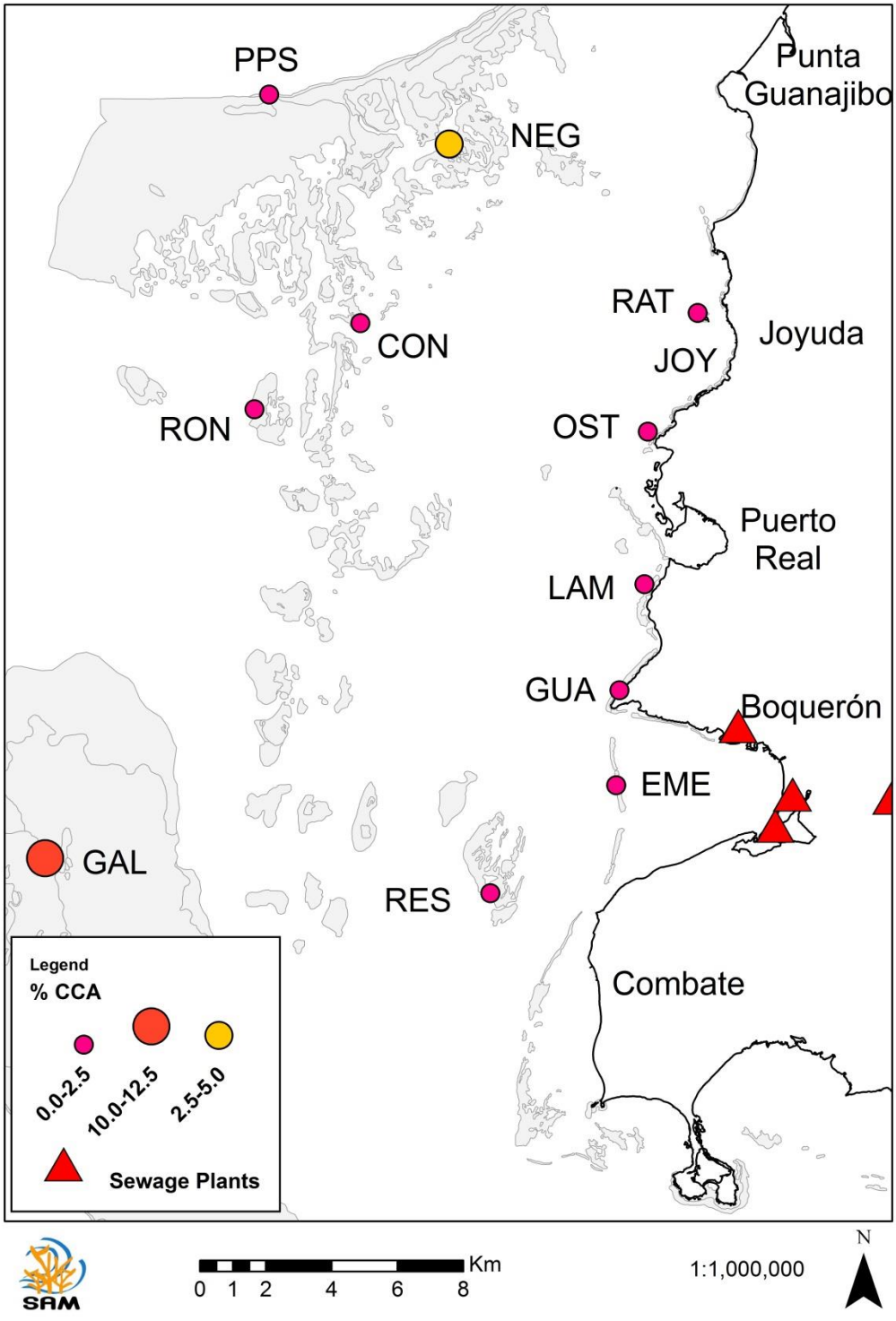

FIGURE 60. Cross-shelf spatial patterns of percent crustose coralline algal (CCA) cover.

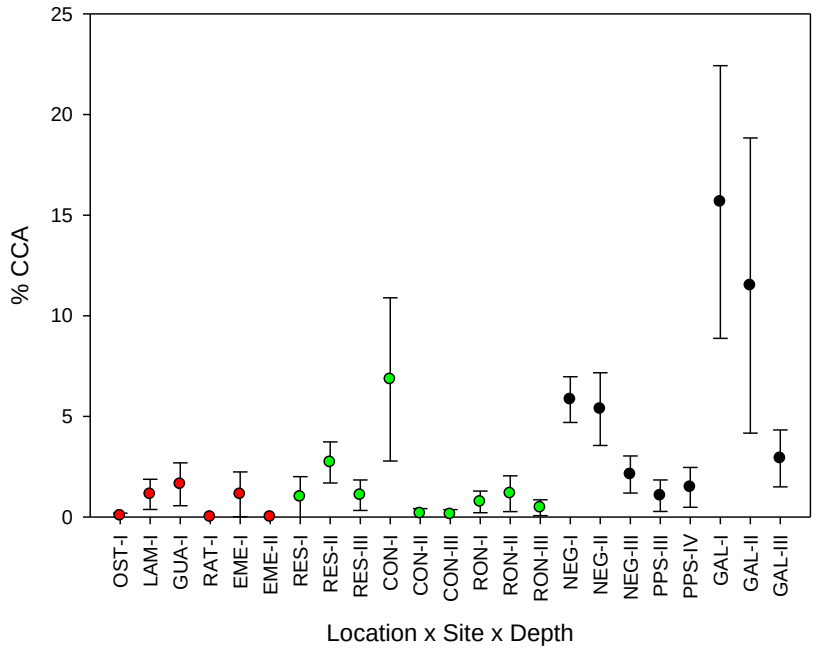

FIGURE 61. Percent crustose coralline algal (CCA) cover across sites. Red circles= Inshore sites; Green circles= Mid-shelf sites; Black circles= Outer shelf sites. Mean±95% confidence interval.

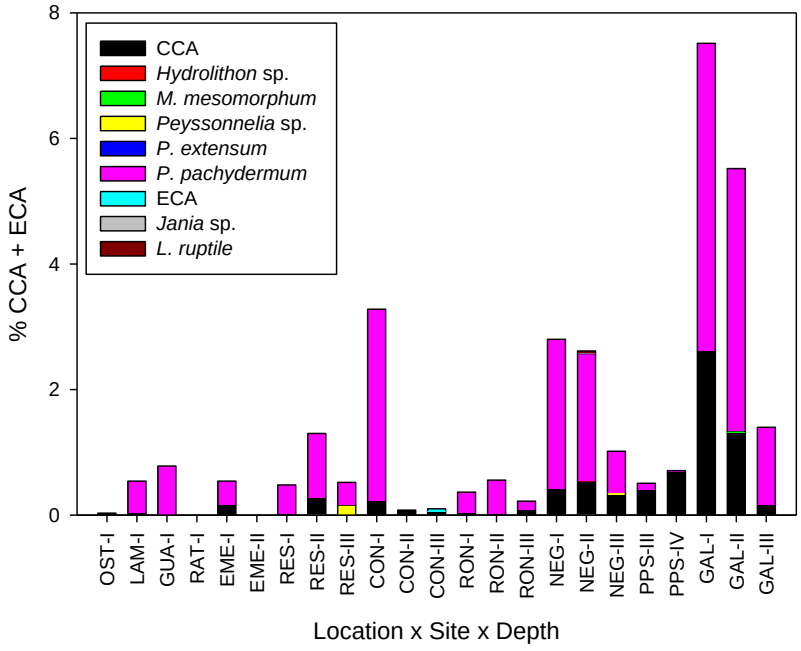

FIGURE 62. Percent relative crustose coralline (CCA) + erect calcareous algae (ECA) cover across sites. Red circles= Inshore sites; Green circles= Mid-shelf sites; Black circles= Outer shelf sites. Mean±95% confidence interval.

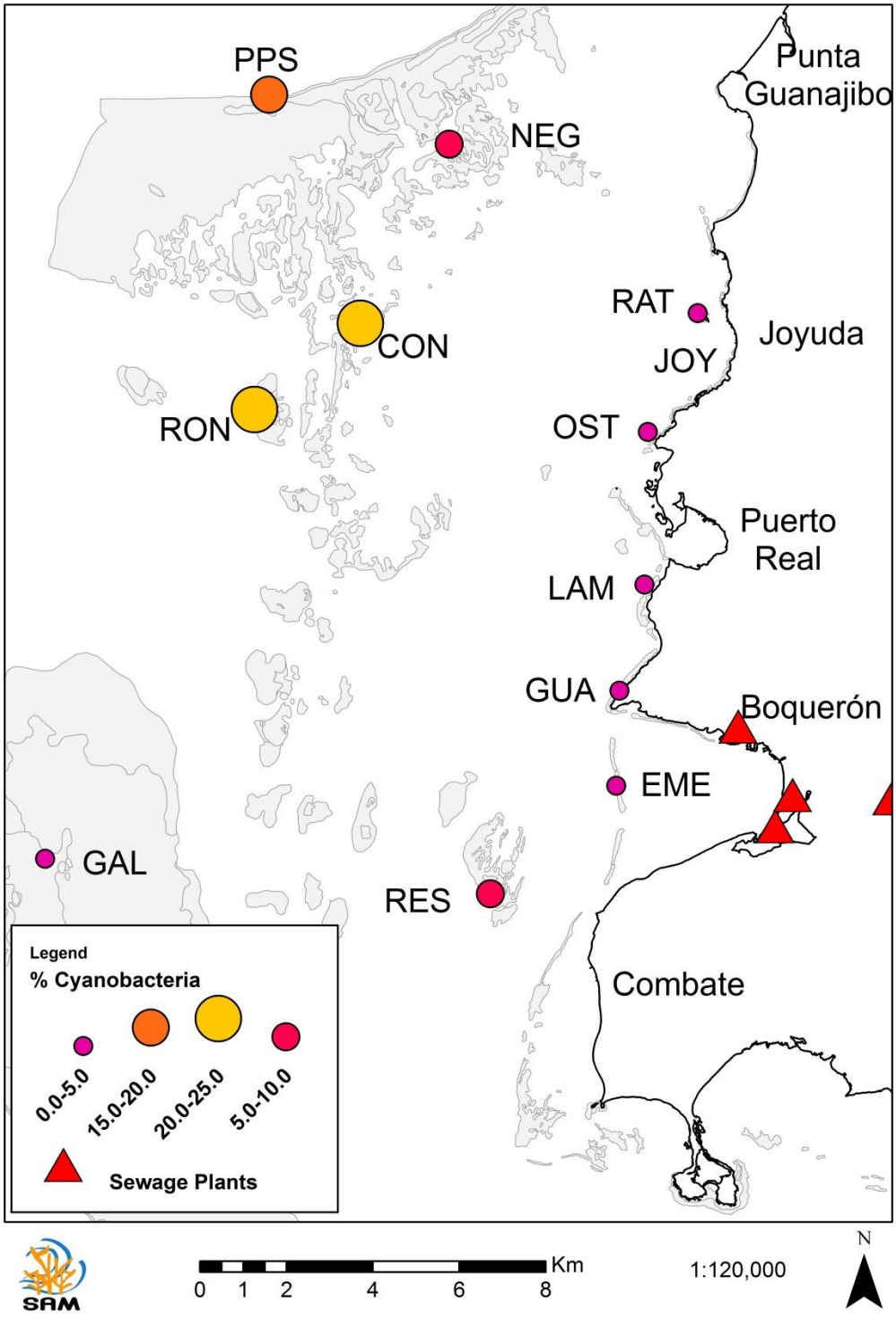

FIGURE 63. Cross-shelf spatial patterns of percent cyanobacterial cover.

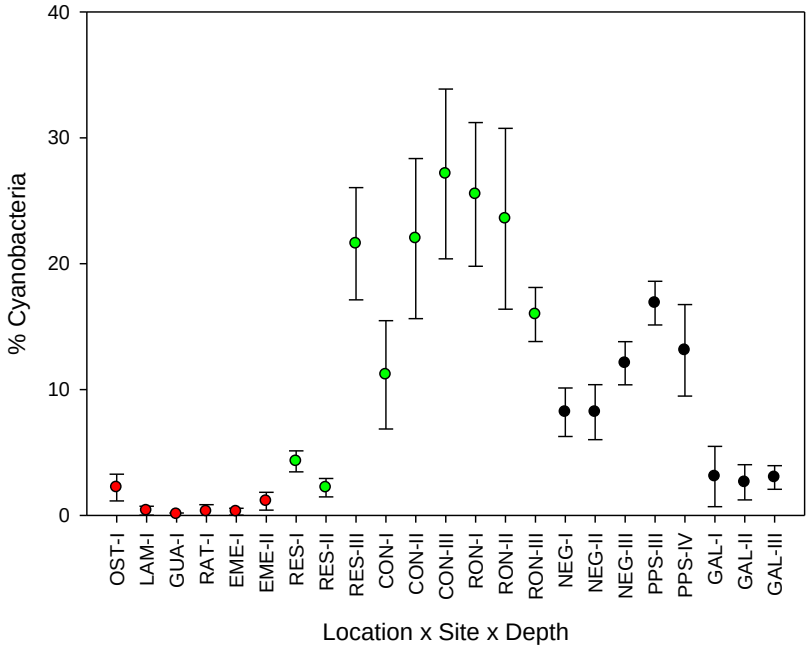

FIGURE 64. Percent cyanobacterial cover across sites. Red circles= Inshore sites; Green circles= Mid-shelf sites; Black circles= Outer shelf sites. Mean±95% confidence interval.

Cyanobacteria showed an interesting spatial pattern that reflected higher abundance across mid-shelf sites, possibly influenced by effluents from either Boquerón Bay (RES), from Guanajibo River (CON, RON, NEG), or from Mayagüez (PPS) (***Figures 63-64***). Mean % cyanobacterial cover was 0.7% across inshore sites, with a highest value of only 2.2% at the <5 m depth zone of OST and a lower value of less than 0.1% at the <5 m depth zone of GUA. Mean % cyanobacterial cover was an impressive 17.1% across mid-shelf sites, with a minimum value of 2.2% at the 5-10 m depth zone of RES and a highest value at the 10-15 m zone of CON with 27.1%. Mean % cyanobacterial cover was 8.4% across outer shelf sites, with a minimum value of 2.6% at the 5-10 m depth zone of GAL and a highest value at the 10-15 m zone of PPS with 16.9%, right at the shelf edge. These findings suggest that impacts of LBSP, particularly across moderate to deeper reef zones are widespread across the entire shelf and appear to be largely related to the complex cross-shelf oceanic circulation patterns.

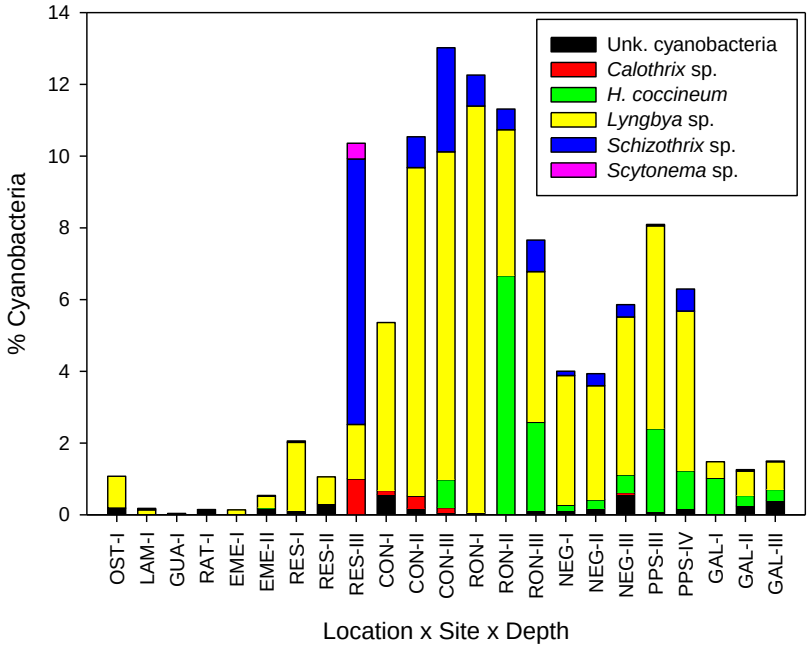

FIGURE 65. Percent relative cyanobacteria cover across sites. Red circles= Inshore sites; Green circles= Mid-shelf sites; Black circles= Outer shelf sites. Mean±95% confidence interval.

Lyngbia spp. was the most common cyanobacterial taxa across the shelf, followed by *Hydrocoleum coccineum*, particularly across mid- to outer shelf sites (***Figure 65***). *Schizotrix* spp. was also common, particularly across mid-shelf sites. *Calothrix* spp. was particularly common at selected mid-shelf sites RES and CON.

Percent frequency of recently dead corals (DCA) was generally low overall (***Figure 66***) and averaged 0.4% across inshore sites, with a maximum of 1.8% at the <5 m depth zone of OST. No DCA were documented at LAM. Mean % DCA was slightly less than 0.6% across mid-shelf sites, with a highest value of 2.2% at the <5 m depth zone of RON. DCA were absent at the <5 m and at the 10-15 m depth zones of RES. Mean % DCA was 0.8% across outer shelf sites, with the lowest frequency at the 15-20 m depth zone on the vertical wall at PPS, and he highest at the 10-15 m zone of GAL with 2.8%.

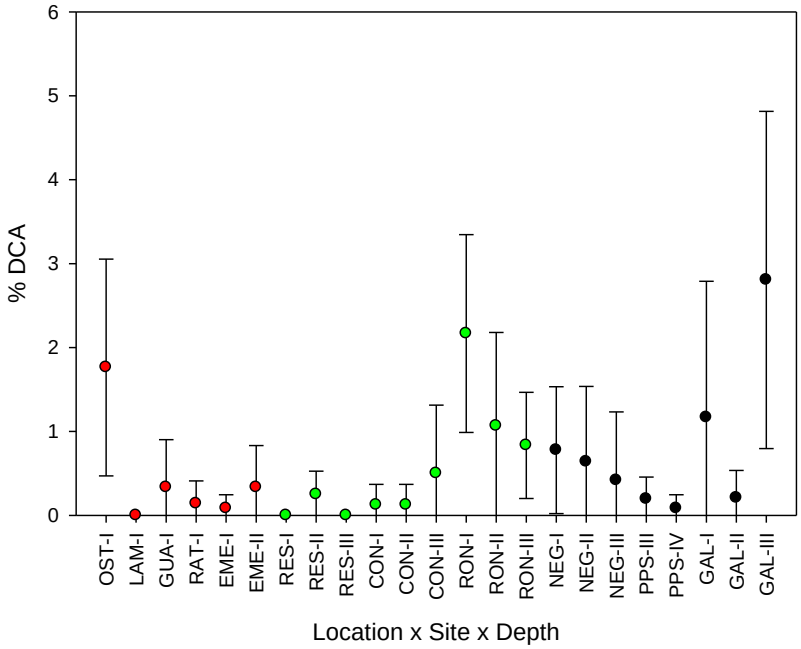

FIGURE 66. Percent frequency recently dead coral with algae (DCA) across sites. Red circles= Inshore sites; Green circles= Mid-shelf sites; Black circles= Outer shelf sites. Mean±95% confidence interval.

Percent frequency of diseased corals showed localized spatial variability probably influenced by local water quality and LBSP (***Figure 67***) and averaged 3.1% across inshore sites, with a maximum of 8.3% at the <5 m depth zone of OST, and a minimum prevalence of 0.4% at the <5 m depth zone of GUA. Mean % prevalence of diseased was 4.7% across mid-shelf sites, with a an impressive highest prevalence of 28.0% at the 10-15 m depth zone of RES, mostly in the form of black band disease (BBD) affecting *Orbicella* spp and *Siderastrea siderea*. The lowest mean prevalence was observed across the <5 m depth zone of RES. Mean % prevalence of diseased corals was 3.5% across outer shelf sites, with the lowest prevalence of 0.5% at the <0.5 m depth zone at GAL, mostly in the form of patchy necrosis (PN) impacting exclusively Elkhorn coral (*Acropora palmata*), and he highest at the 10-15 m zone of GAL with 2.8%, and the highest at the 5-10 m depth zone of GAL, with 10.2%, mostly in the form of PN and in a minor degree BBD. With the exception of mid-shelf 10-15 m depth zone of RES (11.9%), and <5 m depth zone of OST (1.7%), coral bleaching was not a significant factor across sites (***Figure 68***).

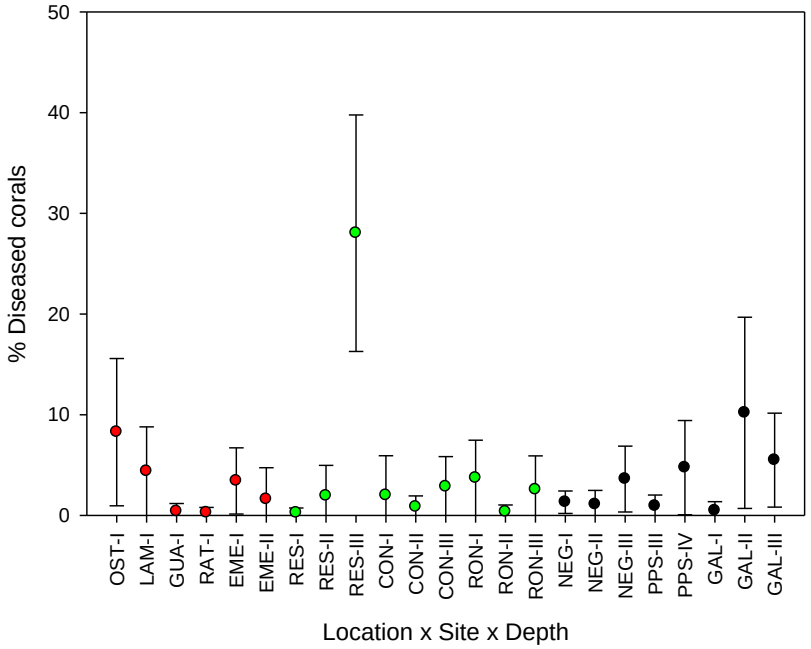

FIGURE 67. Percent prevalence of diseased corals across sites. Red circles= Inshore sites; Green circles= Mid-shelf sites; Black circles= Outer shelf sites. Mean±95% confidence interval.

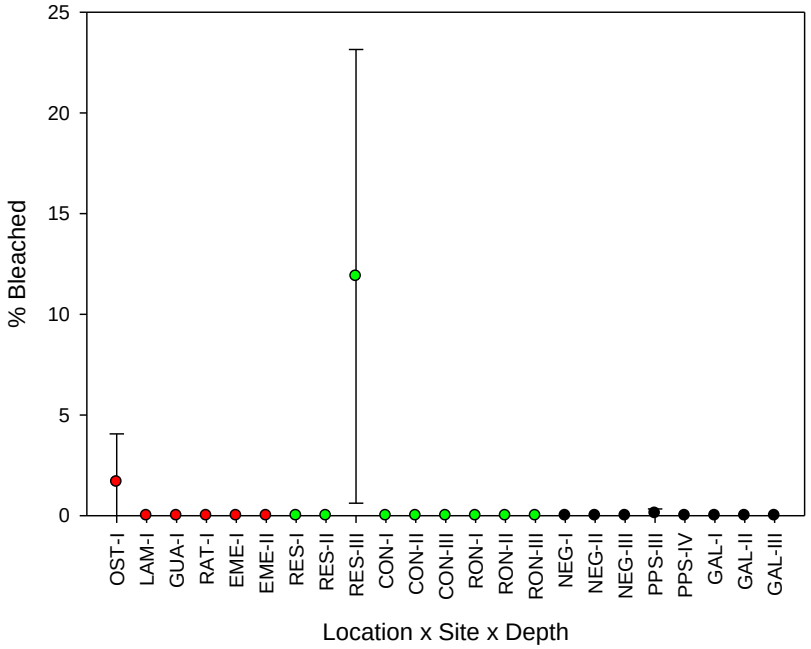

FIGURE 68. Percent frequency diseased corals across sites. Red circles= Inshore sites; Green circles= Mid-shelf sites; Black circles= Outer shelf sites. Mean±95% confidence interval.

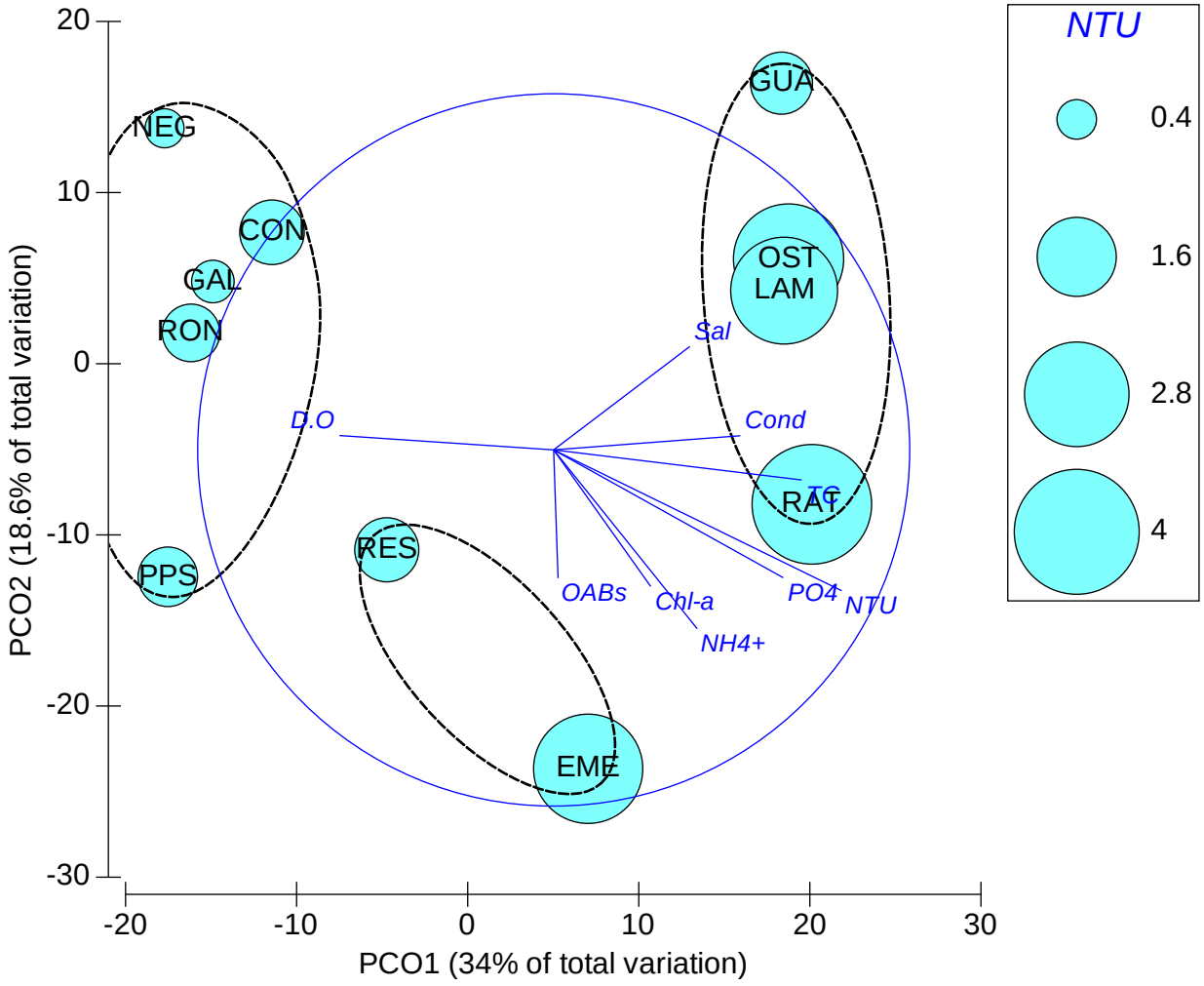

FIGURE 69. Principal component ordination plot (PCO) of coral reef benthic community structure as a function of water quality parameters and across a turbidity gradient (bubbles). Clusters based on 60% similarity cutoff.

PCO analysis showed that benthic coral reef community structure across the western Puerto Rico shelf showed three different clustering patterns as a function of water quality parameters (***Figure 69***). This PCO show results highlighting turbidity spatial patterns (bubbles). A first cluster of inshore sites RAT, OST, LAM, and GUA were explained higher turbidity, PO_4 and sea surface temperature (SST), followed by salinity, conductivity. A second cluster was composed by EME and RES, and was largely explained by NH_4^+, and in a lesser extent by chlorophyll-*a* and optical brighteners concentration (OABs). A final cluster included mid-shelf CON, RON, and outer shelf NEG, PPS, and GAL, which were largely explained by higher dissolved oxygen

concentration. This PCO explained 53% of the observed cross-shelf spatial variability in coral recruit community structure.

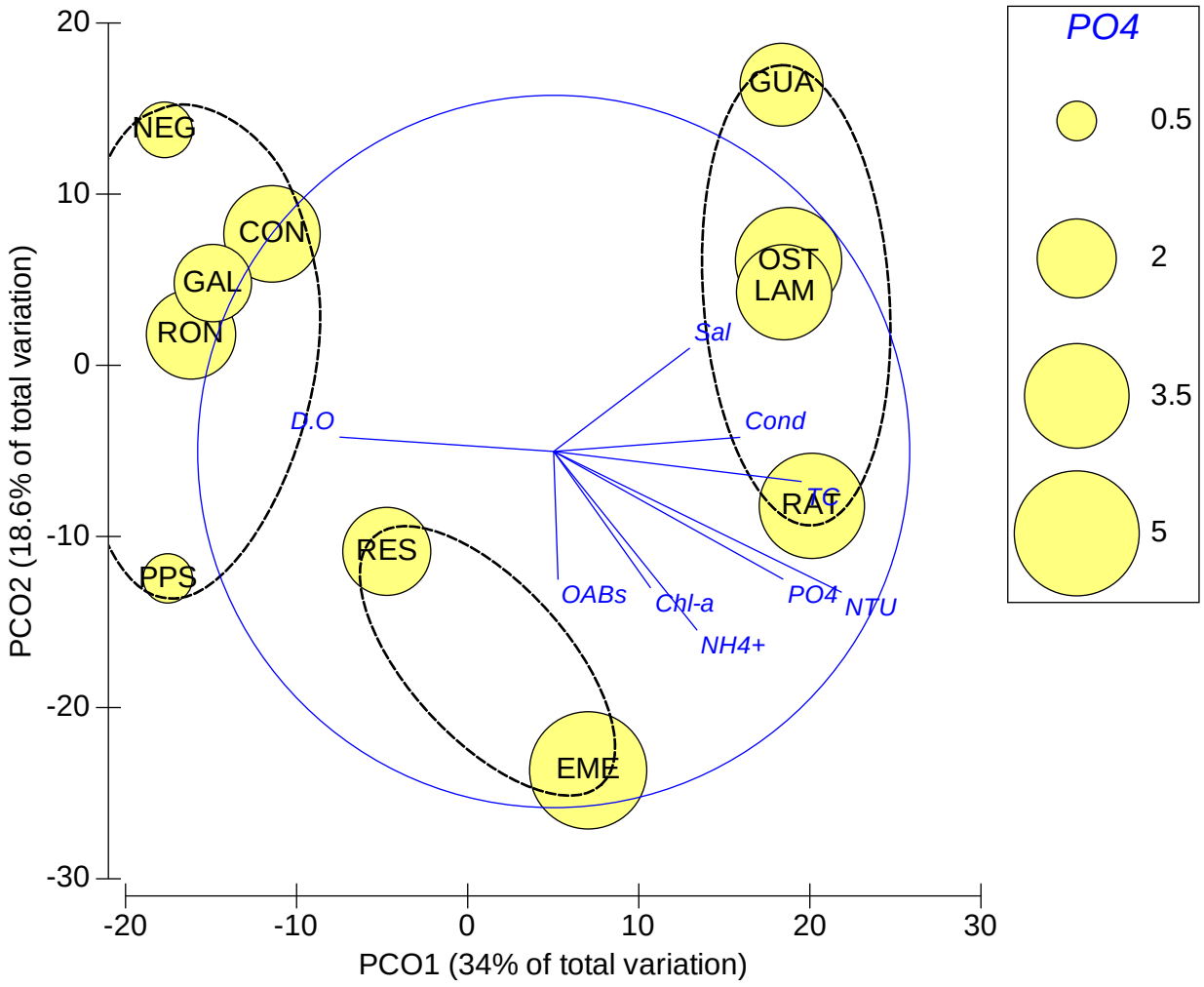

FIGURE 70. Principal component ordination plot (PCO) of coral reef benthic community structure as a function of water quality parameters and across a phosphate (PO_4) concentration (μM) gradient (bubbles). Clusters based on 60% similarity cutoff.

Figure 70 shows PO_4 spatial patterns, while ***Figure 71*** shows NH_4^+ spatial patterns. These three examples suggest that these three parameters seem to affect coral reef benthic community structure. A multivariate stepwise regression analysis using the BVSTEP routine confirmed that the best combination of variables explaining benthic community structure spatial patterns was a combination of turbidity, PO_4 and NH_4^+ (correlation= 0.589, $p<0.05$).

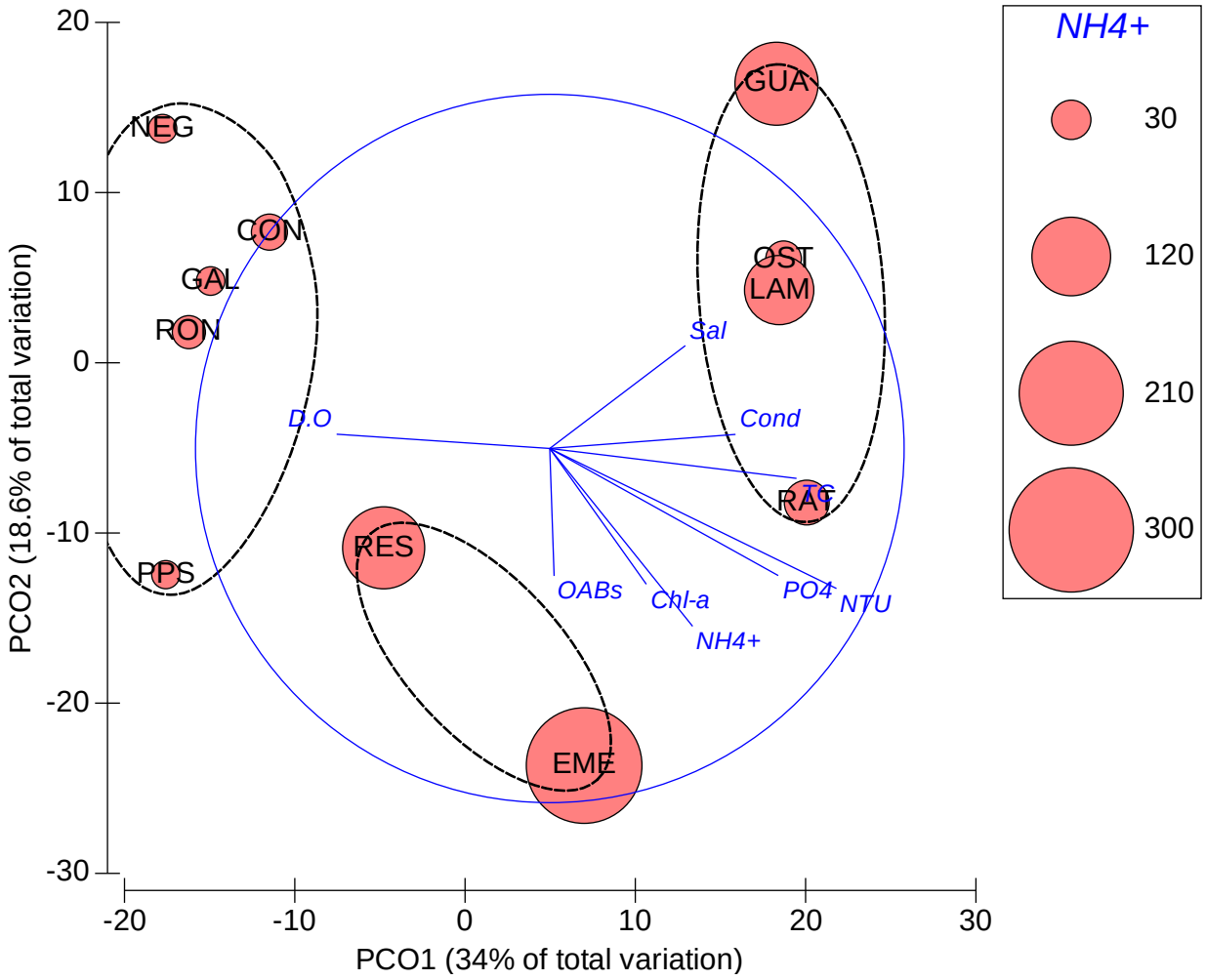

FIGURE 71. Principal component ordination plot (PCO) of coral reef benthic community structure as a function of water quality parameters and across a ionized ammonium (NH_4^+) concentration (µM) gradient (bubbles). Clusters based on 60% similarity cutoff.

Further, a multivariate correlation analysis using the RELATE routine and following a Spearman Rank correlation procedure showed that there was a highly significant correlation between the coral reef benthic community structure matrix and the matrix of water quality parameters (R= 0.42, *p*=0.0020).

A 'linkage tree' of coral reef benthic community structure based on the BIOENV routine to environmental variables was carried out (***Figure 72***). Binary split on basis of the best single environmental variable was thresholded to maximise the ANOSIM R statistic for the two groups formed. The first split (A) in the assemblage data is between sites 8, 10, 11 (RON, PPS, GAL) in

the left side of the tree, and the second group was composed of sites 1-7, 9 (RAT, OST, LAM, GUA, EME, RES, CON, NEG) in the right side of the tree. This division is also reflected in the multi-dimensional scaling (MDS) plot of the test with an ANOSIM of R= 0.57 and B= 85.9% (***Figure 73***). It is characterized by low ionized ammonium to the left of the tree (NH_4^+ Euclidean distance < -0.677) at outer shelf sites PPS and GAL, and at mid-shelf site RON, in high NH_4^+ Euclidean distance > -0.546) to the right side of the tree (***Figure 72***). Alternatively, the same split of sites was obtained by choosing high turbidity to the left of the tree (Turbidity Euclidean distance < -0.555) at outer shelf sites PPS and GAL, and at mid-shelf site RON, and high turbidity (Turbidity Euclidean distance < -0.677) to the right side of the tree (***Figure 72***). ANOSIM R was the same whichever of the two variables was used as they gave the same split of biotic data.

Moving down the tree, split (D) provides the second most strong explanation of spatial patterns with a split between sites 1-6 (RAT, OST, LAM, GUA, EME, RES, CON) to the left and site 7 (NEG) to the right, with low optical brighteners to the left (OABs<0.304) and high optical brighteners to the right (OABs >0.931), and an ANOSIM R= 1.00, and B= 80.7% (***Figure 72***). But split A offered the best solution.

In synthesis, LINKTREE analysis showed that variation in NH_4^+ and turbidity explained most of the spatial variation observed in coral reef benthic community structure. In conclusion, coral reef benthic community structure is being largely influenced by LBSP stress gradients across the entire western Puerto Rican shelf. Coral assemblages are showing signs of stress gradient and so are compromising the long-term reef accretion sustainability and ecosystem resilience.

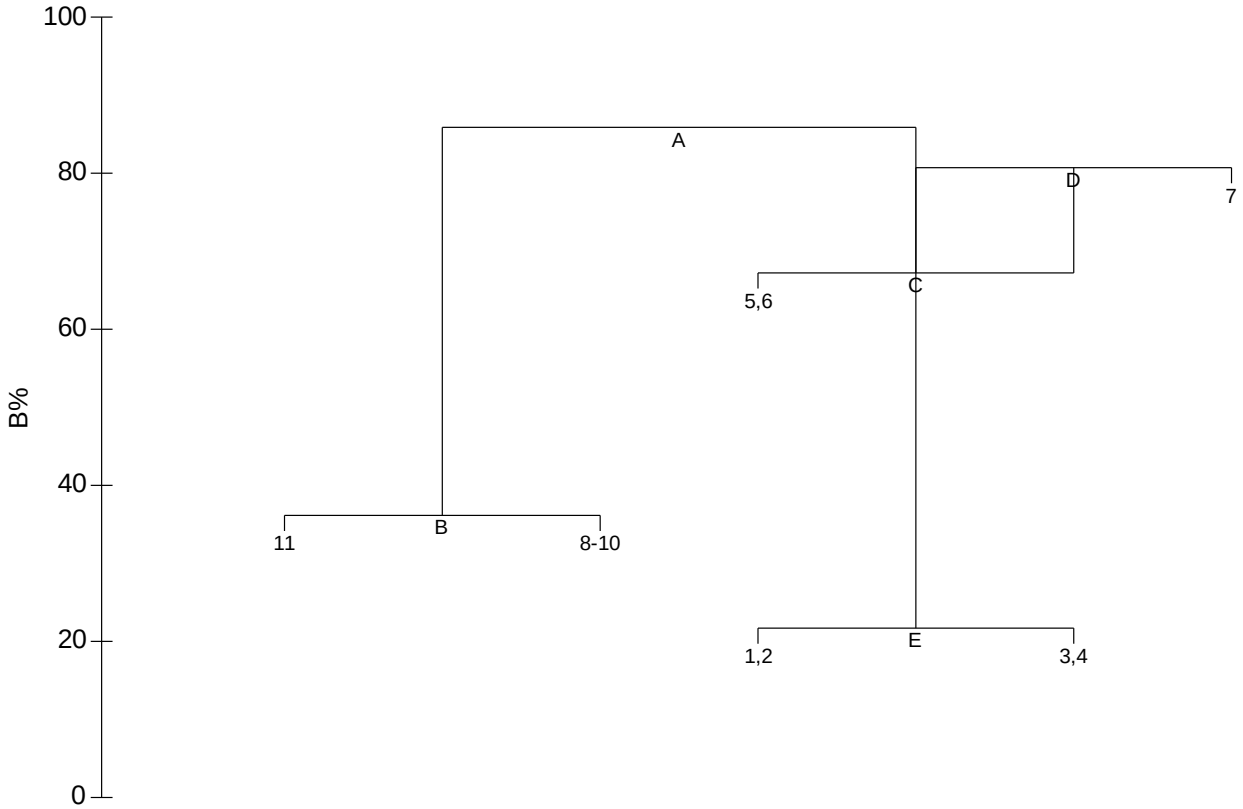

A->B,C= R: 0.57, B%: 85.9, NH4+<-0.677(>-0.546), NTU<-0.555(>-0.463)
B->(11),(8-10)= R: 0.56, B%: 36.1, Sal<-1.84(>-0.791), Cond<-2.01(>-1.22), Chl-*a*<-0.81(>-0.319), D.O>1.72(<1.39)
C->(5,6),D= R: 0.47 B%: 67.2, Sal<-0.267(>8.16E-2), D.O>-0.226(<-0.418)
D->E,(7)= R: 1.00 B%: 80.7, OABs<0.304(>0.931)
E->(1,2),(3,4)= R: 0.75 B%: 21.7, Chl-*a*>1.16(<6.2E-2), NH_4^+<-9.43E-2(>0.756), TC<0.212(>1.03), Sal>0.777(<0.256), PO_4>0.842(<0.4), OABs>4.87E-2(<-8.29E-2), NTU>1.17(<1.06), D.O<-0.528(>-0.453)
Sample numbers for plot 1)RAT;2)OST;3)LAM;4)GUA;5)EME;6)RES;7)CON;8)RON;9)NEG;10)PPS;11)GAL

FIGURE 72. LINKTREE analysis of coral reef benthic community structure as a function of water quality parameters. Data was log_{10}-transformed and normalized for analysis. Numbers are Euclidean distances. B%= 'between group' average rank as % of maximum possible.

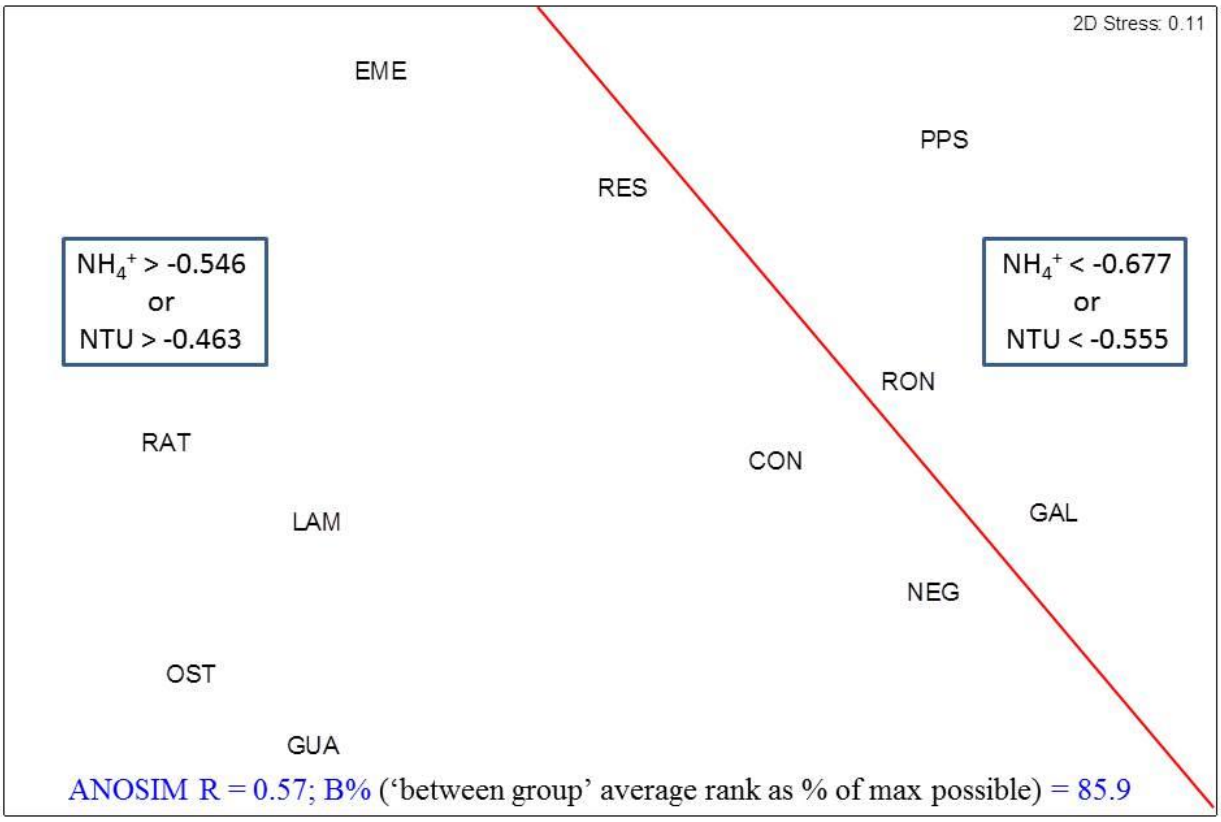

FIGURE 73. Multi-dimensional scaling (MDS) plot of the first stage in a 'linkage tree' of coral reef benthic community structure to environmental variables. Binary split on basis of the best single environmental variable, thresholded to maximise the ANOSIM R statistic for the two groups formed.

So far, this study has confirmed that benthic coral reef communities are showing evidence of impacts by chronic LBSP in the form of altered spatial distributions of multiple coral and algal taxa, with particular distance gradients (i.e., increasing percent living coral cover with increasing distance from LBSP). Multivariate PCO further confirmed these patterns. In spite of the fact that multiple coral reef show high benthic spatial heterogeneity due to structural construction by scleractian corals, percent living coral cover remains low, regardless of depth and distance from the shore. This suggests that coral reef benthic communities are showing a highly limited natural recovery ability, probably as a combined result of chronic LBSP impacts (which foster increased algal growth) and impacts by climate change-related factors (see Hernández-Delgado et al.,

2014). Therefore, coral recruit spatial patterns have become a critical component to address the spatial patterns of LBSP influences across the shelf.

TABLE 3. Summary of a three-way PERMANOVA test of coral recruit community structure

Variable	d.f.	Pseudo-F	*p*
Geographic location	2,147	10.31	<0.0001
Site	10,139	4.39	<0.0001
Depth	3,146	3.10	0.0004
Location x Site	10,139	4.39	<0.0001
Location x Depth	8,141	3.97	<0.0001
Site x Depth	22,127	3.01	<0.0001
Location x Site x Depth	22,127	3.01	<0.0001

C. Coral recruit communities

Coral recruit community structure showed a highly significant variation among all geographic zones, sites and depth zones, suggesting a strong effect associated to the LBSP gradient and to depth (***Table 3***). PCO analysis suggested that coral recruit community structure produced three general clustering patterns (***Figure 74***). A first cluster was dominated by inshore sites EME and RAT, which had very limited abundance of Scleractinians. This cluster was explained by *Gorgonia ventalina* recruits. A second cluster was composed by inshore sites OST and GUA, which was largely explained by *Siderastrea radians* recruits, which is an ephemeral species, dominant under high disturbance regimes, characterized by frequent (lunar) recruitment cycles, but very high mortality rates. The final large cluster is composed by mid-shelf and outer shelf sites plus inshore site LAM, and is explained by a combination of several Scleractinian species. Inshore site LAM was explained by *S. radians*, and RES by *G. ventalina*. RON was largely explained by *Millepora alcicornis* recruitment. PPS was better explained by *S. siderea* recruits, while NEG, CON, and GAL were better explained by a group of Scleractinian recruits, including *Porites porites*, *Undaria tenuifolia*, *U. agaricites*, and *Agaricia lamarcki*. Recruits of these species were largely absent from inshore sites.

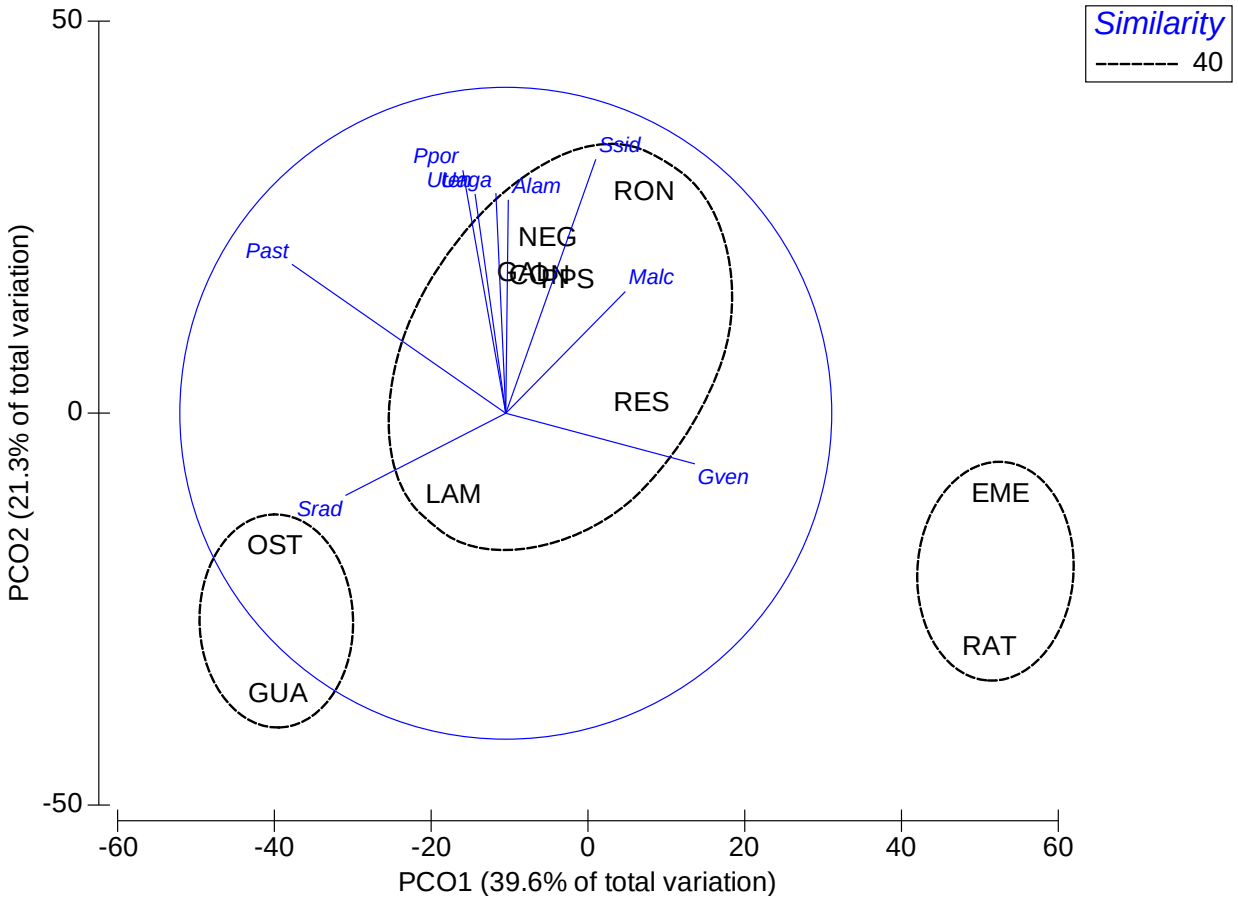

FIGURE 74. Principal component ordination plot of coral recruit communities among study sites. Clusters based on 40% similarity cut off level. Vectors based on a 0.70 correlation. This model explained 60.9% of the observed variation.

A spatial gradient of increasing coral recruit abundance with increasing distance from LBSP was also evident for several species, including *Porites porites*, *Undaria agaricites*, *Siderastrea siderea*, and *Orbicella faveolata* (***Figure 75***). Coral recruit density averaged 1.1 colonies/m^2 across inshore reef sites, with the lowest value of 0.4 colonies/m^2 at the <5 m depth zone of RAT and the highest value of 2.1 colonies/m^2 at the <5 m depth zone of LAM (***Figure 76***). Coral recruit density averaged 4.1 colonies/m^2 across mid-shelf sites, with the lowest value of 1.0 colonies/m^2 at the 10-15 m depth zone at RES and the highest value of 8.4 colonies/m^2 at the <5 m depth zone of RON. Mean coral recruit density across outer shelf sites was 7.7 colonies/m^2 across mid-shelf sites, with the lowest value of 4.8 colonies/m^2 at the <5 m depth zone at NEG and the highest value of 16.0 colonies/m^2 at the 10-15 m depth zone of GAL.

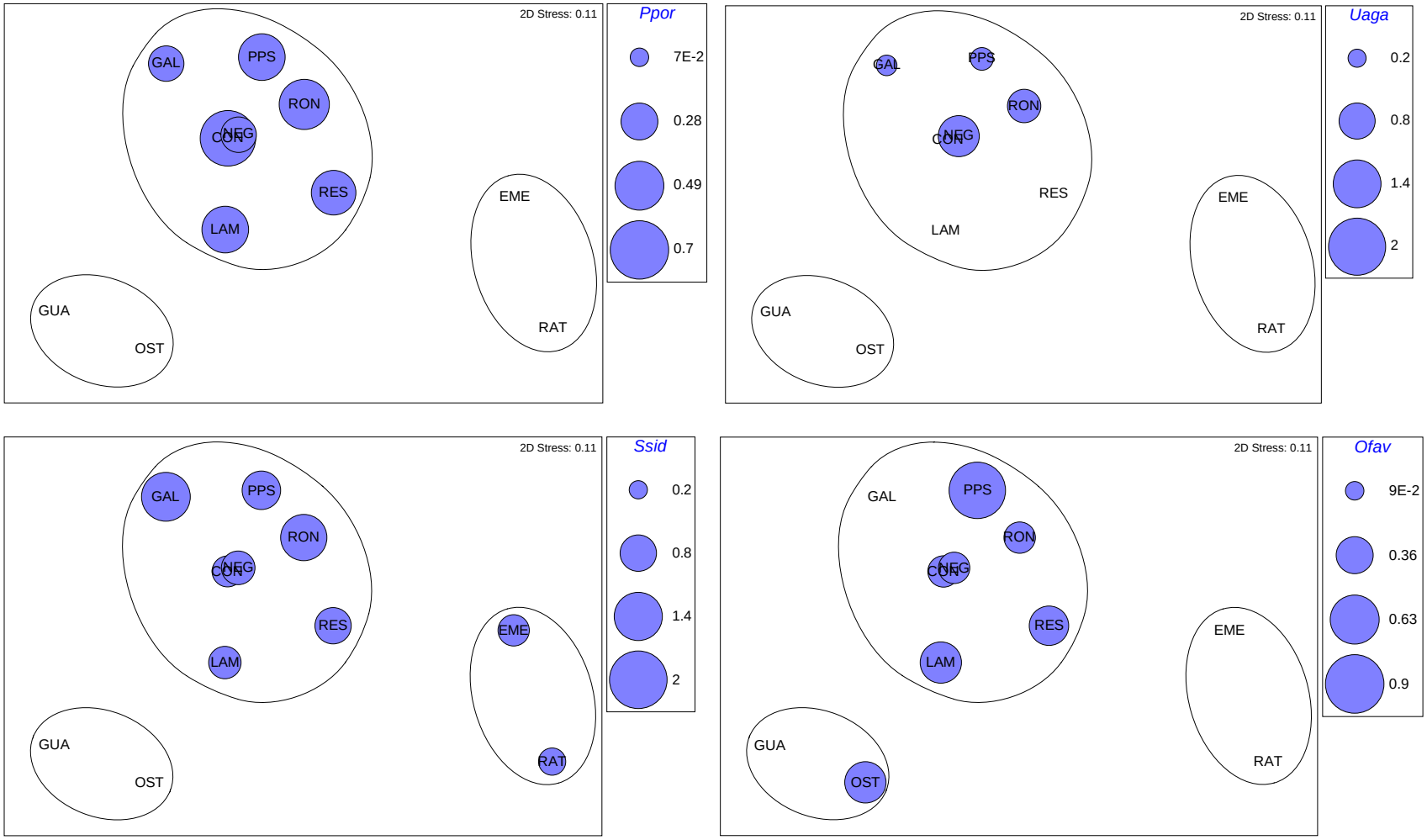

FIGURE 75. Bubble plots based on a MDS analysis of the spatial distribution of four Scleractinian coral species along a LBSP gradient. From top left: A) *Porites porites* (Ppor); B) *Undaria agaricites* (Uaga); C) *Siderastrea siderea* (Ssid); and D) *Orbicella faveolata*. Clustering patterns based on 40% similarity cut off level.

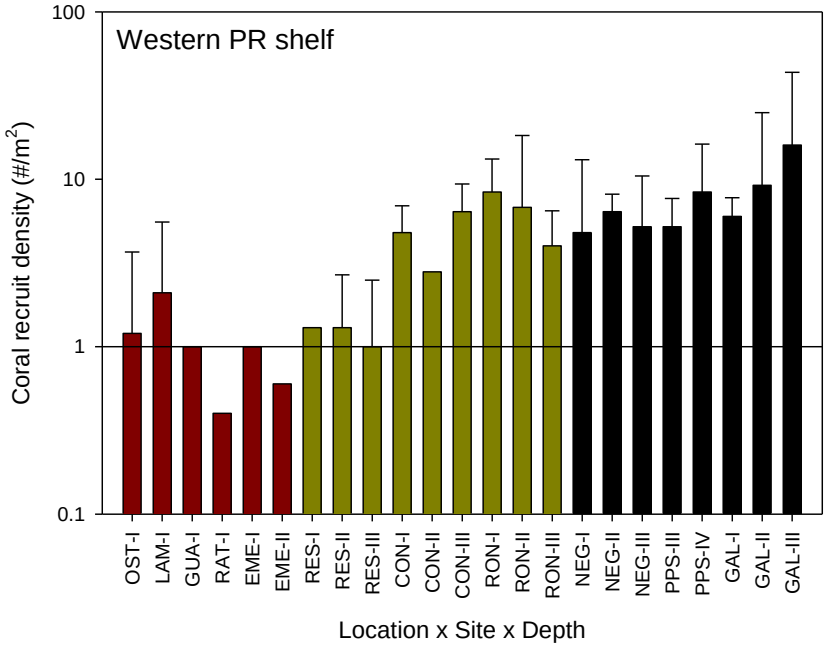

FIGURE 76. Total coral recruit density across sites. Red bars= Inshore sites; Gold bars= Mid-shelf sites; Black bars= Outer shelf sites. Mean±95% confidence interval.

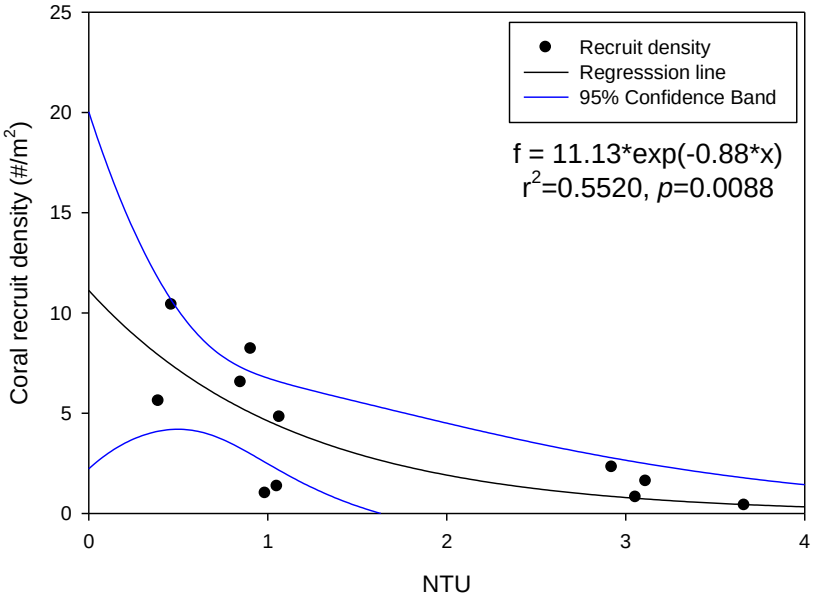

FIGURE 77. Non-linear regression between total coral recruit density and turbidity.

There was a significant (r^2=0.5520, *p*=0.0088) non-linear negative correlation between coral recruit density and water turbidity (***Figure 77***). There was also a significant (r^2=0.5203, *p*=0.0122) linear positive correlation between coral recruit density and dissolved oxygen concentration (***Figure 78***). Coral recruit density showed also a significant (r^2=0.7464, *p*=0.0006) non-linear negative correlation between and NH_4^+ (***Figure 79***).

Scleractinian coral recruit species distribution was largely variable among sites across the LBSP distance gradient (***Figure 80***). *Porites astreoides*, *Siderastrea siderea*, and *S. radians* were the dominant Scleractinian recruit species across inshore sites. *Siderastrea siderea*, *P. astreoides*, and *P. porites* were the dominant Scleractinian recruits across mid-shelf sites. *Siderastrea siderea*, *P. astreoides*, and *Undaria agaricites* were the dominant Scleractinian recruits across outer shelf sites.

Octocoral recruit density was low across the entire shelf, with mean densities that never exceeded 0.2 colonies/m^2 across inshore sites, 1.2 colonies/m^2 across mid-shelf sites, and 0.8 colonies/m^2 across outer shelf sites (***Figure 81***). Octocoral recruits species composition showed a significant difference among all geographic locations. *Gorgonia ventalina* recruits were present only at the <5 m depth zone of EME, while *Plexaura hommomalla* was present only at the <5 m depth zone of LAM. No other octocoral recruits were documented across other inshore sites. *Briareum asbestinum* was present only at the 5-10 m depth zone of RES, while *Eunicea calyculata* was present at the <5 m depth zone of CON. No other octocoral recruits were present across mid-shelf sites. *Muriceopsis flavida* and *E. fusca* were present at the <5 m depth zone of GAL, while *P. hommomalla* was only present at the 5-10 m depth zone of GAL.

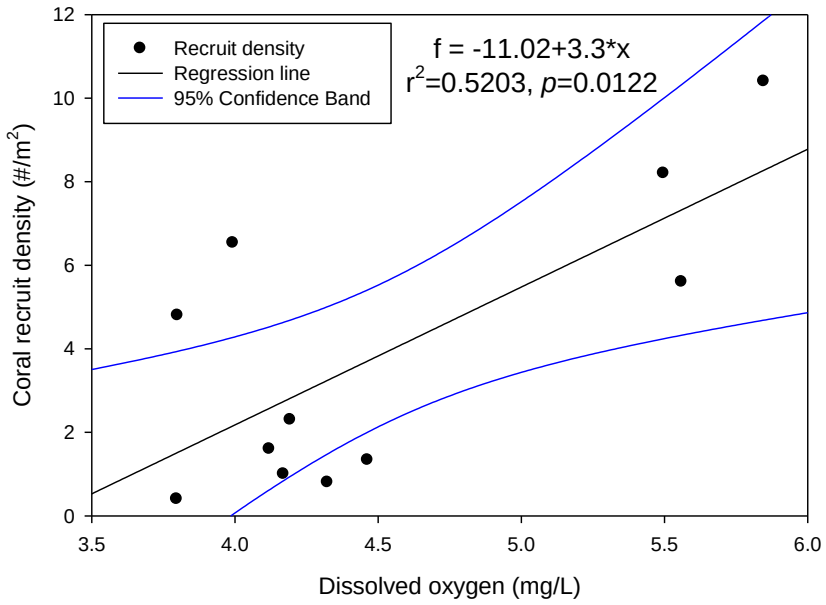

FIGURE 78. Linear regression between total coral recruit density and dissolved oxygen concentration.

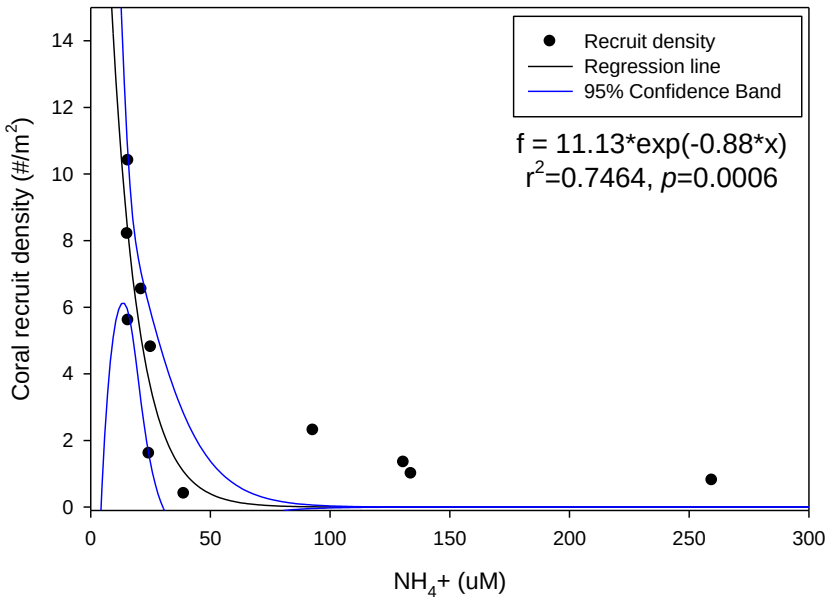

FIGURE 79. Non-linear regression between total coral recruit density and. ammonium (NH_4^+) concentration.

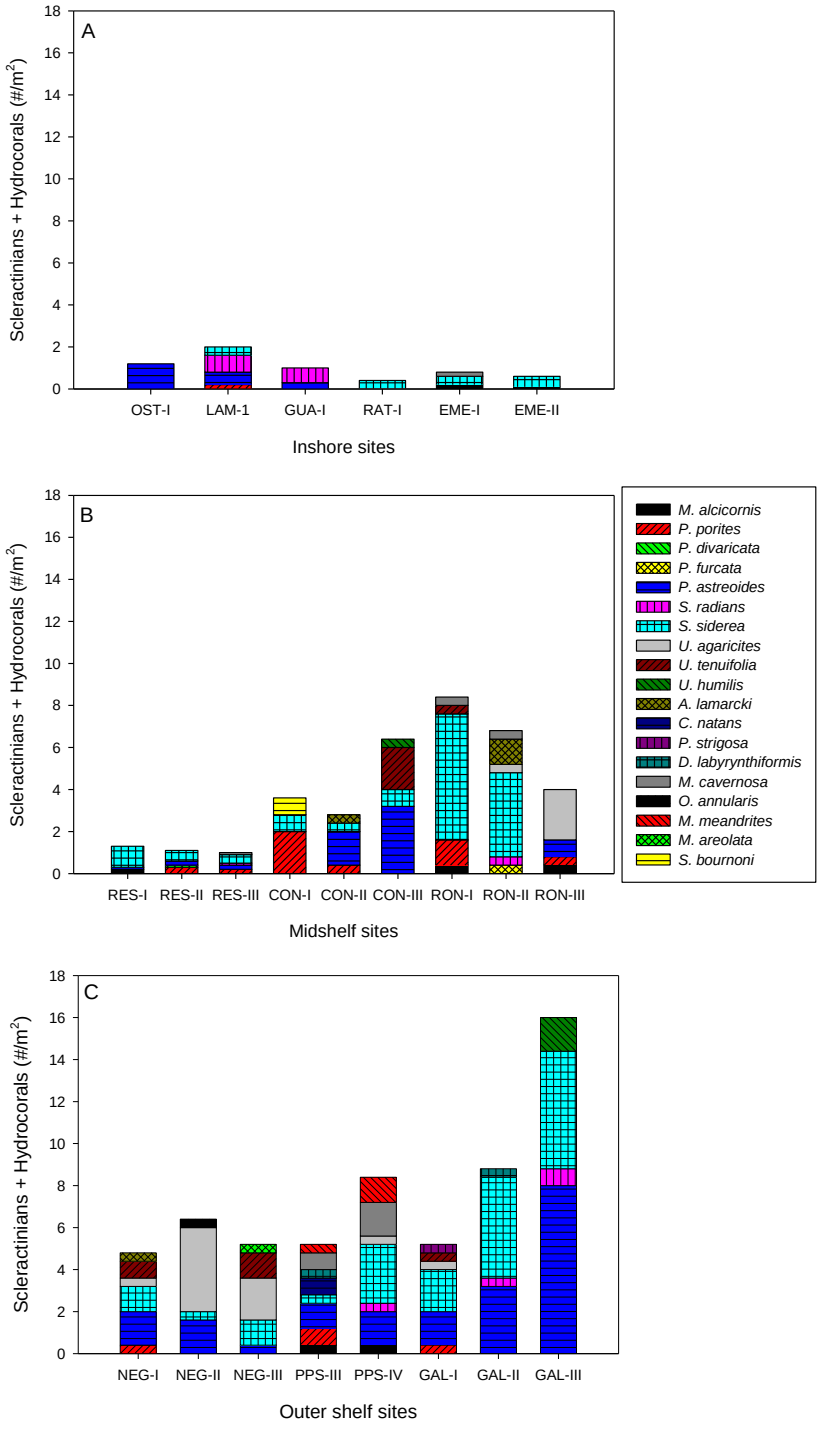

FIGURE 80. Mean scleractinian coral and hydrocoral recruit density across study sites: A) Inshore reefs; B) Mid-shelf reefs; and C) Outer shelf reefs. I= <5 m, II= 5-10 m, III= 10-15 m; IV= 15-20 m.

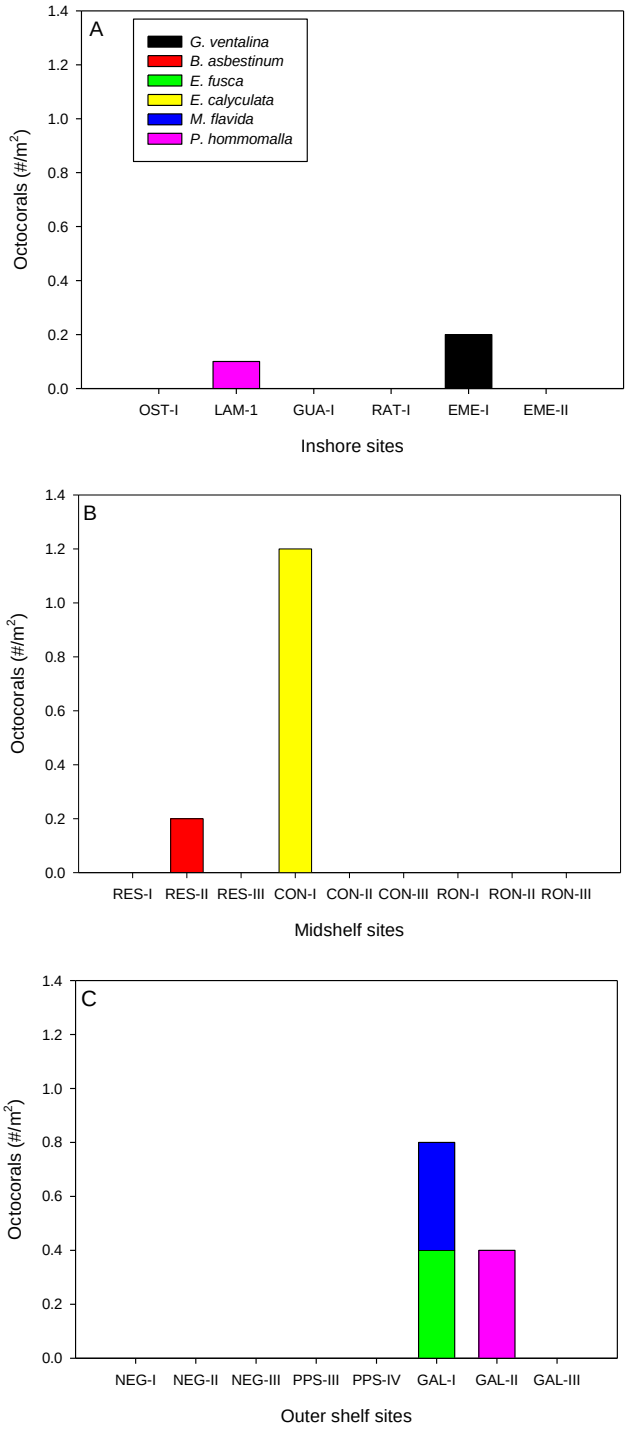

FIGURE 81. Mean octocoral recruit density across study sites: A) Inshore reefs; B) Mid-shelf reefs; and C) Outer shelf reefs. I= <5 m, II= 5-10 m, III= 10-15 m; IV= 15-20 m.

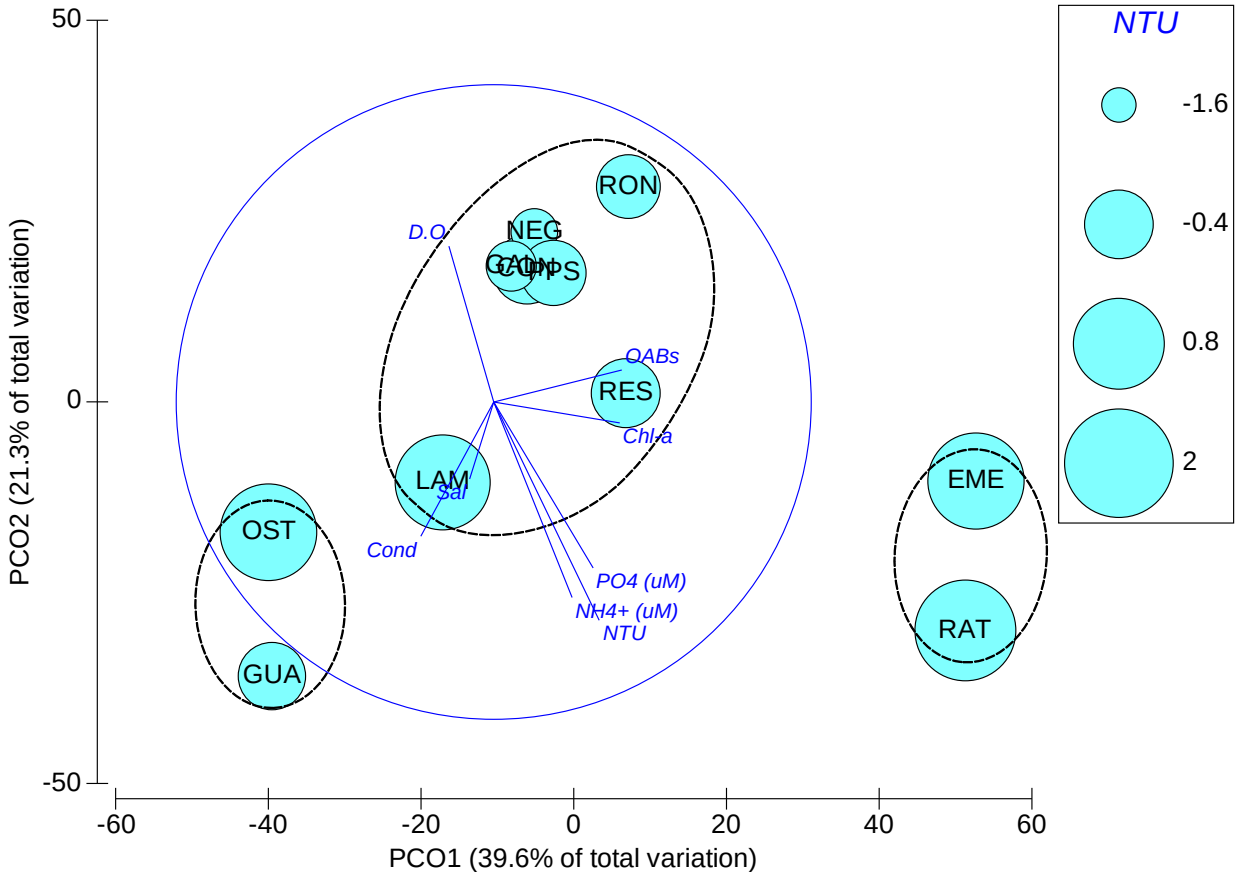

FIGURE 82. Principal component ordination plot (PCO) of coral recruit community structure as a function of water quality parameters and across a turbidity gradient (bubbles). Clusters based on 40% similarity cutoff level. This model explained 60.9% of the observed variation.

PCO analysis showed that coral recruit community structure across the western Puerto Rico shelf showed three different clustering patterns as a function of water quality parameters (***Figure 82***). This PCO show results highlighting turbidity spatial patterns (bubbles). A first cluster of inshore sites RAT and EME were explained higher turbidity, PO_4 and NH_4^+. A second cluster was composed by OST and GUA, and was largely explained by salinity. A final large cluster was explained by the rest of the water quality parameters, with RES explained by OABs and chlorophyll-*a*, and the rest of the mid- and outer shelf sites explained by dissolved oxygen concentration. This PCO explained 61% of the observed cross-shelf spatial variability in coral recruit community structure.

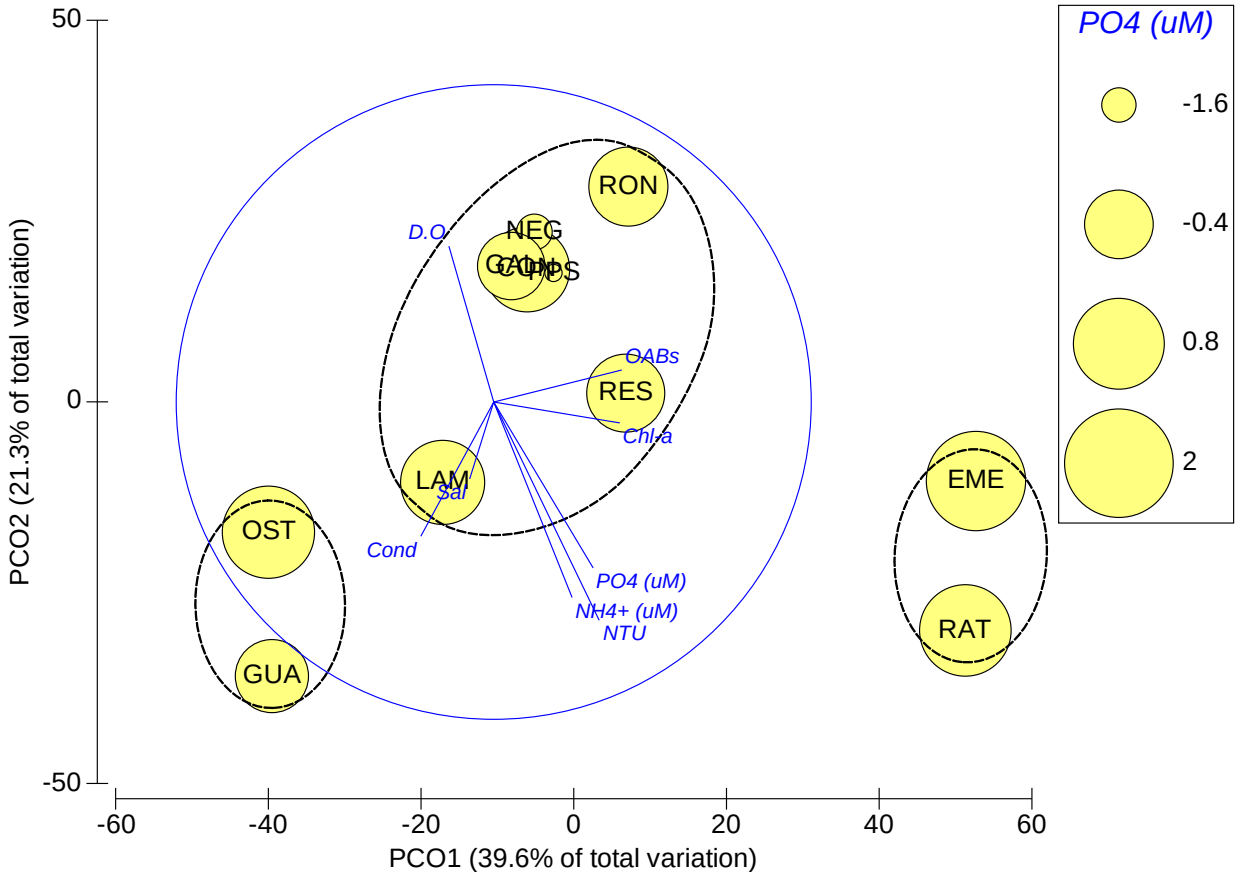

FIGURE 83. Principal component ordination plot (PCO) of coral recruit community structure as a function of water quality parameters and across a phosphate (PO_4) concentration (µM) gradient (bubbles). Clusters based on 40% similarity cutoff level. This model explained 60.9% of the observed variation.

Figure 83 shows PO_4 spatial patterns, while ***Figure 84*** shows NH_4^+ spatial patterns. These three examples suggest that these three parameters seem to affect coral recruit community structure. BIOENV and BVSTEP analyses showed that the coral recruit biotic matrix and the water quality matrix showed a correlation of 0.463 based on the combination of turbidity, chlorophyll-*a*, and PO_4 concentrations. This suggests that although LBSP could have been an important factor influencing coral recruit spatial patterns, other potential non-local, regional-global factors (i.e., climate change) could have significantly influenced coral recruitment trends across surveyed sites.

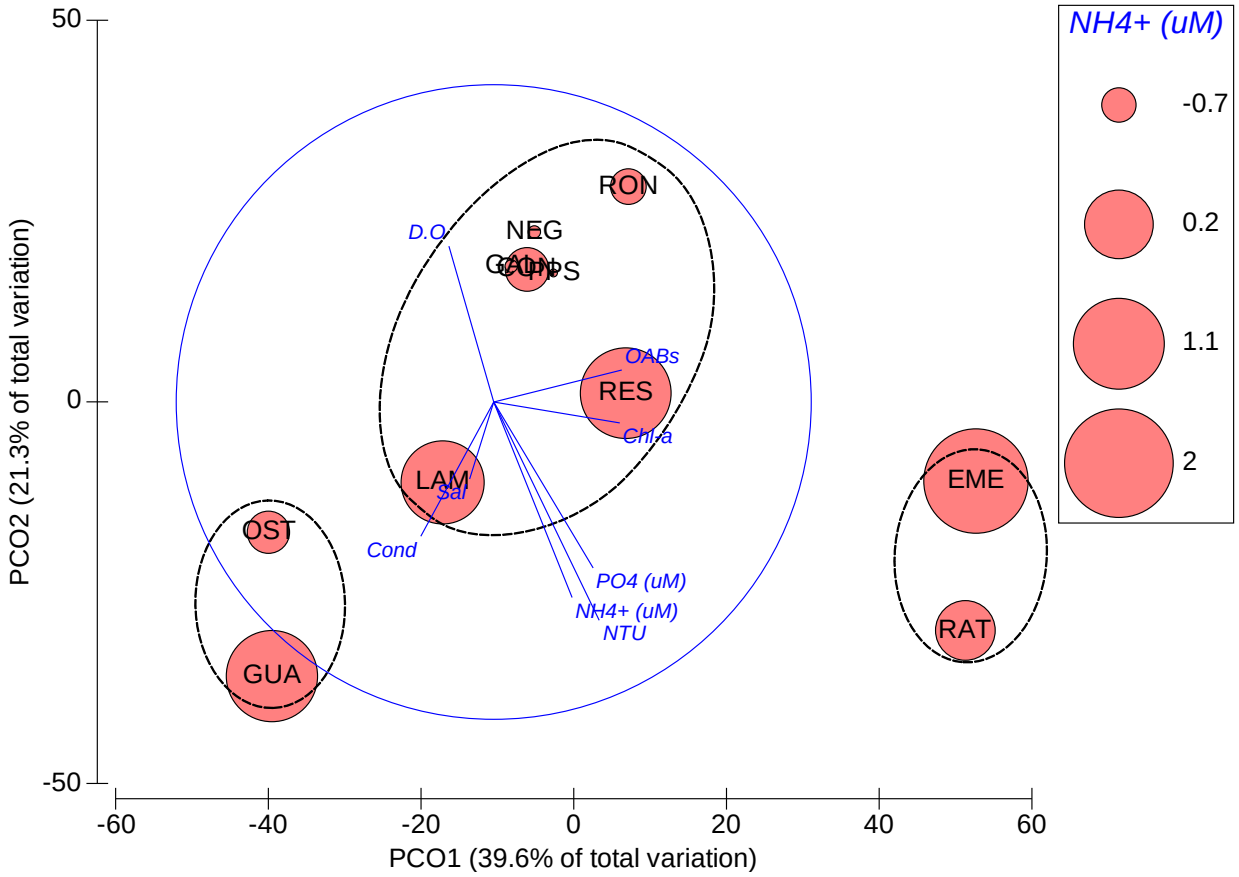

FIGURE 84. Principal component ordination plot (PCO) of coral recruit community structure as a function of water quality parameters and across a ionized ammonium (NH_4^+) concentration (µM) gradient (bubbles). Clusters based on 60% similarity cutoff level. This model explained 60.9% of the observed variation.

A 'linkage tree' of coral recruit community structure based on the BIOENV routine to environmental variables was carried out (***Figure 85***). Binary split on basis of the best single environmental variable was thresholded to maximise the ANOSIM R statistic for the two groups formed. The first split (A) in the assemblage data is between site 1 (RAT) in the left side of the tree, and the rest in the right side of the tree. This division is also reflected in the MDS plot of the test with an ANOSIM of R= 0.68 and B= 85.9% (***Figure 86***). It is characterized by a high turbidity (Euclidean distance > 1.45) to the left of the tree at inshore site RAT, and low turbidity (Euclidean distance < 1.17) to the right side of the graph (***Figure 85***).

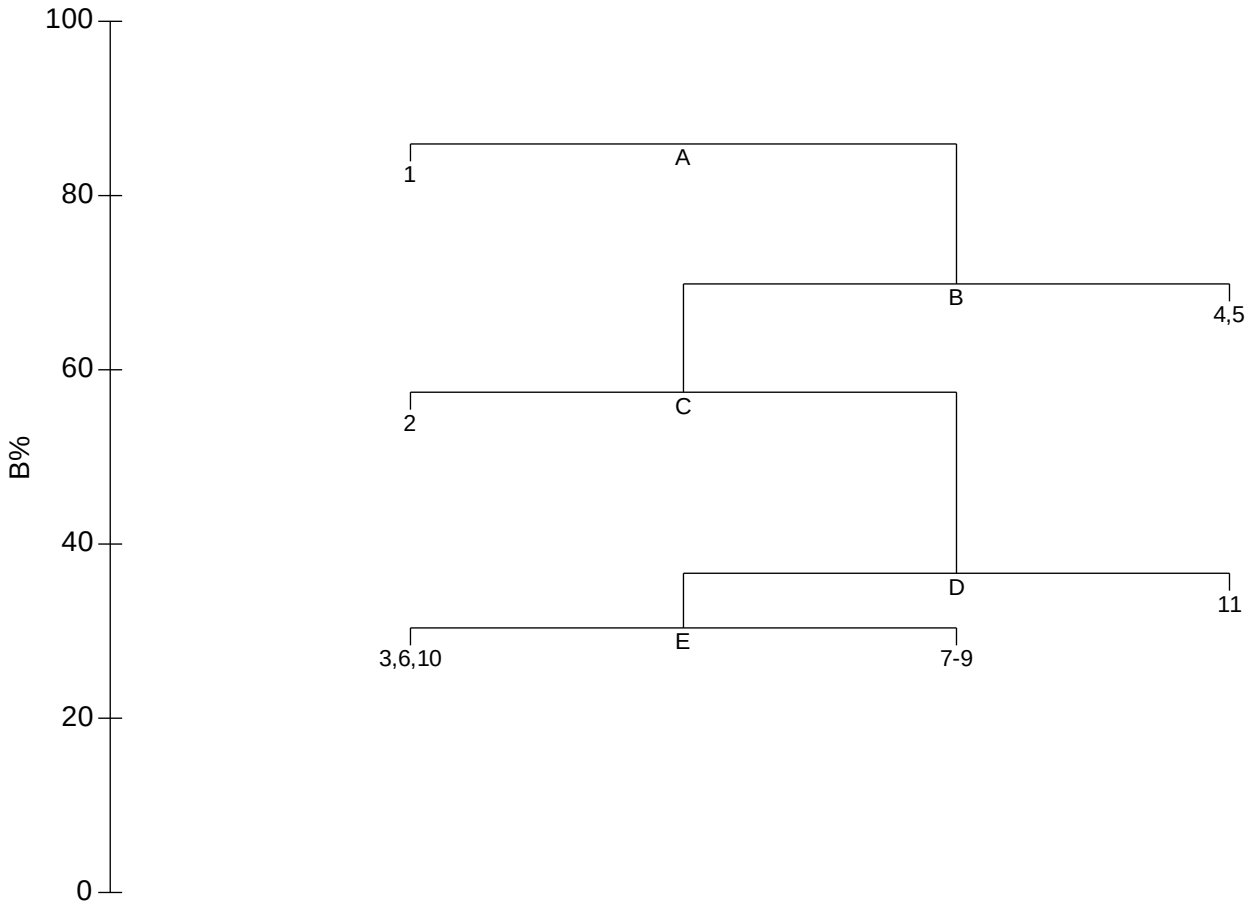

A->(1),B= R: 0.68, B%: 85.9, NTU>1.45(<1.17), D.O<-1.03(>-1.03)
B->C,(4,5)= R: 0.67, B%: 69.9, NH4+(<1.09(>1.12)
C->(2),D= R: 0.78 B%: 57.4, Chl-a>1.46(<0.286), PO4 (uM)>0.888(<0.453), Cond>0.898(<0.755), NTU>1.17(<1.06)
D->E,(11)= R: 0.44 B%: 36.6, Cond>-1.22(<-2.01), Sal>-1.32(<-1.84), D.O<1.39(>1.72)
E->(3,6,10),(7-9)= R: 0.67 B%: 30.4, Sal<8.16E-2(>0.256)
Sample numbers for plot 1)RAT;2)OST;3)LAM;4)GUA;5)EME;6)RES;7)CON;8)RON;9)NEG;10)PPS;11)GAL

FIGURE 85. LINKTREE analysis of coral recruit community structure as a function of water quality parameters. Data was $\log_{10}$-transformed and normalized for analysis. Numbers are Euclidean distances. B%= 'between group' average rank as % of maximum possible.

Alternatively, the same split of sites was obtained with low dissolved oxygen concentration (Euclidean distance < -1.03) to the left of the tree at inshore site RAT, and high dissolved oxygen concentration (Euclidean distance > -1.03) to the right of the tree (***Figure 85***). ANOSIM R was the same whichever of the two variables was used as they gave the same split of biotic data.

Moving down the tree, split (B) provides the second most strong explanation of spatial patterns with a split between sites 4-5 (GUA, EME) to the right and the rest to the left, with low NH_4^+ to the left (Euclidean distance < 1.09) and high NH_4^+ to the right at GUA and EME (Euclidean distance > 1.12), and an ANOSIM R= 0.67, and B= 69.9% (***Figure 87***). Split A offered the best solution.

In synthesis, LINKTREE analysis showed that variation in turbidity and dissolved oxygen concentration explained most of the spatial variation observed in coral recruit community structure. In conclusion, coral recruit community structure is also being largely influenced by LBSP stress gradients across the entire western Puerto Rican shelf. Coral recruit assemblages are also showing signs of a stress gradient and so are compromising the long-term reef recovery ability, accretion sustainability and ecosystem resilience across mot reefs.

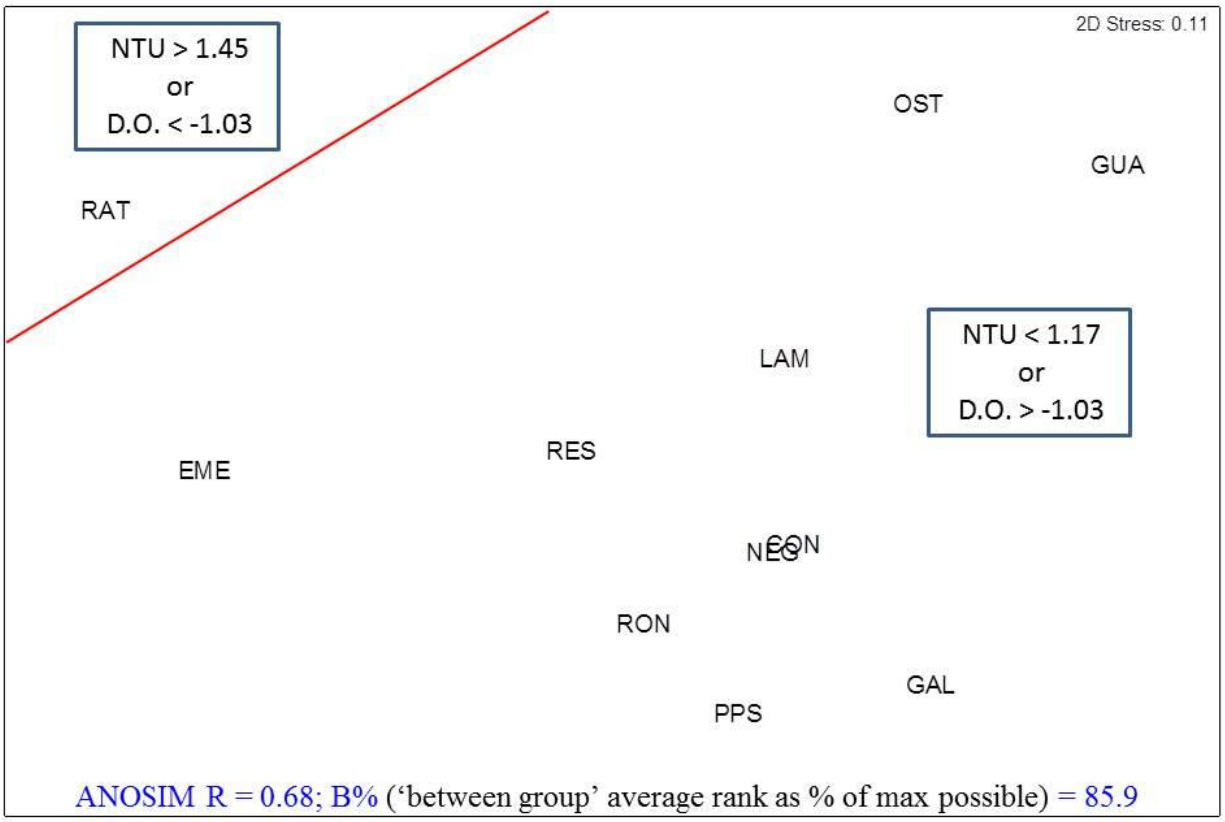

FIGURE 86. Multi-dimensional scaling (MDS) plot of the first stage in a 'linkage tree' of coral recruit community structure to environmental variables. Binary split on basis of the best single environmental variable, thresholded to maximise the ANOSIM R statistic for the two groups formed.

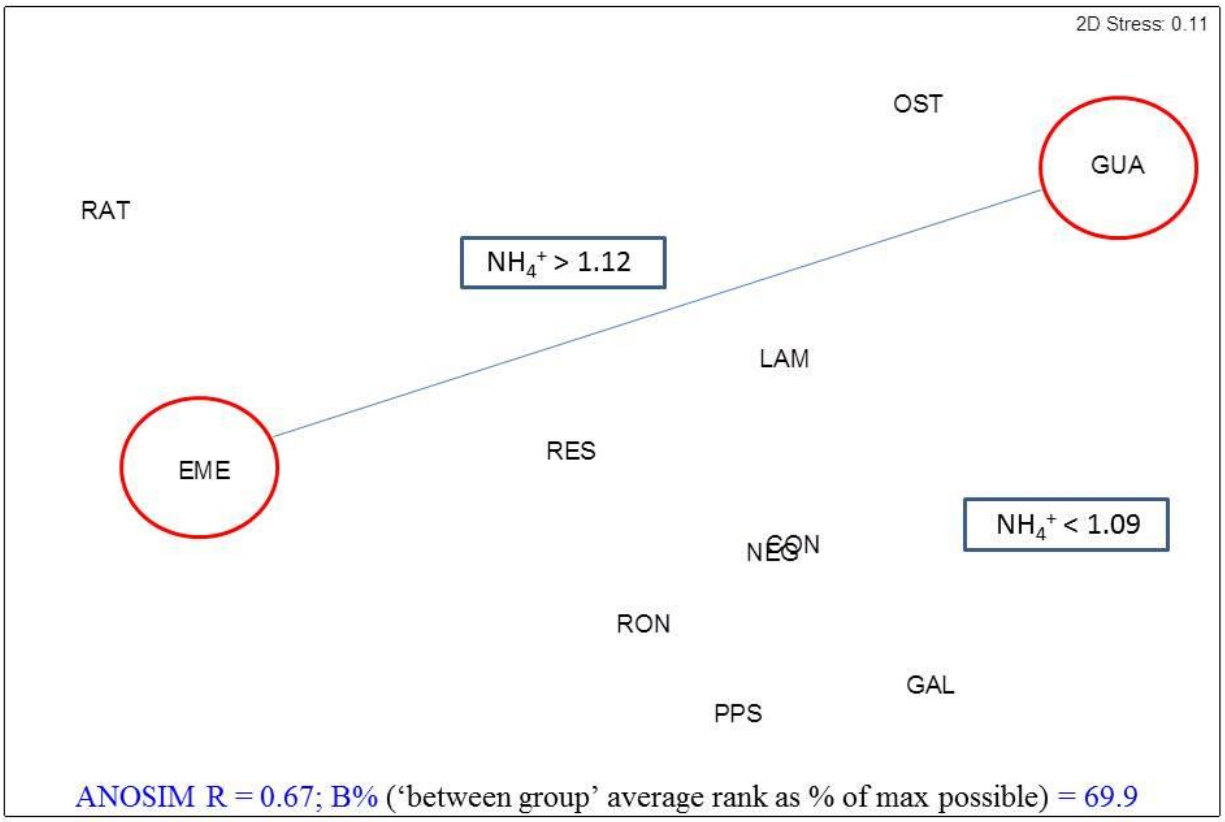

FIGURE 87. Multi-dimensional scaling (MDS) plot of the second stage in a 'linkage tree' of coral recruit community structure to environmental variables. Binary split on basis of the best single environmental variable, thresholded to maximise the ANOSIM R statistic for the two groups formed.

TABLE 4. Summary of a three-way PERMANOVA test of reef fish community structure.

Variable	d.f.	Pseudo-F	*p*
Geographic location	2,94	4.94	<0.0001
Site	10,86	3.59	<0.0001
Depth	3,93	2.70	<0.0001
Location x Site	11,85	3.45	<0.0001
Location x Depth	9,87	2.75	<0.0001
Site x Depth	23,73	2.67	<0.0001
Location x Site x Depth	24,72	2.56	<0.0001

D. Coral reef fish communities

Coral reef fish community structure showed a highly significant variation among all geographic zones, sites and depth zones, suggesting a strong effect associated to geographic location, to the LBSP gradient and to depth (***Table 4***). PCO analysis suggested that coral reef fish community structure produced four general clustering patterns (***Figure 88***). A first cluster was composed by inshore sites RAT and OST, where RAT was explained by the Princess parrotfish (*Scarus taeniopterus*) and the Beaugregory (*Stegastes leucostictus*), and where OST was explained by Yellowtail parrotfish (*Sparisoma rubripinne*). There was also a second large cluster composed by inshore sites LAM, GUA, and EME, mid-shelf sites RES, CON, and RON, and outer shelf site GAL. These were explained by the Bluehead wrasse (*Thalassoma bifasciatum*) and by the Sharpnose puffer (*Canthigaster rostrata*). Outer shelf site NEG constituted an independent cluster mostly explained by multiple fish species, including the French angelfish (*Pomacanthus paru*), the Creole wrasse (*Clepticus parrae*), and the Brown chromis (*Chromis multilineata*). But also a consortium of five fish species explained the separation of NEG as an individual cluster, including the Tobacco fish (*Serranus tabacarius*), the Bermuda chub (*Kyphosus sectatrix*), the Atlantic spadefish (*Chaetodipterus faber*), the Rainbow parrotfish (*Scarus guacamaia*), and the Frillfin goby (*Bathygobius soporator*). Outer shelf site PPS also constituted an independent cluster explained by the Yellowtail snapper, *Ocyurus chrysurus*, and by the Cleaning goby, *Elacatinus genie*, and by wrasse *Bodianus pulchellus*. These spatial patterns evidenced an unequivocal cross-shelf gradient of fish species distribution influenced by reef position and condition, depth, and water quality.

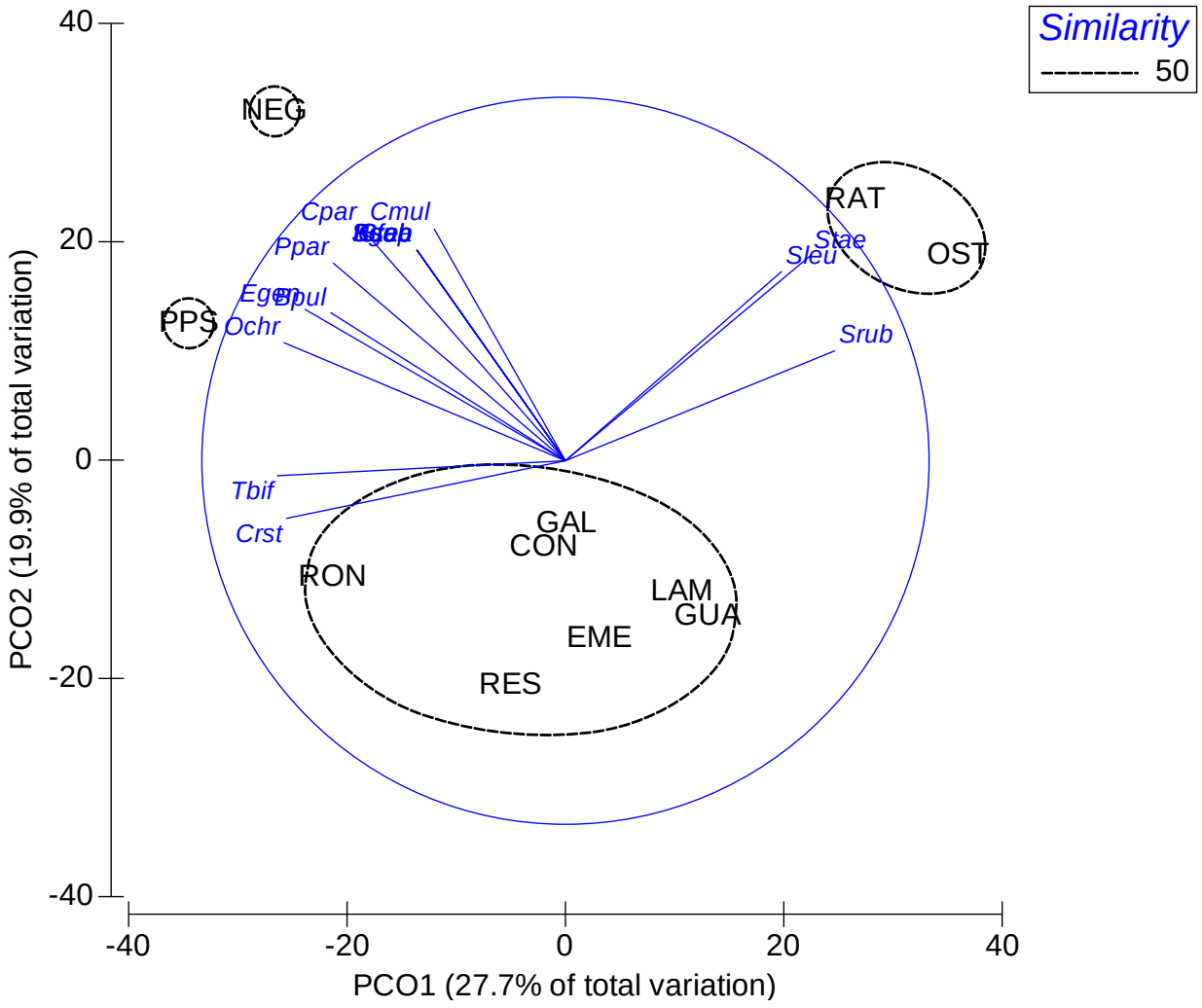

FIGURE 88. Principal component ordination plot of coral reef fish communities among study sites. Clusters based on 50% similarity cut off level. Vectors based on a 0.70 correlation. This model explained 60.9% of the observed variation.

PCO analysis also revealed that the observed spatial clustering pattern in fish community structure was influenced by water quality spatial patterns (***Figure 89***). The inshore cluster composed by RAT and OST was largely explained by turbidity, chlorophyll-*a*, and salinity in a lesser extent. The large cluster formed by inshore sites LAM, GUA, and EME, the mid-shelf RES, CON, and RON, and the outer shelf GAL were explained by PO_4 and NH_4^+ concentrations, and in a lesser extent by conductivity and OABs, particularly across inshore sites. Outer shelf sites PPS and NEG were most likely explained by dissolved oxygen concentration.

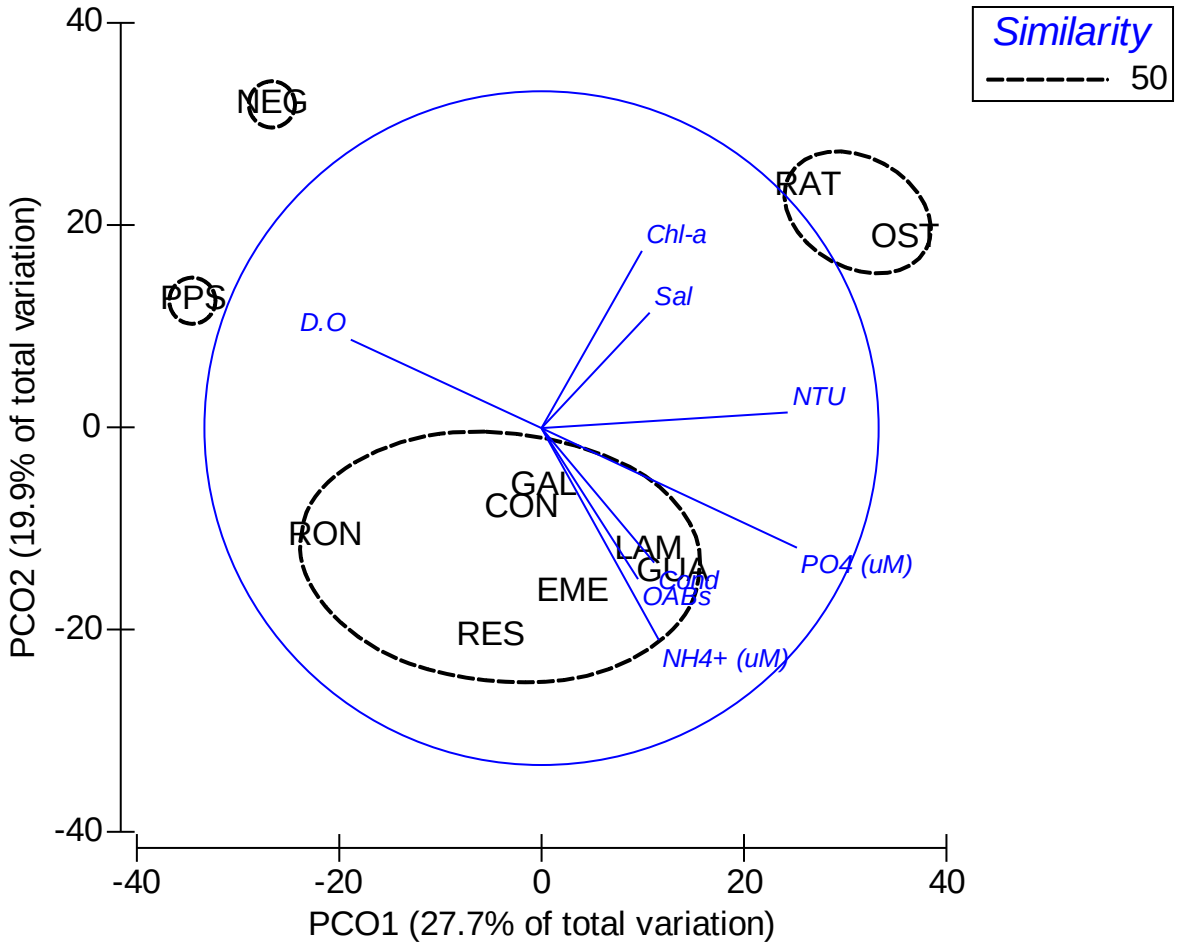

FIGURE 89. Principal component ordination plot of coral reef fish communities among study sites based on water quality spatial patterns. Clusters based on 50% similarity cut off level. This model explained 60.9% of the observed variation.

A % cumulative dominance plot of fish species also evidenced the observed cross-shelf spatial gradient of fish species richness (***Figure 90***). A SIMPER test of indicator fish species based on biomass estimates revealed that parrotfishes (Scaridae) were the most significant indicators of spatial patterns across most surveyed sites (***Table 5***). The Striped parrotfish (*Scarus iserti*) was the most common indicator species across 6 out of 11 sites (55%). Four other parrotfish species, including *Sparisoma rubripinne*, *Sp. viride*, *Sp. aurofrenatum*, and *Scarus taeniopterus*, as well as Labrid *Clepticus parrae* were also indicator species at individual sites. These were the most dominant (=higher mean biomass) across sites.

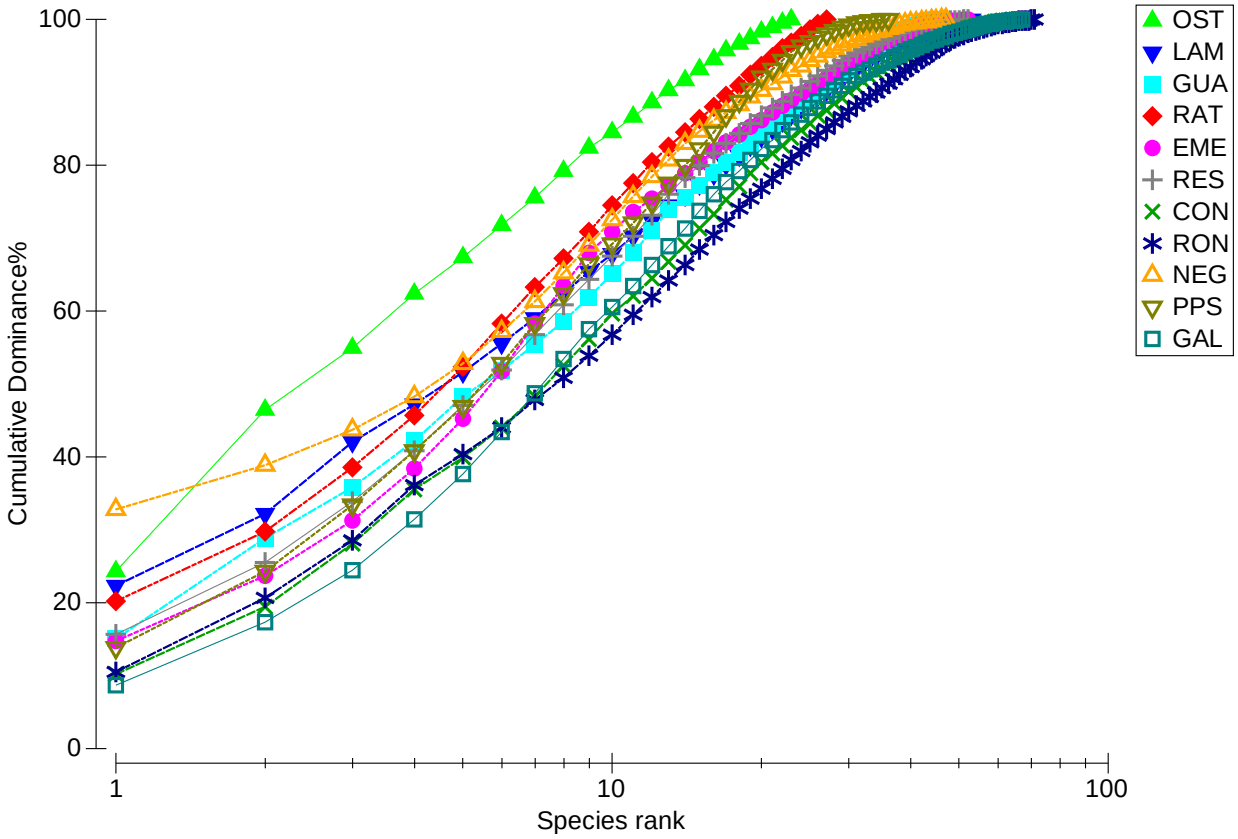

FIGURE 90. Cumulative fish species dominance plot.

TABLE 5. Summary of SIMPER test of the three most dominant coral reef fish species across sites.

Species/Site	% Contrib.	Cum. %
OST		
Sparisoma rubripinne	31.73	31.73
Acanthurus coeruleus	16.40	48.13
Scarus iserti	2.06	63.36
LAM		
Scarus iserti	33.50	33.50
Sparisoma viride	23.24	56.74
Sparisoma rubripinne	8.07	64.81
GUA		
Scarus iserti	29.99	29.99
Acanthurus bahianus	10.85	40.85
Sparisoma viride	10.24	51.09
RAT		
Scarus taeniopterus	26.66	26.66
Stegastes planifrons	21.96	48.62
Scarus iserti	12.49	61.11
EME		
Scarus iserti	23.67	23.67
Acanthurus coeruleus	21.08	44.75
Acanthurus bahianus	15.46	60.21
RES		
Scarus iserti	27.57	27.57
Sparisoma viride	11.80	39.37
Sparisoma aurofrenatum	11.74	51.10
CON		
Sparisoma viride	18.37	18.37
Sparisoma aurofrenatum	15.46	33.83
Scarus iserti	14.41	48.24
RON		
Sparisoma aurofrenatum	20.37	20.37
Sparisoma viride	14.46	34.83
Scarus iserti	13.65	48.48
NEG		
Clepticus parrae	29.84	29.84
Sparisoma viride	14.02	43.86
Scarus iserti	9.74	53.61
PPS		
Scarus iserti	20.84	20.84
Stegastes partitus	9.97	30.82
Cephalopholis fulva	8.84	39.65
GAL		
Scarus iserti	15.24	15.24
Melichthys niger	12.07	27.30
Sparisoma aurofrenatum	9.19	36.50

TABLE 6. Summary of percent dissimilarities in coral reef fish assemblages across sites.

Sites	LAM	GUA	RAT	EME	RES	CON	RON	NEG	PPS	GAL
OST	74	73	66	73	75	71	78	86	82	74
LAM	-	72	73	75	67	69	73	81	80	72
GUA		-	76	71	69	70	75	84	80	74
RAT			-	75	74	69	76	80	81	71
EME				-	66	69	75	82	76	74
RES					-	63	66	77	74	66
CON						-	62	76	74	62
RON							-	77	75	66
NEG								-	79	76
PPS									-	77
GAL										-

There was also a spatial gradient of increasing mean dissimilarities in fish assemblages with increasing distance from the shore (***Table 6***). Mean % dissimilarity within inshore sites was 72.8%, with a range of 66 to 76%. Mean % dissimilarity within mid-shelf sites was 63.7%, with a range of 62 to 66%. Mean % dissimilarity within outer-shelf sites was 77.3%, with a range of 76 to 79%. Mean % dissimilarity between inshore and mid-shelf sites was 71.7%, and between inshore and outer shelf sites was 78.5%. Mean % dissimilarity between mid-shelf and outer shelf sites was 71.9%. This suggests that geographic distance, and potentially reef condition and a water quality stress gradient could have influenced cross-shelf fish diversity distribution.

TABLE 7. Indicator coral reef fish species analyses across sites based on SIMPER test.

Sites	LAM	GUA	RAT	EME	RES	CON	RON	NEG	PPS	GAL
OST	*Sise*^	*Srub*<	*Stae*<	*Srub*<	*Srub*<	*Srub*<	*Srub*<	*Cpar*^	*Srub*<	*Srub*<
LAM	-	*Sise*<	*Sise*<	*Sise*<	*Sise*<	*Sise*<	*Sise*<	*Cpar*^	*Sise*<	*Sise*<
GUA		-	*Stae*<	*Svir*<	*Svir*^	*Svir*^	*Saur*^	*Cpar*^	*Cpar*^	*Mnig*^
RAT			-	*Stae*<	*Stae*<	*Stae*<	*Stae*<	*Cpar*^	*Cpar*^	*Mnig*^
EME				-	*Sise*^	*Saur*^	*Sbar*^	*Cpar*^	*Cpar*^	*Mnig*^
RES					-	*Sise*<	*Sbar*^	*Cpar*^	*Cpar*^	*Mnig*^
CON						-	*Sbar*^	*Cpar*^	*Cpar*^	*Mnig*^
RON							-	*Cpar*^	*Cpar*^	*Mnig*^
NEG								-	*Cpar*<	*Cpar*<
PPS									-	*Crub*<
GAL										-

^= Higher biomass at the site above. <= Higher biomass at the site in the left.

SIMPER analysis also allowed determining indicator species of spatial differences among all sites (***Table 7***). The Striped parrotfish (*Scarus iserti*), followed by the Princess parrotfish (*Sc. taeniopterus*), was the most important indicator species of differences among inshore sites. The Barracuda (*Sphyraena barracuda*) was the most important indicator species of differences among mid-shelf sites, while the Creole wrasse (*Clepticus parrae*) was the most important indicator among outer shelf sites. Differences between inshore and mid-shelf sites were mostly explained by three parrotfish species, *Sparisoma rubripinne*, *Sc. taeniopterus*, and *Sc. iserti*. Differences between inshore sites and outer shelf sites were mostly explained by *C. parrae*, followed by the Black durgon (*Melichthys niger*). Differences between mid-shelf and outer shelf sites were also mostly explained by these two species, and in a lower extent by the Bar jack (*Carangoides ruber*).

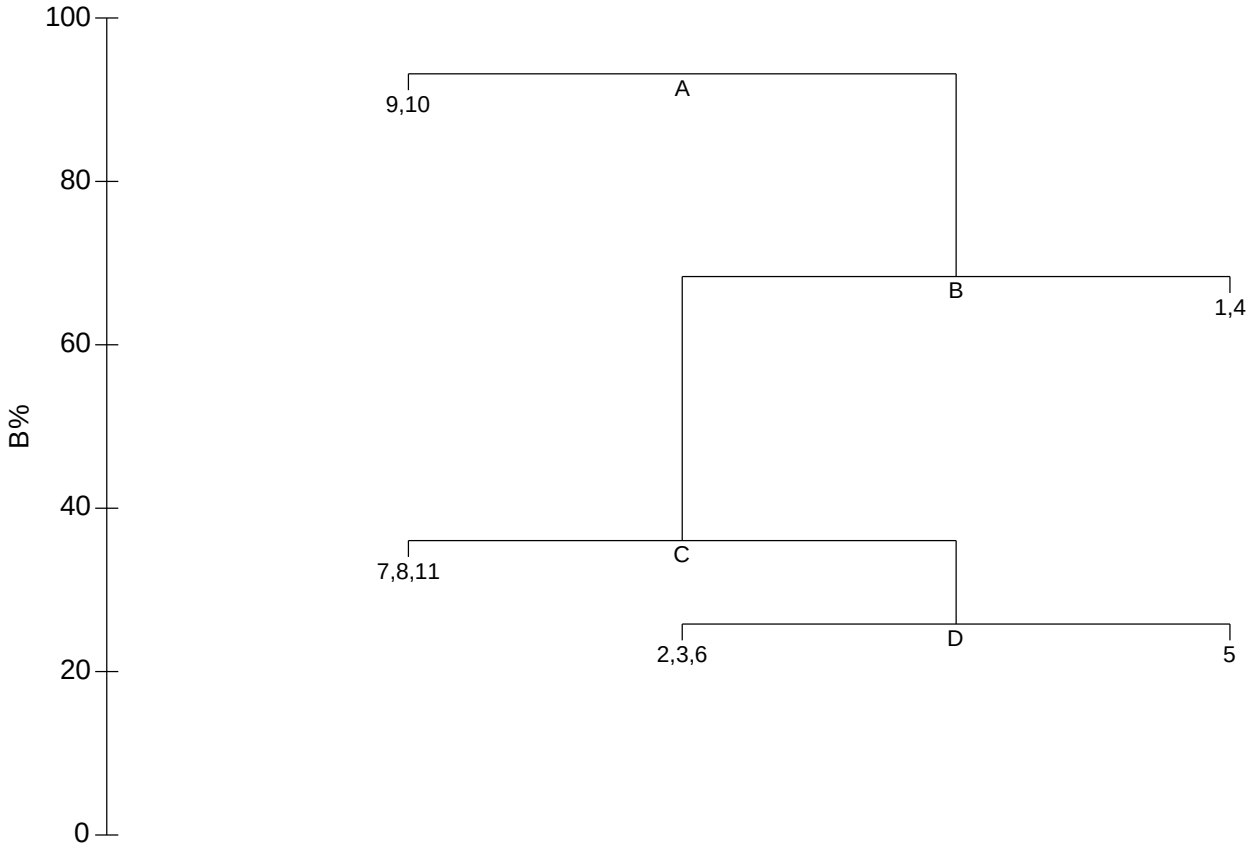

A->(9,10),B= R: 0.83, B%: 93.2, PO_4 < -1.57 (> -0.46), OABs < -1.33 (> -1.19)
B->C,(1,4)= R: 0.90, B%: 68.4, Chl-*a* < 0.88 (>1.16),NTU < 1.14 (> 1.17)
C->(7,8,11),D= R: 0.67 B%: 36.0, NH_4^+ < -0.515 (>0.76)
D->(2,3,6), (5)= R: 0.78 B%: 25.8, OABs < -8.29E-2 (> 1.41), PO_4 < 0.4 (> 1.34), Chl-*a* <6.2E-2 (> 0.88), NH_4^+ <1.12 (> 1.77), NTU <1.06 (> 1.14)
Sample numbers for plot 1)RAT;2)OST;3)LAM;4)GUA;5)EME;6)RES;7)CON;8)RON;9)NEG;10)PPS;11)GAL

FIGURE 91. LINKTREE analysis of coral reef fish community structure as a function of water quality parameters. Data was log_{10}-transformed and normalized for analysis. Numbers are Euclidean distances. B%= 'between group' average rank as % of maximum possible.

A 'linkage tree' of coral reef fish community structure based on the BIOENV routine to environmental variables was carried out (***Figure 91***). Binary split on basis of the best single environmental variable was thresholded to maximise the ANOSIM R statistic for the two groups formed. The first split (A) in the assemblage data is between sites 9 (NEG) and 10 (PPS) in the left side of the tree, and the rest in the right side of the tree. This division is also reflected in the

MDS plot of the test with an ANOSIM of R= 0.83 and B= 93.2% (***Figure 92***). It is characterized by a low PO_4 concentration (Euclidean distance > 1.45) to the left of the tree at outer shelf sites NEG and PPS, and a high PO_4 concentration (Euclidean distance < 1.17) to the right side of the graph (***Figure 91***). Alternatively, the same split of sites was obtained with low OABs concentration (Euclidean distance < -1.33) to the left of the tree at outer shelf sites NEG and PPS, and high OABs concentration (Euclidean distance > -1.19) to the right of the tree (***Figure 91***). ANOSIM R was the same whichever of the two variables was used as they gave the same split of biotic data.

Moving down the tree, split (B) provides the second most strong explanation of spatial patterns with a split between inshore sites 1 (RAT) and 5 (GUA) to the right and the rest to the left, with low chl-*a* concentration to the left (Euclidean distance < 0.88) and high to the right at RAT and GUA (Euclidean distance > 1.16), and an ANOSIM R= 0.90, and B= 68.4% (***Figure 93***). Alternatively, the same split of sites was obtained with low turbidity (Euclidean distance < 1.14) to the left of the tree, and high turbidity (Euclidean distance > 1.17) to the right of the tree at RAT and GUA (***Figure 91***). ANOSIM R was the same whichever of the two variables was used as they gave the same split of biotic data. But split A offered the best solution.

LINKTREE analysis showed that variation in PO_4 and OABs concentrations explained most of the spatial variation observed in the cross-shelf coral reef fish community structure. A multivariate correlation using the RELATE routine showed a strong significant correlation (Rho=0.362, p=0.0027) between the entire fish community matrix and the water quality matrix. Further, BIOENV and BVSTEP analyses showed that the coral reef fish community matrix and the water quality matrix showed a correlation of 0.626 (p<0.05) based on PO_4 concentration. Other factors, besides LBSP, could have also influenced fish community spatial patterns, including fishing impacts and habitat decline associated to climate change.

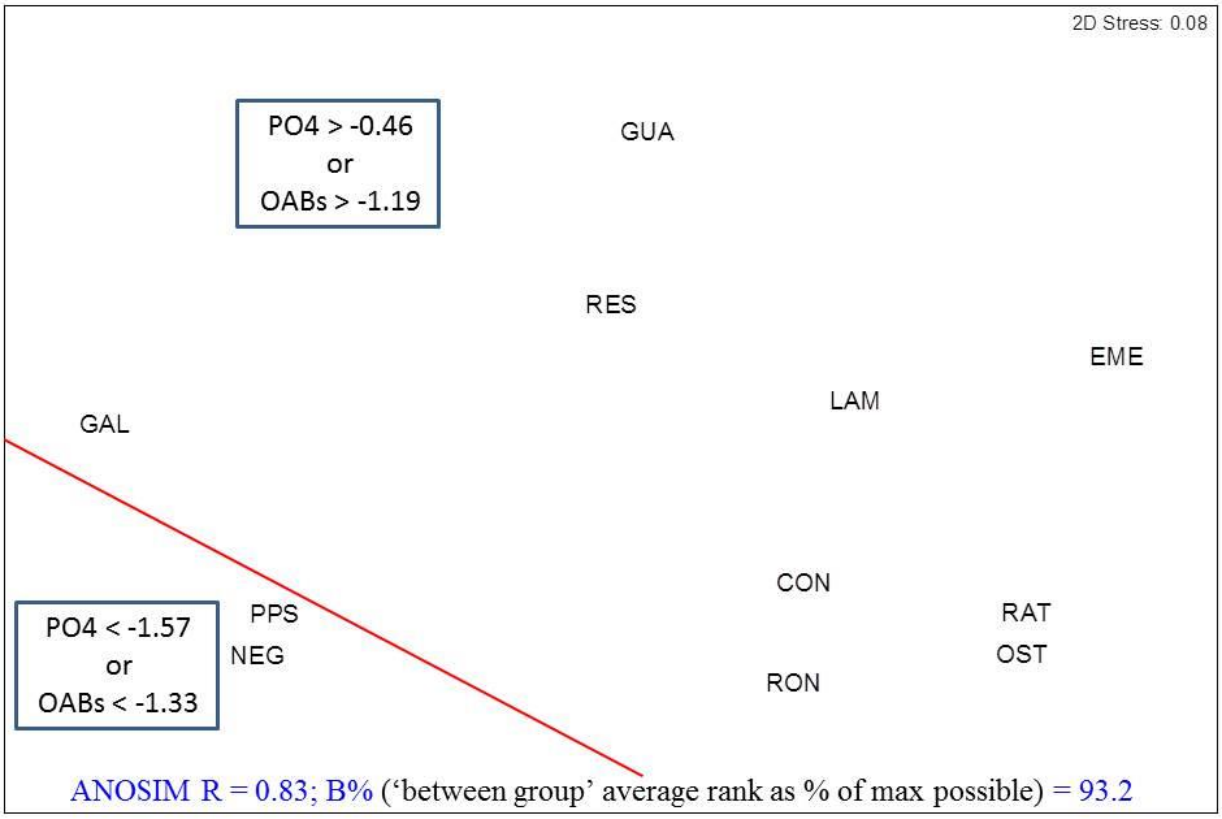

FIGURE 92. Multi-dimensional scaling (MDS) plot of the first stage in a 'linkage tree' of coral reef fish community structure to environmental variables. Binary split on basis of the best single environmental variable, thresholded to maximise the ANOSIM R statistic for the two groups formed.

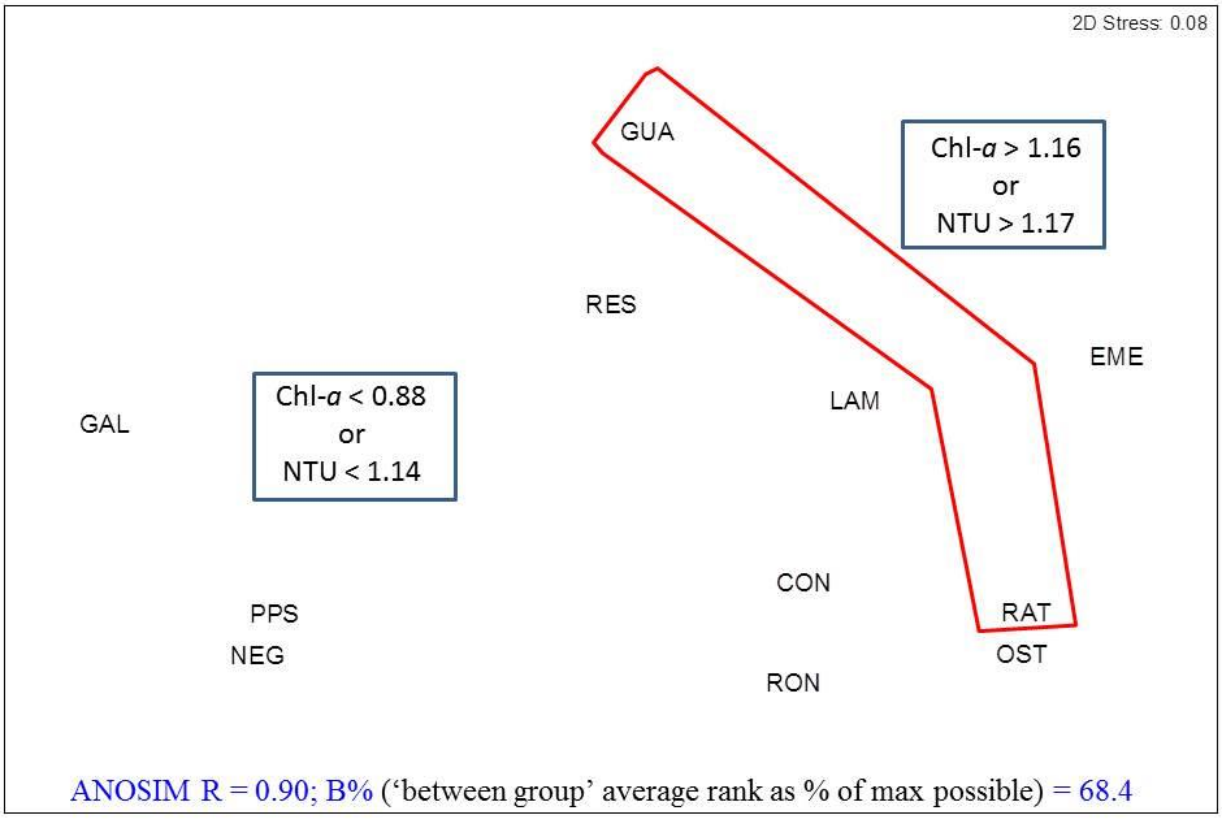

FIGURE 93. Multi-dimensional scaling (MDS) plot of the second stage in a 'linkage tree' of coral reef fish community structure to environmental variables. Binary split on basis of the best single environmental variable, thresholded to maximise the ANOSIM R statistic for the two groups formed.

Mean fish species richness increased with increasing distance from the shore along the documented LBSP gradient (***Figure 94***). Species richness averaged 12.6/count across inshore sites, with a minimum of 9.3 species/count at the 10-15 m depth zone of EME and a maximum of 14.2 species/count at the <5 m depth zone of GUA. Species richness increased to 18.8/count across mid-shelf sites, with a minimum 14.5/count at the <5 m depth zone of RES and a maximum of 27/count at the 10-15 m depth zone of RON. Species richness also averaged 18.8/count across outer shelf sites, with a minimum of 14/count at the 5-10 m depth zone of NEG and at the 10-15 m depth zone of PPS, and a maximum of 27/count at the 10-15 m depth zone of GAL. Significantly polluted and degraded EME site showed the lowest species richness.

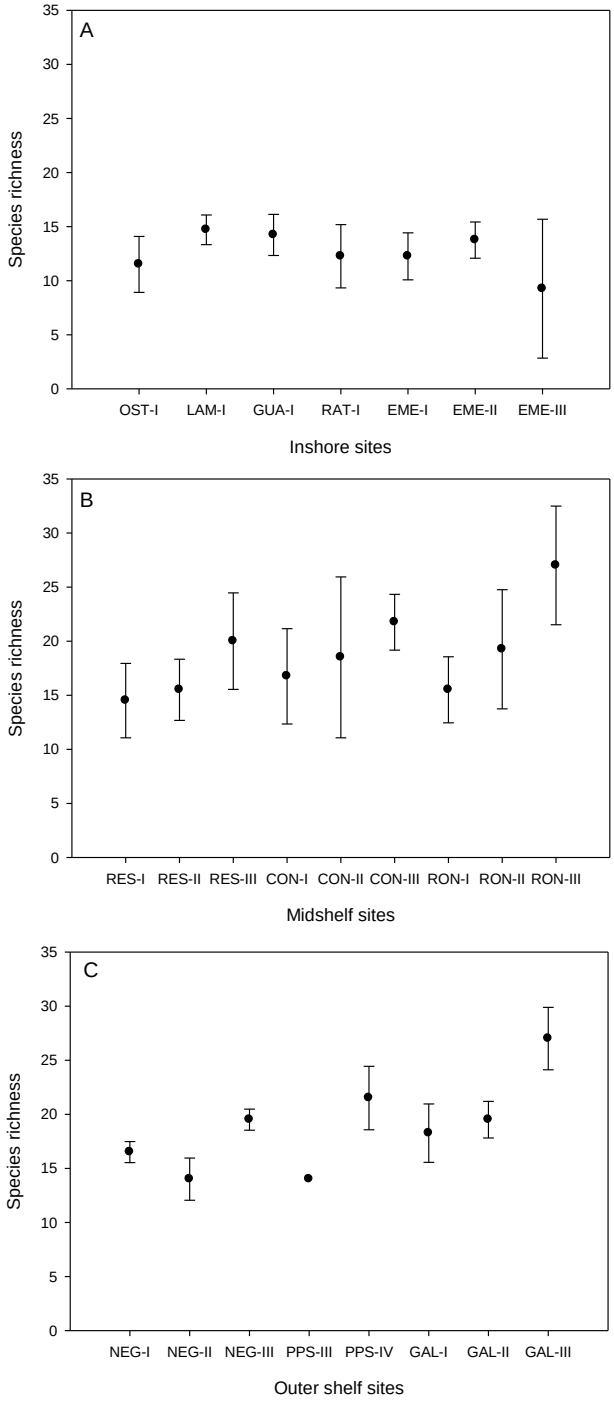

FIGURE 94. Fish species richness across study sites: A) Inshore reefs; B) Mid-shelf reefs; and C) Outer shelf reefs. Mean±95% confidence interval. I= <5 m, II= 5-10 m, III= 10-15 m; IV= 15-20 m.

Mean fish abundance showed a similar increase with increasing distance from the shore along the documented LBSP gradient (***Figure 95***). Fish abundance averaged 92.2/count across inshore sites, with a minimum of 23 individuals/count at the 10-15 m depth zone of EME and a maximum of 204 individuals/count at the <5 m depth zone of LAM, mostly juvenile and semi-adult parrotfishes (Scaridae). Abundance increased to 166/count across mid-shelf sites, with a minimum of 87/count at the 10-15 m depth zone of RES and a maximum of 307/count at the 10-15 m depth zone of RON. Abundance further increased to 409/count across outer shelf sites, with a minimum of 98/count at the 5-10 m depth zone of GAL and a maximum of 1,336/count at the 10-15 m depth zone of NEG. The lowest fish abundances were documented across the most degraded and polluted reef sites.

Mean fish species diversity (H'n) followed the classical Connell (1978) intermediate disturbance hypothesis curve with higher H'n under intermediate disturbance levels and lower H'n under either low or frequent disturbance levels. H'n averaged 1.9567 across inshore sites, with a minimum of 1.7631 at the 10-15 m depth zone of EME and a maximum of 2.2062 at the 5-10 m depth zone of EME (***Figure 96***). H'n increased to 2.1301 across mid-shelf sites, with a minimum of 1.8693 at the 5-10 m depth zone of RON and a maximum of 2.3401 at the 10-15 m depth zone of RES. H'n averaged 1.8089 across outer shelf sites, with a minimum of 1.0080 at the 10-15 m depth zone of NEG and a maximum of 2.3195 at the 10-15 m depth zone of GAL. Declining H'n was often the result of dominance by juvenile and semi-adult parrotfish (Scaridae) guilds across shallow inshore sites, and by Creole wrasse (*Clepticus parrae*) and Yellowtail snapper (*Ocyurus chrysurus*) schools across outer shelf sites. However, benthic structural complexity, sediment deposition and the condition of benthic habitats did influence these results.

Mean fish species evenness (J'n) showed a declining trend with increased distance from the shore and increased dominance by selected species across outer shelf sites (***Figure 97***). J'n averaged 0.7877 across inshore sites, with a minimum of 0.6865 at the <5 m depth zone of OST and a maximum of 0.8588 at the 10-15 m depth zone of EME. J'n increased to 0.7371 across mid-shelf sites, with a minimum of 0.6221 at the 10-15 m depth zone of RON and a maximum of 0.8230 at the <5 m depth zone of RON. J'n averaged 0.6162 across outer shelf sites, with a minimum of 0.3397 at the 10-15 m depth zone of NEG and a maximum of 0.7613 at the 5-10 m depth zone of GAL. Declining J'n was the result of dominance by *C. parrae*) and *O. chrysurus*.

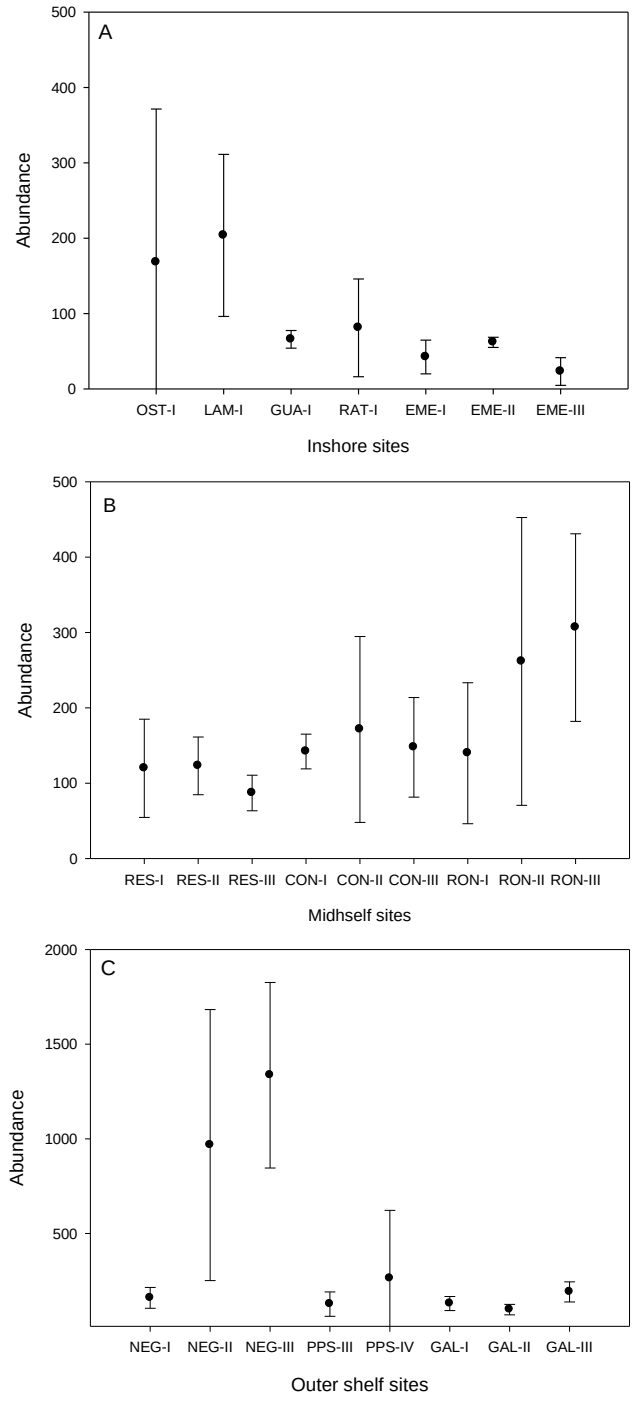

FIGURE 95. Total fish abundance across study sites: A) Inshore reefs; B) Mid-shelf reefs; and C) Outer shelf reefs. Mean±95% confidence interval. I= <5 m, II= 5-10 m, III= 10-15 m; IV= 15-20 m.

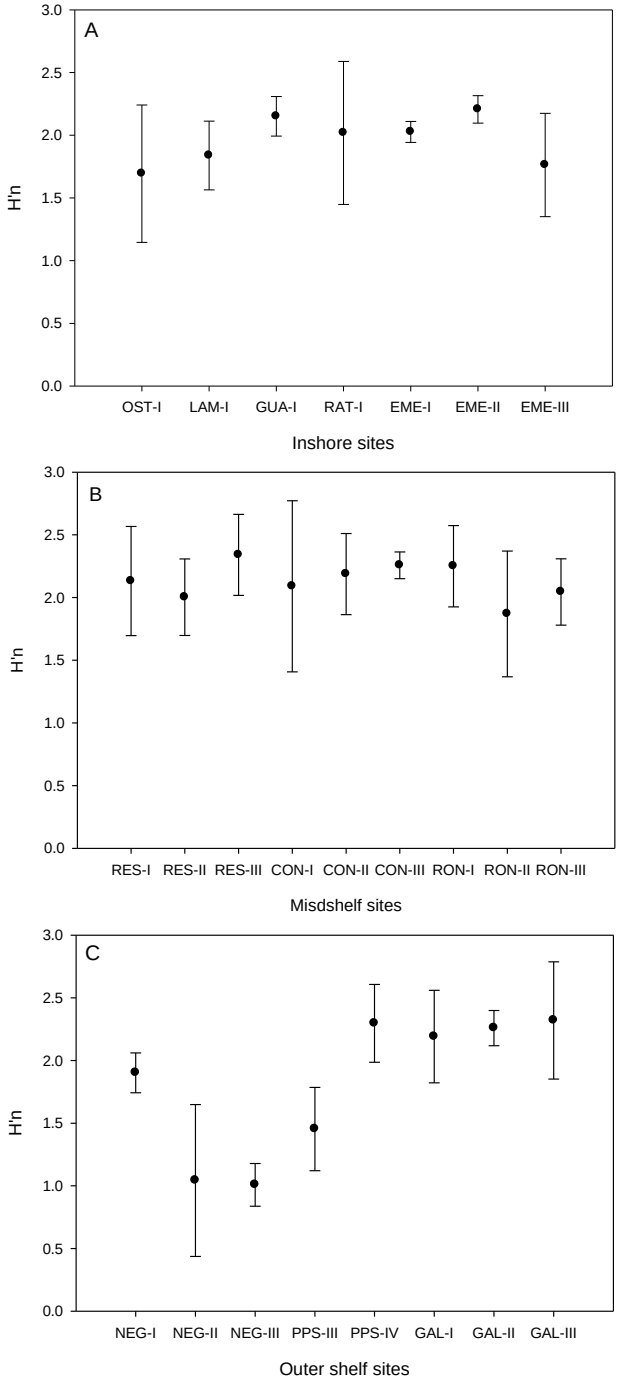

FIGURE. 96. Fish species diversity (H'n) across study sites: A) Inshore reefs; B) Mid-shelf reefs; and C) Outer shelf reefs. Mean±95% confidence interval. I= <5 m, II= 5-10 m, III= 10-15 m; IV= 15-20 m.

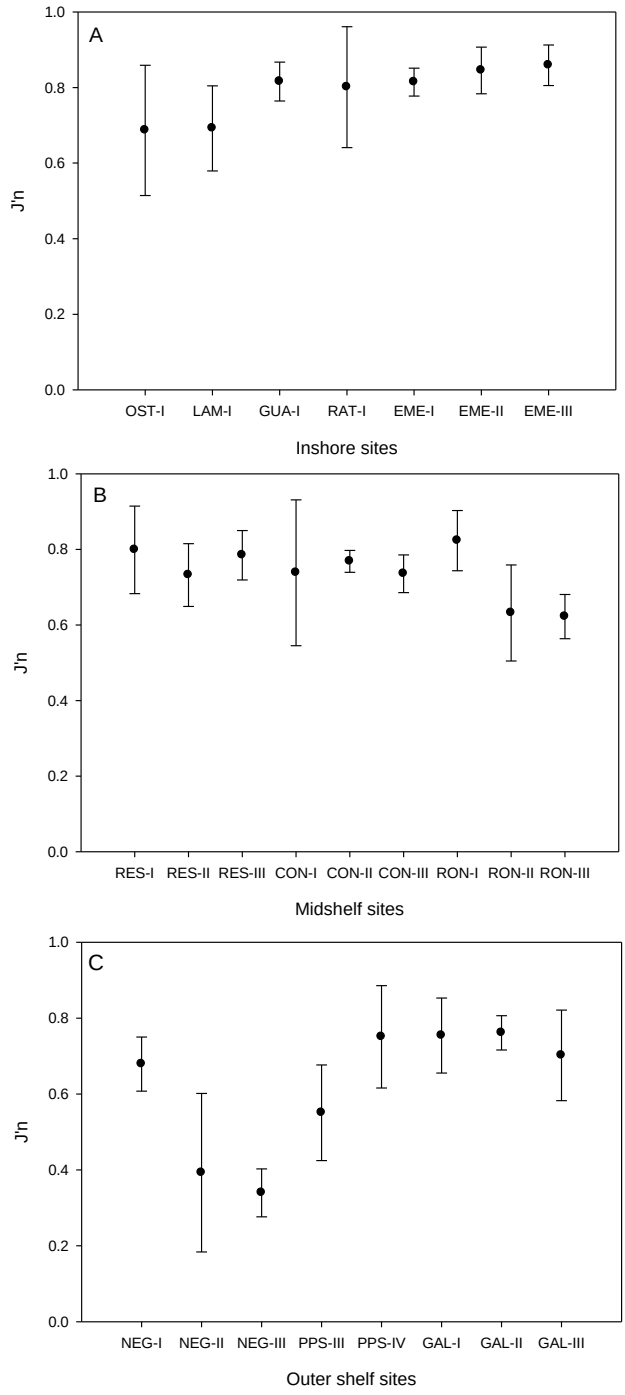

FIGURE. 97. Fish species evenness (J'n) across study sites: A) Inshore reefs; B) Mid-shelf reefs; and C) Outer shelf reefs. Mean±95% confidence interval. I= <5 m, II= 5-10 m, III= 10-15 m; IV= 15-20 m.

Mean total herbivore fish abundance averaged 76.7 individuals/count across inshore sites, with a minimum of 13/count at the 10-15 m depth zone of EME and a maximum of 177/count at the <5 m depth zone of LAM (***Figure 98***). Total herbivore abundance across mid-shelf sites averaged 89 individuals/count, with a minimum of 50/count at the 10-15 m depth zone of RES and a maximum of 131 individuals/count at the 5-10 m depth zone of CON. Total herbivores averaged 42 individuals/count across outer shelf sites, with a minimum of 16 individuals/count at the 10-15 m depth zone of PPS and a maximum of 70 individuals/count at the 10-15 m depth zone of GAL. Overall, total herbivore abundance declined with declining algal cover and distance from the shore. Scrapers were the most abundant functional herbivore guild, followed by browsers and non-denuders (***Figure 99***).

Mean total carnivore fish abundance showed a significant increase with increased distance from the shore, averaging 13 individuals/count across inshore sites, with a minimum of 10/count at the 5-10 m depth zone of RAT and a maximum of 19/count at the <5 m depth zone of LAM (***Figure 100***). Total carnivore abundance across mid-shelf sites averaged 44 individuals/count, with a minimum of 25 individuals/count at the <5 m depth zone of CON and a maximum of 110 individuals/count at the 10-15 m depth zone of RON. Total carnivores averaged 239 individuals/count across outer shelf sites, with a minimum of 43 individuals/count at the 10-15 m depth zone of GAL and a maximum of 805/count at the 10-15 m depth zone of NEG.

Total carnivore guilds showed a significant difference in their assemblages depending on the geographic location (***Figure 101***). For instance, generalist carnivores were proportionately dominant across inshore and mid-shelf sites, while planktivores became more common across mid-shelf sites, and eventually dominated outer shelf sites. Piscivore abundance was particularly concerning. Piscivores averaged only 2.7 individuals/count across inshore sites, with a minimum value of 0.8 individuals/count at the <5 m depth zone of EME and a maximum value of 5.5 individuals/count at the 5-10 m depth zone of EME. Piscivores averaged 3.1 individuals/count across mid-shelf sites, with a minimum of 0.5 individuals/count at the <5 m depth zone of RES, and a maximum of 16 individuals/count at the 10-15 m depth zone of RON. Piscivores averaged 10 individuals/count across outer shelf sites, with none present across the <5 m depth zone of NEG, and a maximum of 64 individuals/count across the 15-20 m deep wall of PPS, mostly the

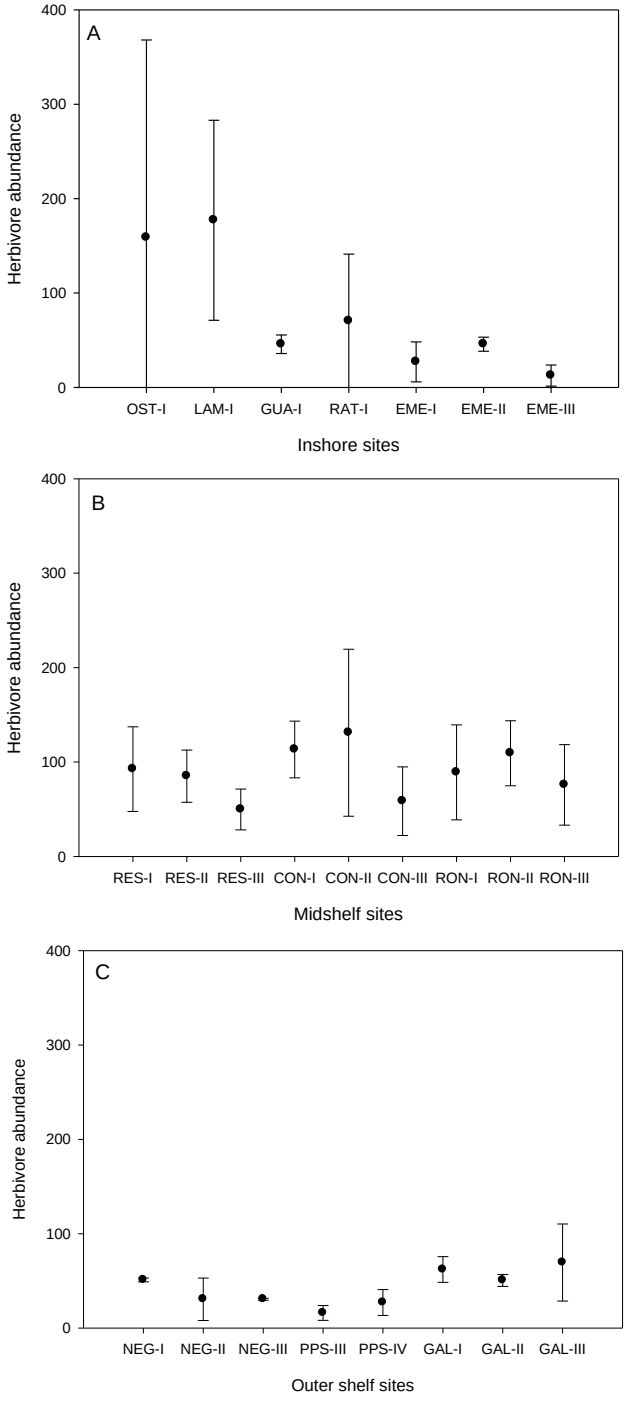

FIGURE 98. Total herbivore abundance across study sites: A) Inshore reefs; B) Mid-shelf reefs; and C) Outer shelf reefs. Mean±95% confidence interval. I= <5 m, II= 5-10 m, III= 10-15 m; IV= 15-20 m.

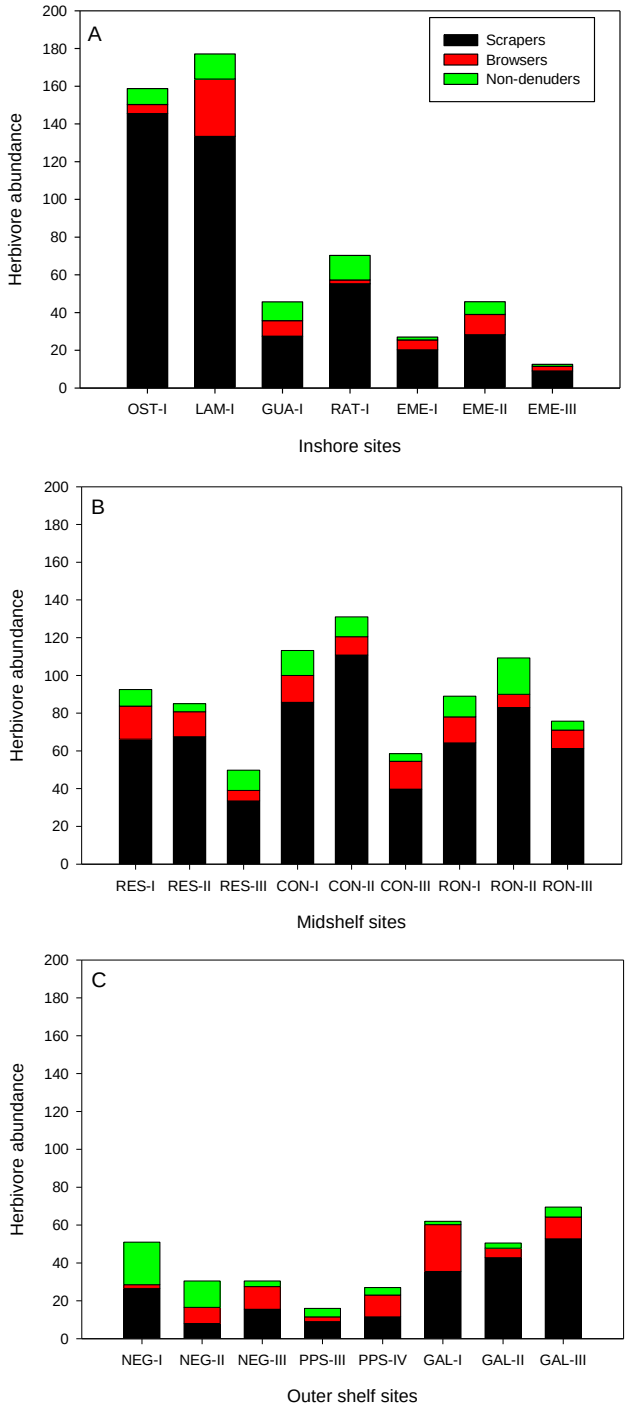

FIGURE 99. Mean herbivore guilds abundance across study sites: A) Inshore reefs; B) Mid-shelf reefs; and C) Outer shelf reefs. Scrapers (Scaridae), Browsers (Acanthuridae), Non-denuders (Pomacentridae). I= <5 m, II= 5-10 m, III= 10-15 m; IV= 15-20 m.

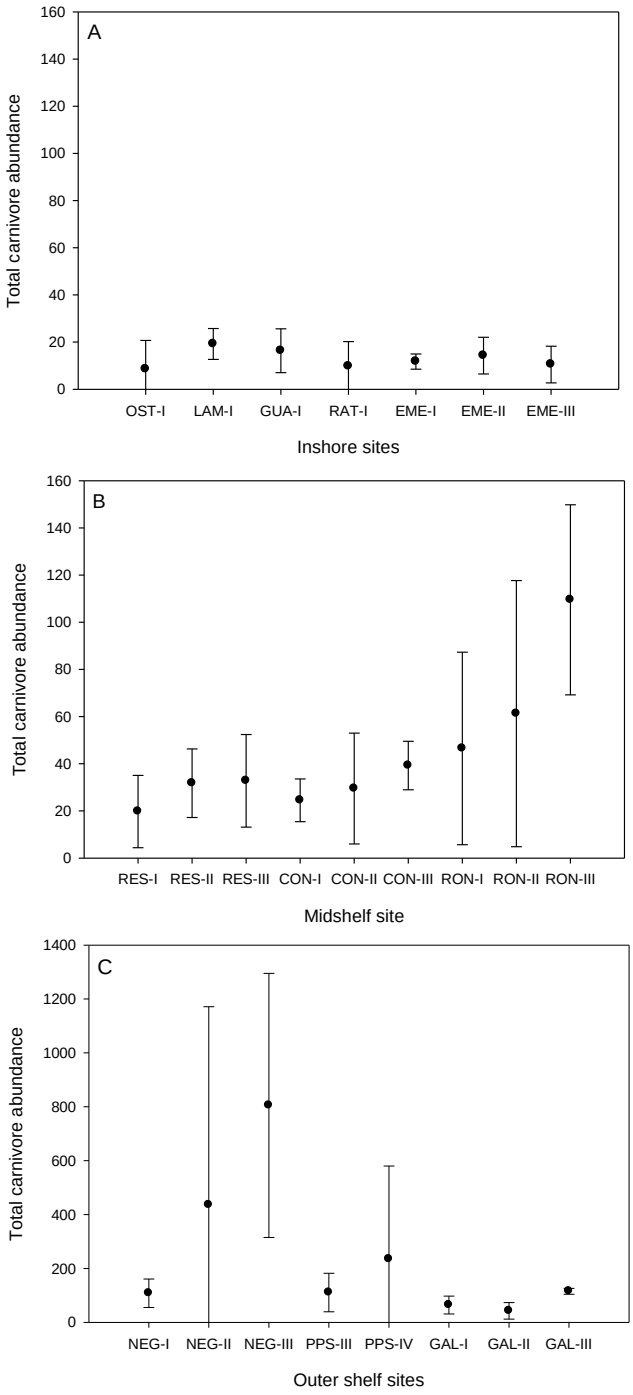

FIGURE 100. Total carnivore abundance across study sites: A) Inshore reefs; B) Mid-shelf reefs; and C) Outer shelf reefs. Mean±95% confidence interval. I= <5 m, II= 5-10 m, III= 10-15 m; IV= 15-20 m.

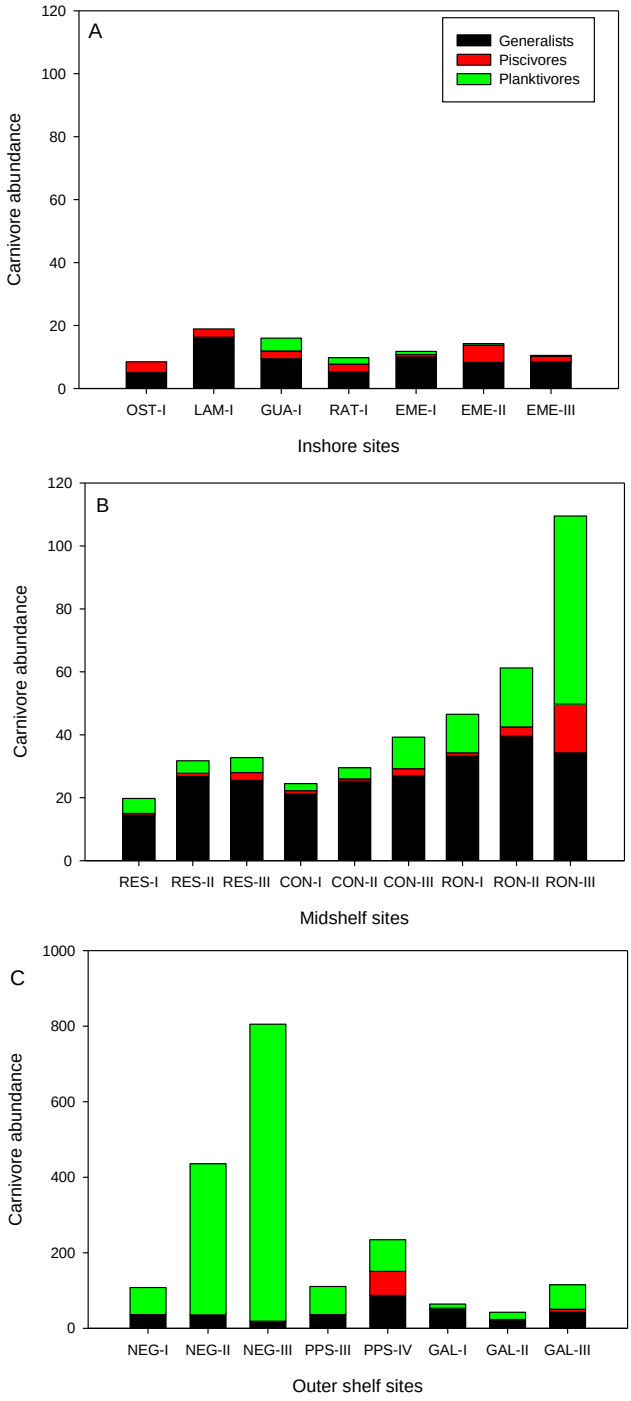

FIGURE 101. Mean carnivore guilds abundance across study sites: A) Inshore reefs; B) Mid-shelf reefs; and C) Outer shelf reefs. I= <5 m, II= 5-10 m, III= 10-15 m; IV= 15-20 m.

Yellowtail snapper, *Ocyurus chrysurus*. These values are very low and share light on possibly significant cross-shelf fishing impacts.

Mean omnivore fish abundance showed a significant increase with increased distance from the shore, averaging less than 3 individuals/count across inshore sites, with none present at the 10-15 m depth zone of EME and a maximum of 4/count at the <5 m depth zone of GUA (***Figure 102***). Omnivore abundance across mid-shelf sites averaged 33 individuals/count, with a minimum of 4/count at the 10-15 m depth zone of RES, and the <5 m depth zone of CON and RON, and a maximum of 121/count at the 10-15 m depth zone of RON. Omnivores averaged 127 individuals/count across outer shelf sites, with none present at the 10-15 m depth zone of PPS and a maximum of 501/count at the 5-10 m depth zone of NEG.

There was a significant increase in mean total fish biomass with increasing distance from the shore along the documented LBSP gradient (***Figure 103***). Total biomass averaged 3,222 g/count across inshore sites, with a minimum of 1,329 g/count at the <5 m depth zone of EME and a maximum of 6,622 g/count at the <5 m depth zone of LAM, mostly juvenile and semi-adult parrotfishes (Scaridae). Total biomass increased to 5,221 g/count across mid-shelf sites, with a minimum of 2,325 g/count at the 5-10 m depth zone of CON and a maximum of 19,291 g/count at the 10-15 m depth zone of RON. Mean total biomass further increased to 15,110 g/count across outer shelf sites, with a minimum of 2,099 g/count at the <5 m depth zone of NEG and a maximum of 51,284 g/count at the 10-15 m depth zone of NEG. The lowest biomass values were documented across the most degraded reef sites.

Mean total herbivore fish biomass averaged 2,392 g/count across inshore sites or a mean 74% of the total observed biomass, with a minimum of 503 g/count at the 10-15 m depth zone of EME and a maximum of 5,550 g/count at the <5 m depth zone of LAM (***Figure 104***). Total herbivore biomass across mid-shelf sites averaged 2,357 g/count or a mean 45% of the total observed biomass, with a minimum of 1,363 g/count at the 10-15 m depth zone of CON and a maximum of 3,060 g/count at the 5-10 m depth zone of RON. Total herbivore biomass averaged 2,941 g/count across outer shelf sites or 19% of the total documented biomass, with a minimum of 689 g/count at the 10-15 m depth zone of PPS and a maximum of 8,104 g/count at the 5-10 m depth zone of NEG. Overall, total herbivore biomass declined with declining algal cover and distance from the shore. Herbivore proportions also declined accordingly. Scraper herbivores were the

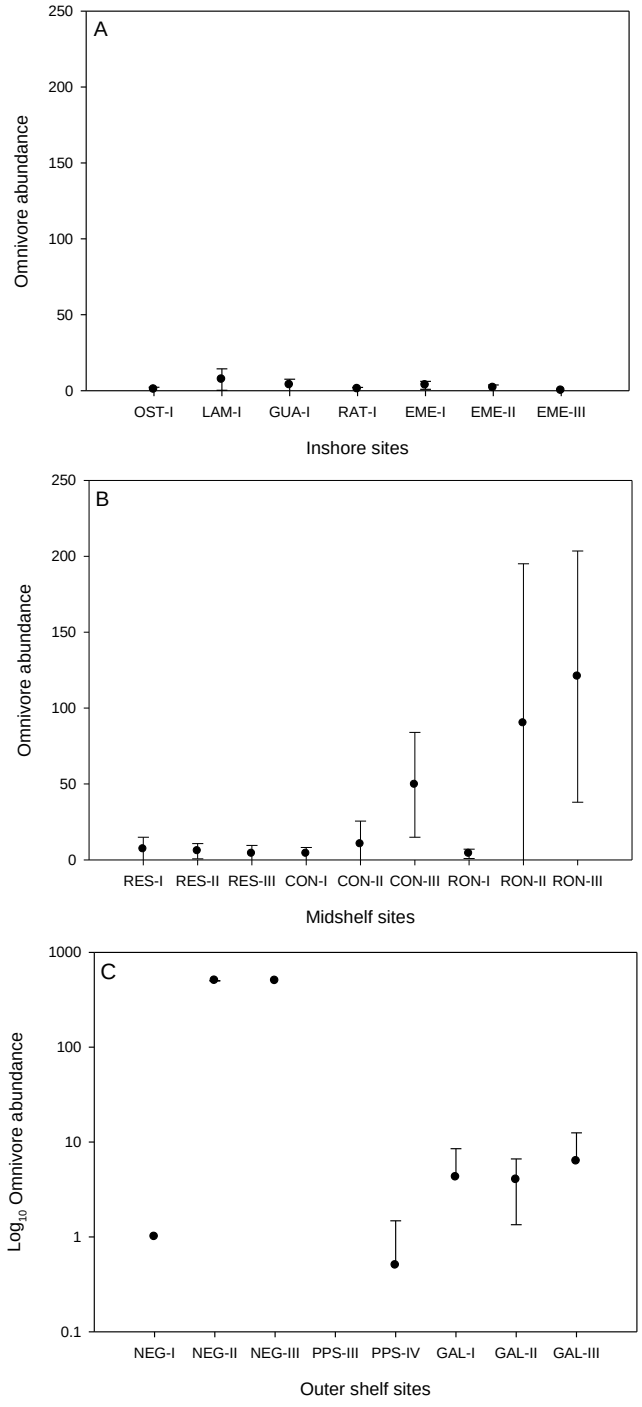

FIGURE 102. Omnivore abundance across study sites: A) Inshore reefs; B) Mid-shelf reefs; and C) Outer shelf reefs. Mean±95% confidence interval. I= <5 m, II= 5-10 m, III= 10-15 m; IV= 15-20 m.

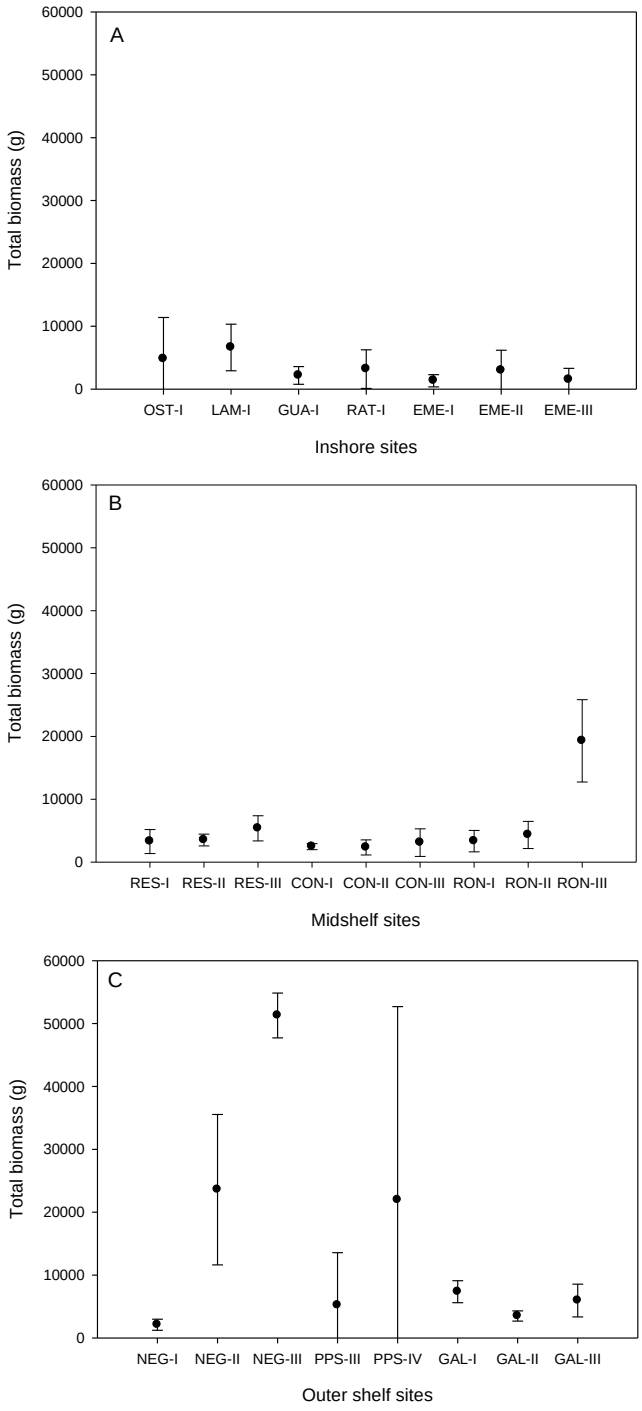

FIGURE 103. Total fish biomass across study sites: A) Inshore reefs; B) Mid-shelf reefs; and C) Outer shelf reefs. Mean±95% confidence interval. I= <5 m, II= 5-10 m, III= 10-15 m; IV= 15-20 m.

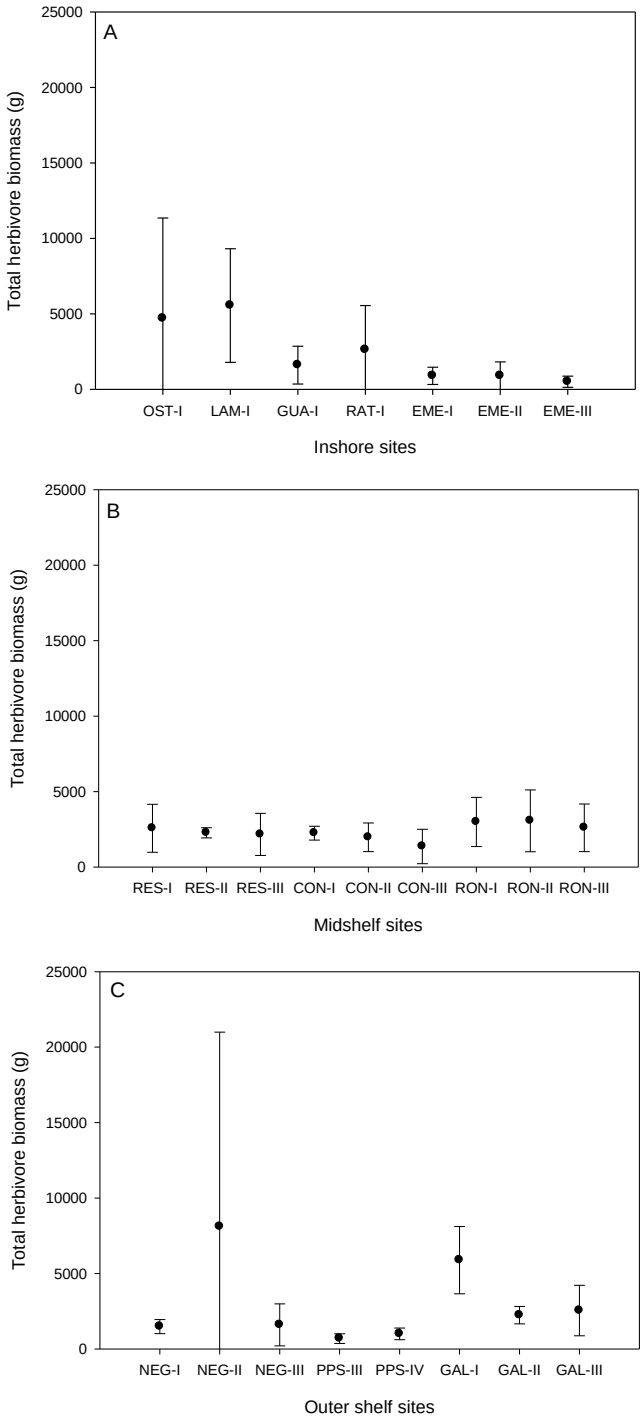

FIGURE 104. Total herbivore biomass across study sites: A) Inshore reefs; B) Mid-shelf reefs; and C) Outer shelf reefs. Mean±95% confidence interval. I= <5 m, II= 5-10 m, III= 10-15 m; IV= 15-20 m.

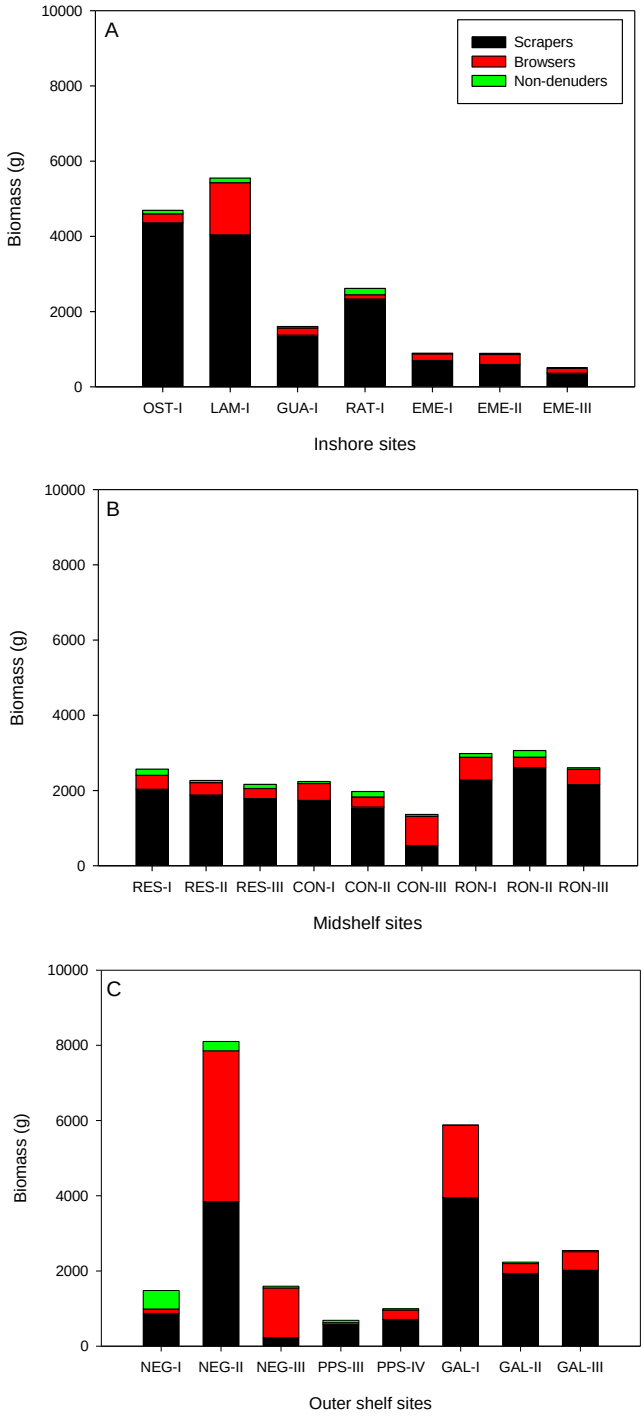

FIGURE 105. Mean herbivore guilds biomass across study sites: A) Inshore reefs; B) Mid-shelf reefs; and C) Outer shelf reefs. Scrapers (Scaridae), Browsers (Acanthuridae), Non-denuders (Pomacentridae). I= <5 m, II= 5-10 m, III= 10-15 m; IV= 15-20 m.

most abundant functional herbivore guild, followed by browsers and non-denuders, although brower biomass increased with distance from the shore (***Figure 105***).

Mean total carnivore fish biomass showed a significant increase with increased distance from the shore, averaging 809 g/count across inshore sites or 25% or the total observed biomass, with a minimum of 83 g/count at the 5-10 m depth zone of OST and a maximum of 2,071 g/count at the 5-10 m depth zone of EME (***Figure 106***). Total carnivore biomass across mid-shelf sites averaged 2,832 g/count or 54% or the total observed biomass, with a minimum of 210 g/count at the <5 m depth zone of CON and a maximum of 16,660 g/count at the 10-15 m depth zone of RON. Total carnivores averaged 11,870 g/count across outer shelf sites or 79% or the total observed biomass, with a minimum of 600 g/count at the 5-10 m depth zone of NEG and a maximum of 49,588 g/count at the 10-15 m depth zone of NEG.

Total carnivore guilds also showed a significant difference in their assemblages depending on the geographic location (***Figure 107***). For instance, generalist carnivore biomass was proportionately dominant across inshore and mid-shelf sites, while planktivores became more common across mid-shelf sites, and eventually dominated outer shelf sites. Piscivore biomass was also concerning. Piscivore biomass averaged only 446 g/count across inshore sites, with a minimum value of less than 5g/count at the <5 m depth zone of OST and a maximum value of 1,853 g/count at the 5-10 m depth zone of EME. Piscivores averaged 1,400 g/count across mid-shelf sites, with a minimum of 49 g/count at the <5 m depth zone of RON, and a maximum of 11,453 g/count at the 10-15 m depth zone of RON. Piscivores averaged 1,778 g/count across outer shelf sites, with none present across the <5 m depth zone of NEG, and a maximum of 11,394 g/count across the 15-20 m deep wall of PPS, mostly *Ocyurus chrysurus*. These values, however, are very low and share light on possibly significant cross-shelf fishing impacts.

Omnivore biomass showed a significant increase with increased distance from the shore, averaging 21 g/count across inshore sites, with none present at the 10-15 m depth zone of EME and a maximum of 53 g/count at the <5 m depth zone of GUA (***Figure 108***). Omnivore biomass across mid-shelf sites averaged 31 g/count, with a minimum of less than 10 g/count at the 10-15 m depth zone of CON and a maximum of 44 g/count at the <5 m depth zone of RES. Omnivores averaged 34 g/count across outer shelf sites, with none present at the 10-15 m depth zone of PPS and <5 m depth zone of GAL, and a maximum of 133 g/count at the 5-10 m depth zone of NEG.

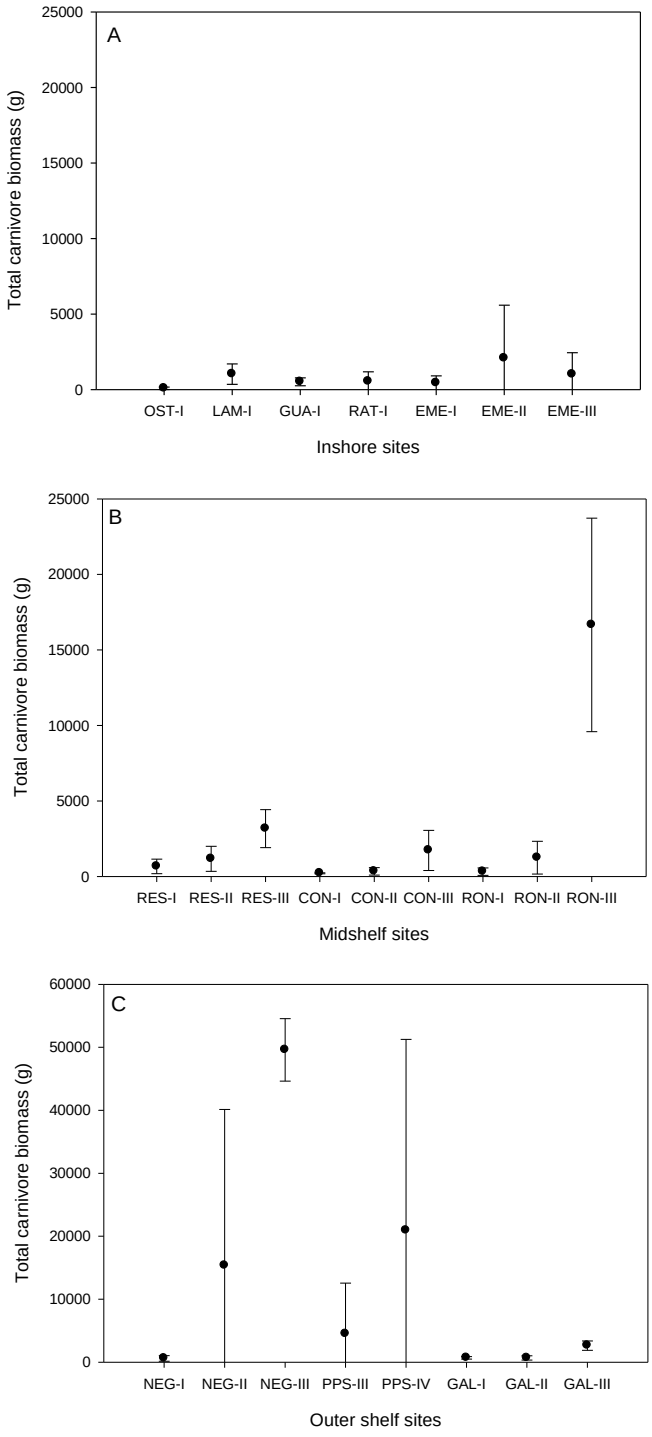

FIGURE 106. Total carnivore biomass across study sites: A) Inshore reefs; B) Mid-shelf reefs; and C) Outer shelf reefs. Mean±95% confidence interval. I= <5 m, II= 5-10 m, III= 10-15 m; IV= 15-20 m.

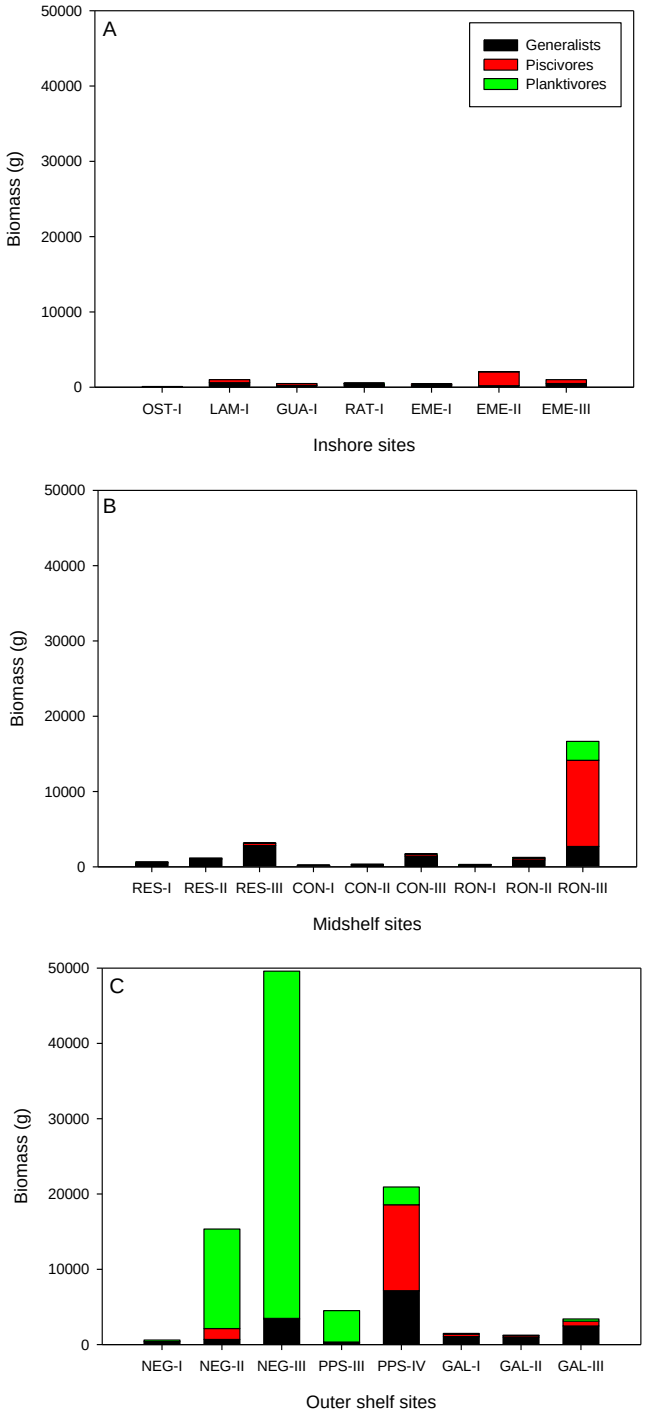

FIGURE 107. Mean carnivore guilds biomass across study sites: A) Inshore reefs; B) Mid-shelf reefs; and C) Outer shelf reefs. I= <5 m, II= 5-10 m, III= 10-15 m; IV= 15-20 m.

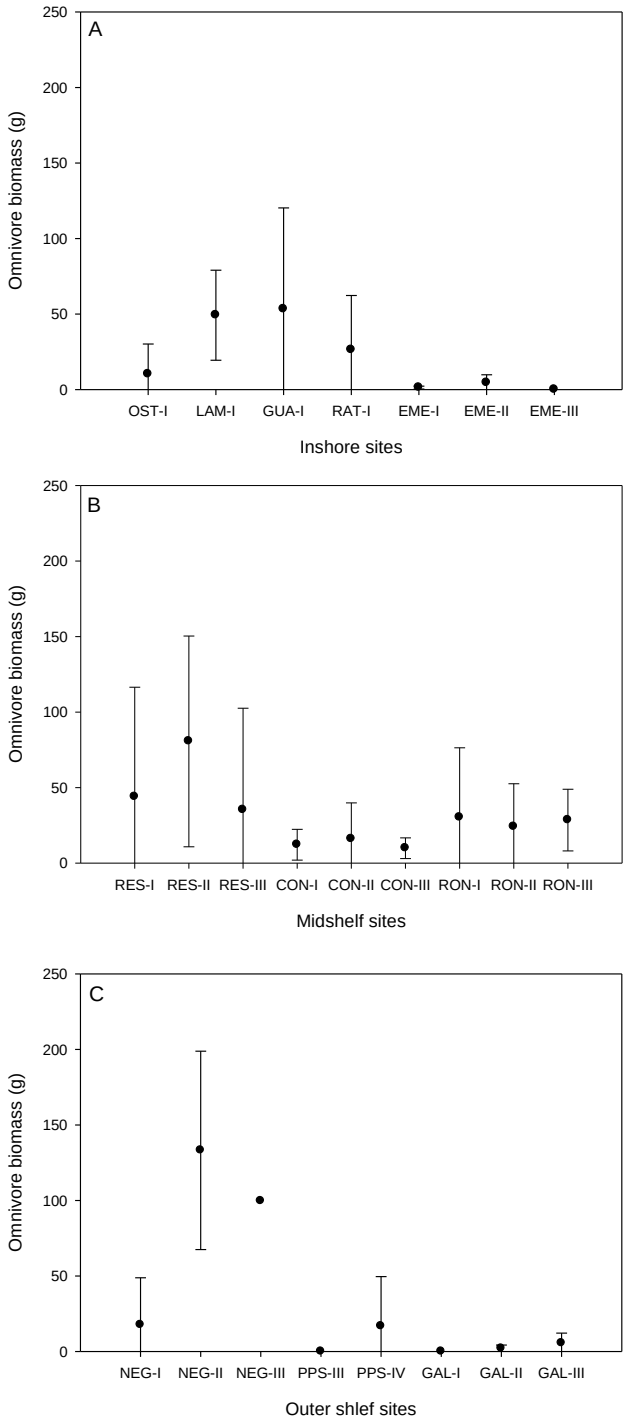

FIGURE 108. Omnivore biomass across study sites: A) Inshore reefs; B) Mid-shelf reefs; and C) Outer shelf reefs. Mean±95% confidence interval. I= <5 m, II= 5-10 m, III= 10-15 m; IV= 15-20 m.

An assessment of selected coral reef fish taxa showed evidence of a potential combination of long-term cross-shelf fishing impacts, depth and reef structural and location effects. Edible grouper subfamily Epinephelinae showed very low abundances across the entire shelf, with a mean Red Hind (*Epinephelus guttatus*) abundance of 0.07 individuals/count across inshore reefs, 0.33/count across mid-shelf sites, and 0.19/count across outer shelf sites (***Figure 109***). No Rock hind (*E. adscensionis*) were observed across inshore sites, 0.06/count was documented across mid-shelf sites, and 0.19/count across outer shelf sites. Less than 0.04 individuals/count of Graysby (*Cephalopholis cruentata*) were observed across inshore sites, less than 0.03/count across mid-shelf sites, and 0.13/count across outer shelf sites. No individuals of Coney (*C. fulva*) were observed across in shore sites, 0.22/count was observed across mid-shelf sites, and 0.44/count across outer shelf sites. Grouper abundance showed a general trend of increase with increasing distance, but mean abundances were overall very low (less than 1 individual/count), which implies potential chronic fishing impacts. The other interesting observations were that Epinehelinae assemblages showed significant variability across sites, and that *E. adscencionis* and *C. fulva* were completely absent across inshore sites.

Snappers (Lutjanidae) species composition also showed remarkable variability across sites, with increasing abundance with increasing distance from the shore (***Figure 110***). Mean Gray snapper (*Lutjanus griseus*) abundance was 0.04 individuals/count across inshore reefs, 0.03/count across mid-shelf sites, and none across outer shelf sites. Schoolmaster (*L. apodus*) abundance averaged 0.22/count across inshore sites, 0.31/count was documented across mid-shelf sites, and 0.59/count across outer shelf sites. Only 0.05 individuals/count of Dog snapper (*L. jocu*) were observed across inshore sites, none across mid-shelf sites, and 0.03/count across outer shelf sites. Mutton snapper (*L. analis*) showed an abundance of 0.04/count across in shore sites, none across mid-shelf sites, and 0.03/count across outer shelf sites. Lane snapper (*L. synagris*) showed an abundance of only 0.01/count across in shore sites, 0.03/count was observed across mid-shelf sites, and none across outer shelf sites. Mahogany snapper (*L. mahogoni*) showed an abundance of 0.06/count across in shore sites, none across mid-shelf sites, and none across outer shelf sites. Finally, Yellowtail snapper (*Ocyurus chrysurus*) showed an abundance of 1.25/count across in shore sites, with 0.89/count across mid-shelf sites, and 4.09/count across outer shelf sites. The abundance of *O. chrysurus* and *L. apodus* showed a general trend of increase with increasing distance.

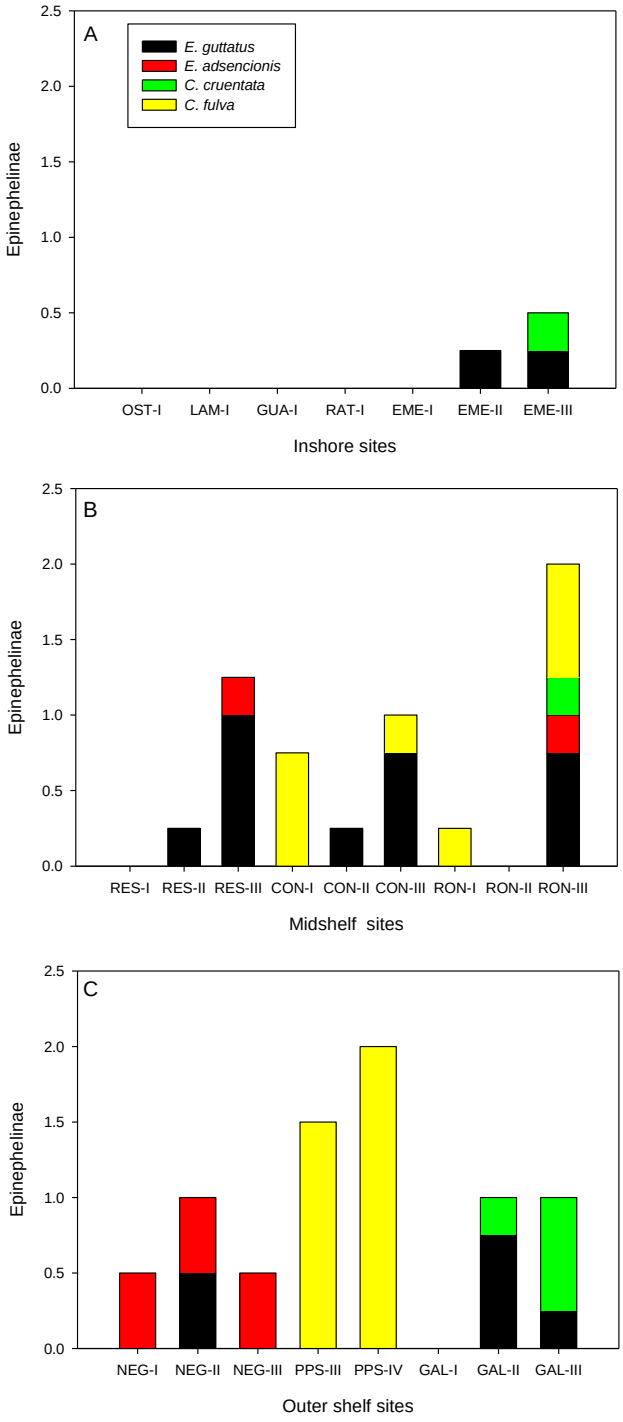

FIGURE 109. Edible groupers (sub-family Epinephelinae) abundance across study sites: A) Inshore reefs; B) Mid-shelf reefs; and C) Outer shelf reefs. Mean±95% confidence interval. I= <5 m, II= 5-10 m, III= 10-15 m; IV= 15-20 m.

Snappers (Lutjanidae) species composition also showed remarkable variability across sites, with increasing abundance with increasing distance from the shore (***Figure 110***). Mean Gray snapper (*Lutjanus griseus*) abundance was 0.04 individuals/count across inshore reefs, 0.03/count across mid-shelf sites, and none across outer shelf sites. Schoolmaster (*L. apodus*) abundance averaged 0.22/count across inshore sites, 0.31/count was documented across mid-shelf sites, and 0.59/count across outer shelf sites. Only 0.05 individuals/count of Dog snapper (*L. jocu*) were observed across inshore sites, none across mid-shelf sites, and 0.03/count across outer shelf sites. Mutton snapper (*L. analis*) showed an abundance of 0.04/count across in shore sites, none across mid-shelf sites, and 0.03/count across outer shelf sites. Lane snapper (*L. synagris*) showed an abundance of only 0.01/count across inshore sites, 0.03/count was observed across mid-shelf sites, and none across outer shelf sites. Mahogany snapper (*L. mahogoni*) showed an abundance of 0.06/count across in shore sites, none across mid-shelf sites, and none across outer shelf sites. Finally, Yellowtail snapper (*Ocyurus chrysurus*) showed an abundance of 1.25/count across inshore sites, with 0.89/count across mid-shelf sites, and 4.09/count across outer shelf sites. The abundance of *O. chrysurus* and *L. apodus* showed a general trend of increase with increasing distance.

Grunts (Haemulidae) species composition showed remarkable variability across sites, but mostly depending on depth and reef physical structure (***Figure 111***). Tomtate (*Haemulon aurolineatum*) abundance was 0.17 individuals/count across inshore reefs, 0.67/count across mid-shelf sites, and 5.0/count across outer shelf sites. Smallmouth grunt (*H. chrysargyreum*) abundance averaged 0.29/count across inshore sites, and none across mid-shelf and outer shelf sites. No individuals of Sailors choice (*H. parrai*) were observed across inshore sites, 0.03/count across mid-shelf sites, and none across outer shelf sites. Spanish grunt (*H. macrostomum*) showed an abundance of 0.02/count across in shore sites, 0.11/count across mid-shelf sites, and none across outer shelf sites. Margate (*H. album*) was absent across in shore sites, but had 0.03/count across mid-shelf sites, and none across outer shelf sites. White grunt (*H. plumieri*) showed an abundance of 0.24/count across inshore sites, 0.47/count across mid-shelf sites, and 0.06/count across outer shelf sites. Caesar grunt (*H. carbonarium*) was also absent across inshore sites, but had 0.14/count across mid-shelf sites, and 0.19/count across outer shelf sites. Bluestriped grunt (*H. sciurus*) showed an abundance of 0.02/count across inshore sites, and none across mid-shelf and outer shelf sites. Finally, French grunt (*H. flavolineatum*) showed an abundance of 0.38/count

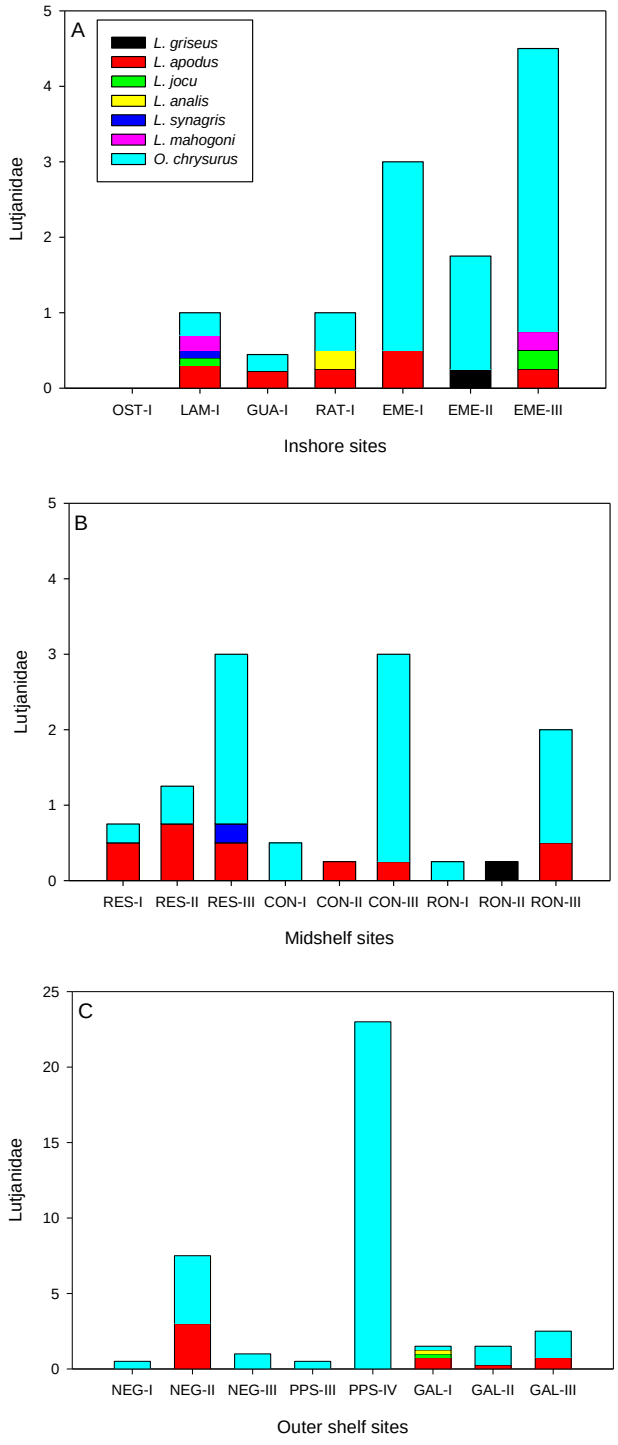

FIGURE 110. Snappers (family Lutjanidae) abundance across study sites: A) Inshore reefs; B) Mid-shelf reefs; and C) Outer shelf reefs. Mean±95% confidence interval. I= <5 m, II= 5-10 m, III= 10-15 m; IV= 15-20 m.

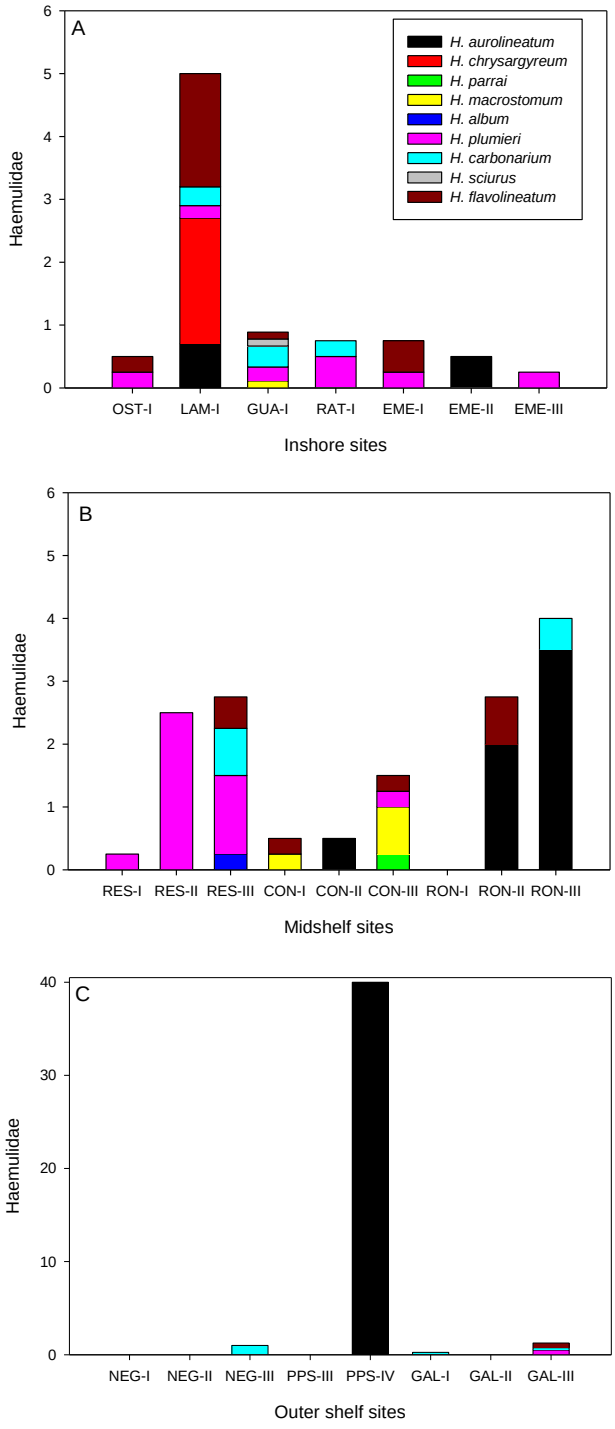

FIGURE 111. Grunts (family Haemulidae) abundance across study sites: A) Inshore reefs; B) Mid-shelf reefs; and C) Outer shelf reefs. Mean±95% confidence interval. I= <5 m, II= 5-10 m, III= 10-15 m; IV= 15-20 m.

across inshore sites, with 0.19/count across mid-shelf sites, and 0.06/count across outer shelf sites. The abundance of *H. aurolineatum* and *H. carbonarium* showed a general trend of increase with increasing distance. All other species showed a spatial variation trend which seemed to be more related to a combination of depth and reef benthic spatial heterogeneity across shallower zones.

Parrotfishes (Scaridae) were the most abundant taxa across sites, but their species composition showed variable assemblages across sites (***Figure 112***). Yellowtail parrotfish (*Sparisoma rubripinne*) abundance was 15.18 individuals/count across inshore reefs, 1.11/count across mid-shelf sites, and 1.47/count across outer shelf sites. Redtail parrotfish (*Sp. chrysopterum*) abundance averaged 0.08/count across inshore sites, 0.47/count was documented across mid-shelf sites, and 0.22/count across outer shelf sites. Stoplight parrotfish (*Sp. viride*) averaged 4.16/count across inshore sites, 11.06/count across mid-shelf sites, and 3.16/count across outer shelf sites. Redband parrotfish (*S. aurofrenatum*) showed an abundance of 2.35/count across inshore sites, 12.89/count across mid-shelf sites, and 3.78/count across outer shelf sites. Bucktooth parrotfish (*Sp. radians*) showed an abundance of only 0.28/count across in shore sites, 0.03/count was observed across mid-shelf sites, and was absent across outer shelf sites. Greenblotch parrotfish (*Sp. atomarium*) was absent across inshore sites, had 1.92/count across mid-shelf sites, and was also absent across outer shelf sites. Queen parrotfish (*Scarus vetula*) had an abundance of 0.19/count across inshore sites, 0.56/count across mid-shelf sites, and 0.78/count across outer shelf sites. Striped parrotfish (*Sc. iserti*) averaged 23.07/count across inshore sites, 34.44/count across mid-shelf sites, and 12.69/count across outer shelf sites. Princess parrotfish (*Sc. taeniopterus*) averaged 14.42/count across inshore sites, 5.53/count across mid-shelf sites, and 2.88/count across outer shelf sites. Rainbow parrotfish (*Sc. guacamaia*) was absent across inshore and mid-shelf sites, but averaged 0.19/count across outer shelf sites. Finally, Bluelip (*Cryptotomus roseus*) showed an abundance of 0.14/count across inshore sites, and was absent across mid-shelf and outer shelf sites. Parrotfish distribution was largely influenced by depth and distance from the shore, in particular for species such as *Sp. rubripinne, Sc. iserti,* and *Sc. taeniopterus*. Shallow, degraded inshore reefs such (OST, LAM, RAT still have a critical function as nursery grounds and support very high densities of juvenile and semi-adult individuals. Also, Scarid abundance seems to be affected by algal distribution patterns. Species vulnerable to fishing (*Sc. vetula, Sc. guacamaia*) showed a limited distribution.

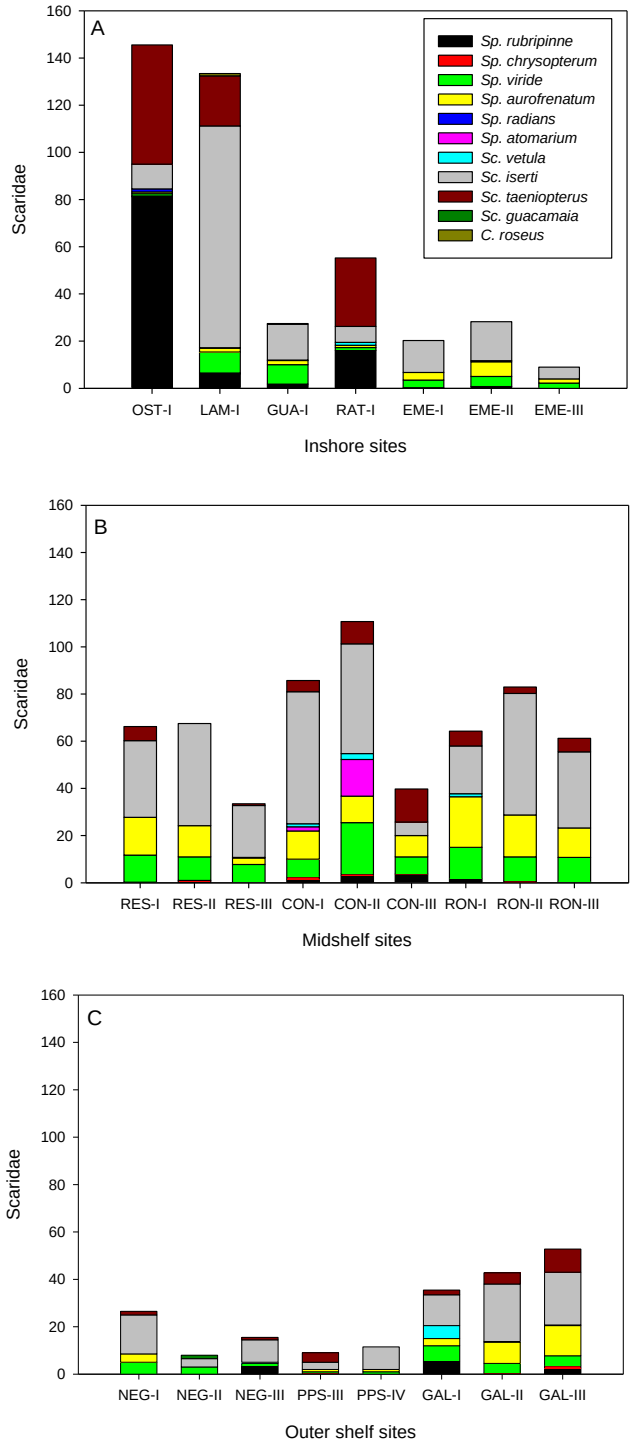

FIGURE 112. Parrotfishes (family Scaridae) abundance across study sites: A) Inshore reefs; B) Mid-shelf reefs; and C) Outer shelf reefs. Mean±95% confidence interval. I= <5 m, II= 5-10 m, III= 10-15 m; IV= 15-20 m.

The abundance of butterflyfishes (Chaetodontidae) was overall low and showed slight variation depending on overall reef condition (***Figure 113***). Foureye butterflyfish (*Chaetodon capistratus*) abundance was 1.10 individuals/count across inshore reefs, 1.47/count across mid-shelf sites, and 0.88/count across outer shelf sites. Banded butterflyfish (*C. striatus*) abundance averaged 0.18/count across inshore sites, 0.08/count was documented across mid-shelf sites, and was absent across outer shelf sites. Spotfin butterflyfish (*C. ocellatus*) averaged 0.07/count across inshore sites, had none across mid-shelf sites, and averaged 0.06/count across outer shelf sites. Finally, Reef butterflyfish (*C. sedentarius*) was absent across inshore sites, and had 0.03/count across mid-shelf sites, and 0.19/count across outer shelf sites.

The abundance of damselfish (Pomacentridae) showed significant species-specific spatial variability (***Figure 114***). The Brazilian damselfish (*Stegastes fuscus*) abundance was 0.10 individuals/count across inshore reefs, and was absent across mid-shelf and outer shelf sites. Threespot damselfish (*S. planifrons*) abundance averaged 4.69/count across inshore sites, 6.78/count across mid-shelf sites, and 5.47/count across outer shelf sites. Cocoa damselfish (*S. variabilis*) averaged 0.07/count across inshore sites, 1.53/count across mid-shelf sites, and 0.34/count across outer shelf sites. Beaugregory (*S. leucostictus*) averaged 1.36/count across inshore sites, 0.03/count across mid-shelf sites, and 0.40/count across outer shelf sites. Bicolor damselfish (*S. partitus*) averaged 0.04/count across inshore sites, 2.39/count across mid-shelf sites, and 8.53/count across outer shelf sites. Dusky damselfish (*S. adustus*) averaged 0.82/count across inshore sites, 0.67/count across mid-shelf sites, and 0.06/count across outer shelf sites. Longfin damselfish (*S. diencaeus*) averaged 0.82/count across inshore sites, 0.61/count across mid-shelf sites, and 0.94/count across outer shelf sites. Finally, Yellowtail damselfish (*Microspathodon chrysurus*) averaged 0.20/count across inshore sites, 1.11/count across mid-shelf sites, and 2.66/count across outer shelf sites. *Stegastes planifrons* showed consistently high densities across the shelf, regardless of depth and distance from the shore. But species such as *S. leucostictus* and *S. adustus* were more abundant across shallow inshore sites, while species such as *S. partitus* and *M. chrysurus* were more abundant across outer shelf and deeper sites exposed to stronger circulation.

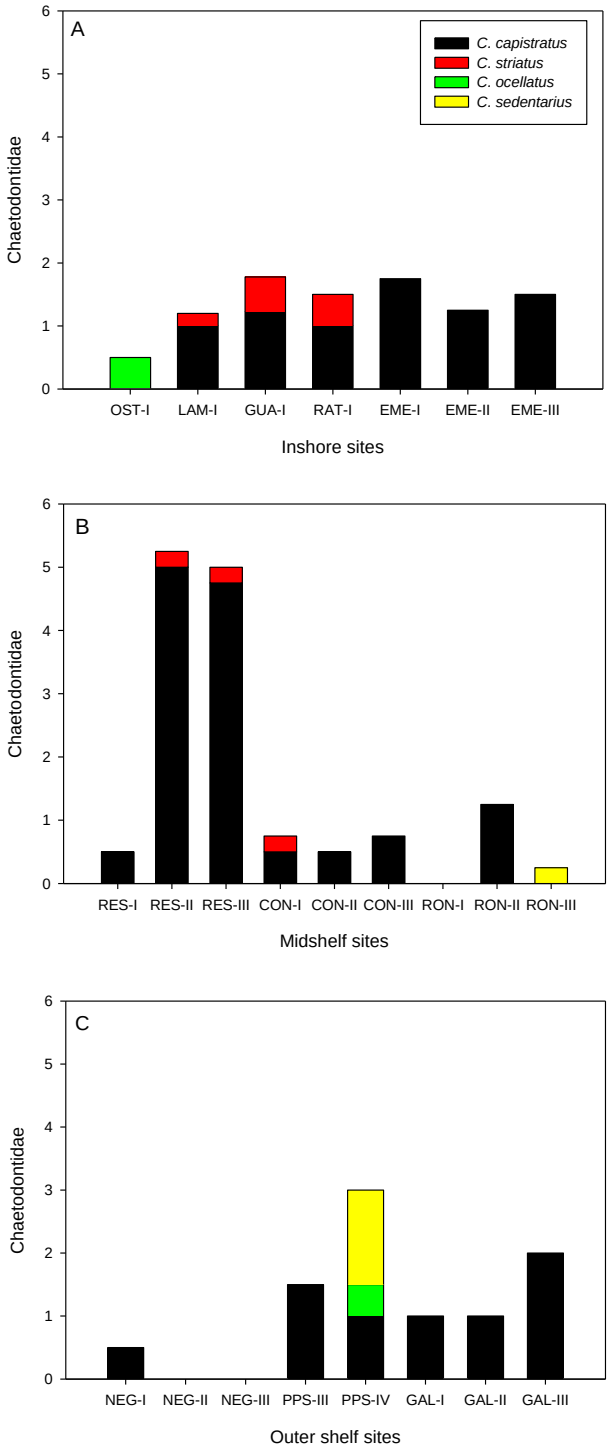

FIGURE 113. Butterflyfishes (family Chaetodontidae) abundance across study sites: A) Inshore reefs; B) Mid-shelf reefs; and C) Outer shelf reefs. Mean±95% confidence interval. I= <5 m, II= 5-10 m, III= 10-15 m; IV= 15-20 m.

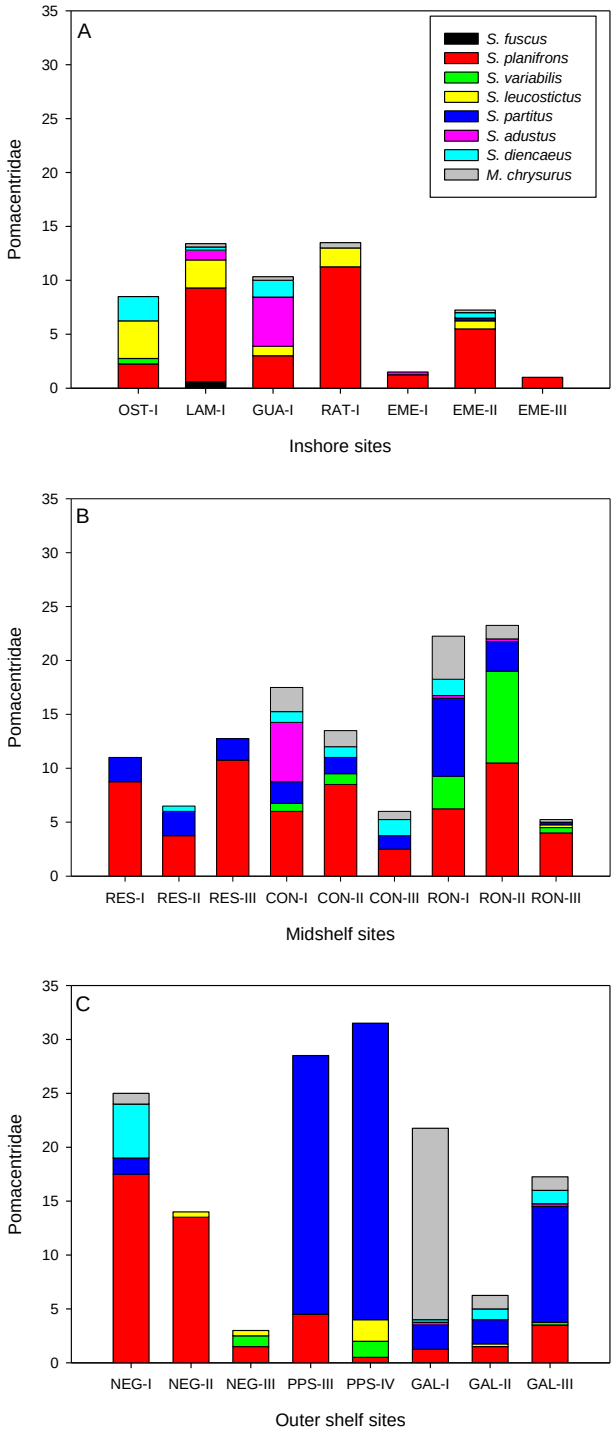

FIGURE 114. Damselfishes (family Pomacentridae) abundance across study sites: A) Inshore reefs; B) Mid-shelf reefs; and C) Outer shelf reefs. Mean±95% confidence interval. I= <5 m, II= 5-10 m, III= 10-15 m; IV= 15-20 m.

IV. DISCUSION

a. LBSP cross-shelf spatial gradient

This study showed important evidence that there were signs of a LBSP gradient across the western Puerto Rico shelf and that chronic water quality decline has significantly affected the face of coral reef benthic communities, coral recruit assemblages, and have indirectly affected reef fish communities. A snapshot view of LBSP showed that particularly turbidity and PO_4 and NH_4^+ concentrations increased along inshore sites, while dissolved oxygen concentration declined along inshore waters. It is particularly concerning that EME reef site and to some extent GUA are being exposed to recurrent pulses of sewage effluents from four different sewage treatment facilities at Boquerón Bay. Elevated PO_4, NH_4^+, chlorophyll-a, and OABs concentrations suggest at EME suggest that tidal cycles may continuously expose coral reef adjacent to Boquerón Bay to recurrent sewage pollution and eutrophication impacts. In the other hand, turbidity, OABs resulted fairly high at other inshore sites such as JOY, RAT, and OST. Their proximity to Joyuda Bay and Puerto Real Bay continuously expose these sampling sites to recurrent polluted water pulses. But a particular concern was water quality conditions across outer shelf sites, where dissolved nutrient concentrations and chlorophyll-*a* concentrations exceeded recommended levels for healthy coral reefs. Pollution across outer shelf sites may also come from other significant sources such as the Río Guanajibo, Río Yagüez, and the Mayagüez Bay.

Previous studies have suggested that PO_4 concentration on coral reef habitats should not exceed 0.3 µM (Lapointe and Clark, 1992), and that any concentration above 1.5 µM would be too high for coral reefs (Lapointe and Matzie, 1996). Our study showed mean PO_4 concentration of 3.46 µM across inshore sites, of 2.67 µM across mid-shelf sites, and of 1.23 µM across outer shelf sites. These values resulted 10.5 times above the recommended concentration for healthy coral reefs across inshore sites, 7.9 times across mid-shelf sites, and 3.1 times across outer shelf sites. These results suggest that PO_4 pollution pulses are a concerning shelf-wide scale phenomenon. Previous studies in Puerto Rico have also shown previous high PO_4 concentrations significantly impacting coral assemblages along the northern coast (Díaz-Ortega and Hernández-Delgado, 2014).

NH_4^+ concentrations above 24 μM have been deemed as too high, when the recommended concentration for coral reefs should not exceed 0.1 μM (Lapointe and Clark, 1992). We obtained mean NH_4^+ concentrations that ranged of 98.09 μM across inshore sites, with even an alarming 260 μM mean value at EME during an ebbing tide. Mean NH_4^+ concentration was 59.09 μM across mid-shelf sites, and 15.63 μM across outer shelf sites. Observed NH_4+ concentrations across inshore sites exceeded 981 times the recommended concentration for healthy coral reefs. The observed NH_4^+ mean concentration at EME, which is located just at the mouth of Boquerón Bay, exceeded by 2,599 times the recommended limits for healthy coral reefs. Concentrations also exceeded the recommended limits 590 times across mid-shelf sites, and 155 times across outer shelf sites. Such levels were also attained in previous studies across the Vega Baja coast in northern Puerto Rico, where coral reefs are rapidly declining (Díaz-Ortega and Hernández-Delgado, 2014). But the spatial scale of the observed patterns in this study seems to be unprecedented.

Another key concern associated to sewage and eutrophication impacts was the elevated cross-shelf mean chlorophyll-*a* concentration range found in this study in comparison to the recommended concentration for coral reef waters of 0.3-0.5 μg/L (Lapointe and Clark, 1992; Otero, 2009). Mean chlorophyll-*a* concentration was 2.38 μg/L across inshore sites, 2.07 μg/L across mid-shelf sites, and 2.12 μg/L across outer shelf sites. These values were up 3.8 to 6.9 times higher than recommended limits for healthy coral reefs across inshore sites, 3.1 to 5.9 times across mid-shelf sites, and 3.2 to 6.1 times across outer shelf sites.

Mean dissolved oxygen concentration in this study was also highly concerning, when any concentration below 2.5 mg/L is considered hypoxic (Lapointe and Matzie, 1996). Mean dissolved oxygen concentration was 4.12 mg/L across inshore sites, 4.09 mg/L across mid-shelf sites, and 5.63 mg/L across outer shelf sites. These values, although far from hypoxic levels, were still concerning as we consider them low for open waters across the shelf and may evidence the chronic state and the large spatial scale of water quality decline as a result of LBSP.

Water quality data in this study was fairly limited as we had no temporal replication. Nonetheless, PCO analysis of observed spatial patterns of water quality explained 74.3% of the variation, confirming observed clustering pattern among inshore, mid-shelf and outer shelf sites

across a LBSP gradient. Documented spatial patterns were also highly consistent with findings of cross-shelf scale pollution patterns documented by Bonkosky et al. (2009). Turbidity patterns were also consistent with previous unpublished observations from year 2000 (Hernández-Delgado, unpub. data). Therefore, it was reasonable to assume that observed spatial patterns of water quality conditions in this study were highly consistent with chronic large-scale degradation at least over the last two decades and that the observed LBSP stress gradient in the form of chronic turbidity and eutrophication, mostly associated to sewage pollution, represent a nearly permanent state.

b. Coral reef benthic community structure

Benthic community structure showed a highly significant variation along the observed LBSP stress gradient. Coral species richness, H'n, J'n and percent living cover increased with increasing distance from LBSP. In contrast, overall algal cover increased across inshore and some of the mid-shelf sites. Further, algal taxonomic composition also showed a significant variation across the documented water quality stress gradient. PCO analysis explained 56.4% of the spatial variation in benthic community structure and showed a spatial clustering pattern of surveyed sites that closely resembled spatial clustering patterns associated to the documented LBSP gradient. Turbidity and the concentration of PO_4 and NH_4^+ were the most significant water quality parameters that explained spatial patterns in benthic community structure. LINKTREE analysis also showed that the combination of high NH_4^+ concentration and high turbidity was the most influencing factor on the observed spatial variation in benthic community structure. The rest of the observed variation in benthic community structure could have resulted from natural variability associated to coral reef spatial heterogeneity, depth and local oceanographic circulation patterns.

c. Coral recruit community structure

Similarly, coral recruit community structure was significantly influenced by the observed LBSP spatial gradient. Coral recruit abundance increased with increasing distance from LBSP. Also, species assemblages showed significant variation with increasing distance from the shore. Further, recruit abundance increased with increasing dissolved oxygen concentration, and declined with increasing turbidity and NH_4^+ concentration. PCO analysis explained 61% of the

spatial variation observed in coral recruit assemblages, mostly as a result of influences by turbidity, NH_4^+ and PO_4. LINKTREE analysis confirmed that the combination of high turbidity and low dissolved oxygen concentration was the most influencing condition affecting the spatial distribution of coral recruits. Other factors could have included coral reef spatial heterogeneity, depth and local oceanographic circulation patterns. Nevertheless, observed patterns were pretty revealing and concerning as the lack of abundant coral recruitment, particularly of large reef-building species implies, with few exceptions across outer shelf sites, a widespread natural lack of recovery potential from disturbance across inshore and most of the surveyed mid-shelf coral reef sites.

d. Coral reef fish community structure

Coral reef fish community structure also showed a highly significant cross-shelf spatial variation influenced by a combination of factors. There was a significant general increase in species richness, total abundance and biomass, H'n, J'n, total carnivore abundance and biomass, piscivore abundance and biomass, and omnivore abundance and biomass with increasing distance from the shore. PCO analysis explained 48% of the observed spatial patterns, mostly as a result of the spatial variation in the concentration of NH_4^+ and PO_4, and in turbidity. LINKTREE analysis suggested that the combination between high PO_4 and OABs concentrations explained most of the observed variation in fish community structure across the observed LBSP gradient. These findings were highly consistent with previous observations of Bejarano and Appeldoorn (2013) that found declining fish community assemblages across turbid environments. The rest of the observed variation in this study could have resulted from influences by local factors such as depth, benthic spatial heterogeneity, reef condition and position, and local oceanographic circulation patterns.

Four additional important findings were documented in this study. First, the distribution of many selected fishery-targeted species showed very low cross-shelf abundances, though many of them showed an increasing abundance with increasing distance from the shore. This may imply the combination of potential LBSP impacts but moreover chronic fishing impacts, particularly across inshore and mid-shelf sites. That was the case of members of the edible groupers in subfamily Epinephelinae and snappers (Lutjanidae). The second important finding is that the abundance of

potential indicator species, such as butterflyfishes (Chaetodontidae), the Yellowtail damselfish (*Microspathodon chrysurus*), and the Bicolor damselfish (*Stegastes partitus*) increased with increased distance from the shore, across the documented LBSP spatial patterns. Other cryptic fish species also increased along the LBSP gradient, with many completely absent across inshore sites (data not shown). These findings were also consistent with observations from Bejarano and Appeldoorn (2013) and suggest potential indirect LBSP effects on fish community structure mediated by previos chronic benthic habitat degradation and habitat environmental quality decline.

A third important finding was the dominant state of parrotfishes (Scaridae) across most of the surveyed sites. Parrotfishes were the most important taxa explained variability across sites, but juvenile and semi-adult stages were particularly dominant and abundant across shallow, highly-degraded inshore reef sites. This finding has significant implications for the maintenance of regional fisheries as it suggest that, regardless of their coral-depleted state, inshore, turbid and polluted reef habitats still have a critical role as nursery ground for a keystone functional group of scraper herbivores. The fact that we also documented the presence of juvenile and semi-adult stages of several species of snappers (Lutjanidae) and grunts (Haemulidae) across inshore sites stressed out the importance of shallow inshore reef sites as a key component of the ontogenic changes of many fish species. This implies the critical need to: 1) provide the most strong protection to shallow inshore coral reef communities and adjacent habitats; 2) strengthen measures to immediately implement the best management practices (BMPs) possible to reduce LBSP to adjacent coastal waters; 3) to implement long-term ecological monitoring efforts to address ecological spatio-temporal changes in benthic community structure and coral recruitment rates across inshore reef sites; 4) to also address spatio-temporal changes in fish community structure across inshore sites, as well as across other cross-shelf sites in order to improve our understanding of local spatio-temporal connectivity among sites and ontogenic shifts in many commercially-important fish species. Therefore, existing large-scale LBSP stress represents a major concern for the maintenance and natural recovery ability of coral reef fish communities. Critical habitats necessary for natural ontogenic shifts of multiple species are severely degraded and water quality still remains significantly compromised. Also, large-scale influences of pollution from large rivers and from Mayagüez Bay also affect mid-shelf and outer shelf sites across Arrecifes Tourmaline Natural Reserve. Potential effects of LBSP on the long-term

benefits of seasonal fishing closures within the natural reserve still remain largely unknown and must also be addressed.

e. Implications for coral reef functions

Observed LBSP across the western Puerto Rico shelf in the form of high turbidity, eutrophication and sewage pollution is a concern for coral reef resilience and for the conservation and recovery of coral reef functions.

Turbidity, sewage pollution and eutrophication across coastal waters were not only confined to the immediate vicinity of receiving waters and have been shown to potentially extend with tidal and wind-driven currents through large geographic areas across the entire shelf (Bonkosky et al., 2009), negatively impacting extensive coral reef communities (Hernández-Delgado et al., 2010). Similar observations were made across the Vega Baja coast (Hernández-Delgado et al., 2011a,b; Díaz-Ortega and Hernández_Delgado, 2014). Sewage impacts are often associated to eutrophication and turbidity (Pastorok and Bilyard, 1985; Lapointe and Clark, 1992; Lapointe and Matzie, 1996; Cloern, 2001; Díaz-Ortega and Hernández_Delgado, 2014). It has also been associated to altered coral-associated microbial community composition (Sekar et al., 2008), to an increased prevalence coral diseases (Patterson et al., 2002; Kaczmarsky et al., 2005), and to declining coral survival rates (Walker and Ormond, 1982; Pastorok and Bilyard, 1985). Declining coral skeletal extension rates (Tomascik and Sander, 1985), reproductive potential (Tomascik and Sander, 1987), and larval settlement rates (Tomascik, 1991) can also occur under eutrophied/polluted conditions. If chronic, these factors can negatively affect the natural coral reef recovery ability from disturbance. In the long run, it can affect ecosystem resilience, functions, services, and benefits.

Sewage and eutrophication impacts often result in a combination of system- and species-specific responses, as well as cascading direct and indirect effects that could result in major long-term phase shifts in benthic community structure, favoring dominance by fleshy macroalgae and non-reef building taxa (Hernández-Delgado et al., 2010, 2011a). Such phase shifts could be irreversible in long-term scales (Hughes, 1994). Sewage-associated eutrophication impacts can also result in an accelerated reef decline often due to a combination of synergistic impacts, mostly from sediments and turbidity (Meesters et al., 1998; Cloern, 2001; Szmant, 2002). This

combination of factors and their long-term shift from pulse to chronic events may explain why some coral reefs across the entire western Puerto Rico shelf have shown the observed declines.

V. CONCLUSIONS

Coral reef ecosystems across the entire western Puerto Rico shelf were showing unequivocal signs of decline mostly as a result of chronic LBSP impacts. The state of decline is reflected both in benthic community structure and in coral recruit assemblages. But also, impacts have indirectly affected coral reef fish community structure. Evidence from this study supports the long-term chronic nature of the observed state of environmental decline. Observed conditions are biologically unsustainable for all of the surveyed inshore coral reefs and for most of the surveyed mid-shelf reefs. Although surveyed outer shelf reefs were in better shape than inshore and that most of the mid-shelf sites, they were also showing important signs of decline. Impacts by declining coastal water quality and non-point source pollution across the western Puerto Rico shelf has been extensively documented in the past (Bonkosky et al., 2009; Hernández-Delgado et al., 2010), but has still received little attention from Commonwealth and U.S. Federal regulatory agencies to prevent or minimize further damage to these unique resources. Observed chlorophyll-$_a$, PO_4 and NH_4^+ concentrations are very far from sustainable and point out at the paramount importance of implementing specific water quality legal limits for coral reef waters for chlorophyll-*a* (0.3 µg/L), PO_4 (0.3 µM), NH_4^+ (0.1 µM), and a ratio of PO_4:Total N of 7:1 or lower.

There is also an imperative need to eliminate illegal raw sewage dumping from septic tank effluents, malfunctioning sewers, and other non-point sources from properties adjacent to coastal waters a Boquerón Bay, Puerto Real Bay, Joyuda Bay, Bramadero Bay, and Mayagüez Bay, and to Río Guanajibo and Río Yagüez watersheds. It would also be important to implement BMPs to foster an improved management of soil erosion, runoff and sedimentation of small-scale watersheds across coastal adjacent lands. This should also include improving sewer systems and upgrading existing sewage treatment plant facilities, particularly at Boquerón Bay. There is also a need to improve the implementation of erosion-sedimentation controls on any construction activity across adjacent watersheds or coastal waters.

There is also a need to implement a permanent long-term ecological monitoring program for coral reef benthic communities, coral recruitment rates and reef fish communities, in combination with a permanent, standard water quality monitoring program. We also encourage testing methods aimed at coral propagation using local coral genetic clones which are naturally resistant to local water quality conditions. Low-tech coral farming and reef rehabilitation have become critical for helping coral reefs to recover from chronic disturbance.

Local coral reef ecosystems across the western Puerto Rico shelf still represent a critical natural resource with invaluable socio-economic significance. But existing impacts from LBSP can not be sustained for much time and need to be thoroughly addressed through an appropriate, highly-participatory management plan to reduce LBSP threats. But such a plan needs to be coupled to a scientific question-driven and properly designed coastal water quality program and a long-term ecological monitoring program to quantify the long-term impacts of management strategies. This becomes more critical considering that chronic eutrophication has been shown to increase the prevalence of coral diseases and bleaching (Vega-Thurber et al., 2013). Considering current and forecasted climate change-related impacts this will become an even major concern in the near future. Otherwise, we might be at risk of losing one of the most important coral reef ecosystems of the entire northeastern Caribbean region.

VI. ACKNOWLEDGMENTS

This study was possible thanks to funding provided by Protectores de Cuencas, Inc. and Ridge to Reefs, Inc. to Sociedad Ambiente Marino under a Coral Reef Conservation grant from the National Fish and Wildlife Foundation (NFWF). Partial support was also provided by the National Science Foundation (HRD #0734826) through the Center for Applied Tropical Ecology and Conservation (CATEC), and the University of Puerto Rico's Central Administration to E.A. Hernández-Delgado. Our appreciation for the logistical field support provided by the crew of M/V *Tourmarine*, and Capt. Elick Hernández. This publication is a contribution from CATEC's Coral Reef Research Group and SAM's collaborative *Coral Reefs Conservation and Rehabilitation Project*.

VII. LITERATURE CITED

Anderson, M.J., Gorley, R.N., and Clarke, K.R. (2008) *PERMANOVA + for PRIMER: Guide to Software and Statistical Methods*. PRIMER-E: Plymouth, U.K.

Bejarano-Rodríguez, I., Appeldoorn, R. (2013) Seawater turbidity and fish communities on coral reefs of Puerto Rico. *Marine Ecology Progress Series*, 474, 217-226.

Bonkosky, M., Hernández-Delgado, E.A., Sandoz, B., Robledo, I.E., Norat-Ramírez, J., and Mattei, H. (2009) Detection of Spatial Fluctuations of Non-Point Source Fecal Pollution in Coral Reef Surrounding Waters in Southwestern Puerto Rico Using PCR-Based Assays. *Marine Pollution Bulletin*, 58, 45-54.

Clarke, K.R., and Warwick, R.M. (2001) *Change in Marine Communities: An Approach to Statistical Analysis and Interpretation.* 2nd Ed. PRIMER-E, Ltd., Plymouth Marine Laboratory, UK.

Cloern, J. (2001) Our Evolving Conceptual Model of the Coastal Eutrophication Problem. *Marine Ecology Progress Series*, **210**, 223--253.

García-Urueña, R.P. (2004) Dinámica de Crecimiento de Tres Especies de Coral en Relación a las Propiedades Ópticas del Agua. Ph.D. Dissertation, Department of Marine Sciences, University of Puerto Rico, Mayagüez, PR, 138 pp.

Goenaga, C. (1988) The Distribution and Growth of *Montastrea annularis* (Ellis and Solander) in Puerto Rican platform reefs. Ph.D. Dissertation, Department of Marine Sciences, University of Puerto Rico, Mayagüez, PR, 215 pp.

Goenaga, C., and Cintrón, G. (1979) Inventory of the Puerto Rican Coral Reefs. Departamento de Recursos Naturales & National Oceanic and Atmospheric Administration, San Juan, PR, 189 pp.

Goenaga, C., and Canals, M. (1990) Island-Wide Coral Bleaching in Puerto Rico: 1990. *Caribbean Journal of Science*, **26**, 171-175.

Goenaga, C., and Boulon, R. (1992) The State of Puerto Rican Corals: An Aid to Managers. Technical Report, Caribbean Fisheries Management Council, San Juan, PR, 66 pp.

Hernández-Delgado, E.A. (2000) Effects of Anthropogenic Stress Gradients in the Structure of Coral Reef Epibenthic and Fish Communities. Ph.D. Dissertation, Department of Biology, University of Puerto Rico, San Juan, P.R. 330 pp.

Hernández-Delgado, E.A. 2005. Historia natural, caracterización, distribución y estado actual de los arrecifes de coral Puerto Rico. 281-356. *In*, R.L. Joglar (Ed.), *Biodiversidad de Puerto Rico: Vertebrados Terrestres y Ecosistemas. Serie Historia Natural*. Editorial Instituto de Cultura Puertorriqueña, San Juan, PR. 563 pp.

Hernández-Delgado, E.A., Sandoz, B., Bonkosky, M., Mattei, H., and Norat, J. (2010) Impacts of Non-Point Source Sewage Pollution in Elkhorn Coral, *Acropora palmata* (Lamarck), Assemblages of the Southwestern Puerto Rico Shelf. *Proceedings of the 11th International Coral Reefs Symposium*, 747-751.

Hernández-Delgado, E.A., and Sandoz-Vera, B. (2011) Impactos Antropogénicos en los Arrecifes de Coral, 62-72. In, J. Seguinot-Barbosa (Ed.), *Islas en Extinción: Impactos Ambientales en las Islas de Puerto Rico*. Ediciones SM, Cataño, PR 255 pp.

Hernández-Delgado, E.A., Hutchinson-Delgado, Y.M., Laureano, R., Hernández-Pacheco, R., Ruiz-Maldonado, T.M., Oms, J., and Díaz, P.L. (2011a) Sediment Stress, Water Turbidity and Sewage Impacts on Threatened Elkhorn Coral (*Acropora palmata*) Stands at Vega Baja, Puerto Rico. *Proceedings of the Gulf and Caribbean Fisheries Institute*, 63, 83-92.

Hernández-Delgado, E.A., Alvarado, A., Laureano, R., Flynn, K., and Griffin, S. (2011b) Seawall Construction Activities Cause a Localized Mass Mortality of Threatened Elkhorn Coral (*Acropora palmata*) at Vega Baja, Puerto Rico. *Proceedings of the Gulf and Caribbean Fisheries Institute*, 63, 511.

Hernández-Delgado, E.A., Méndez-Lázaro, P.A., Medina-Muñiz, J.L., Nieves-Santiago, A., Cabrera-Molina, J., and Rodríguez-Díaz, I.M. (2012) Chronic Impacts of Sewage and Turbidity on Coral Reefs Within the Tres Palmas Marine Reserve, Rincón, Puerto Rico: I. Threatened Elkhorn coral (*Acropora palmata*) Populations. Final report submitted to Environmental Science Graduate Program, Department of Public Health, University of Puerto Rico – Medical Sciences Campus, and to the Coral Reef Conservation Program, Department of Natural and Environmental Resources, San Juan, Puerto Rico, 70 pp.

Hughes, T.P. (1994) Catastrophes, Phase Shifts, and Large-Scale Degradation of a Caribbean Coral Reef. *Science*, **265**, 1547-1550.

Kaczmarsky, L., Draud, M., and Williams, E. (2005) Is There a Relationship Between Proximity to Sewage Effluent and the Prevalence of Coral Disease. *Caribbean Journal of Science*, **41**, 124--137.

Lapointe, B.E., and Clark, M.E. (1992) Nutrient Inputs from the Watershed and Coastal Eutrophication in the Florida Keys. *Estuaries*, **15**, 465-476.

Lapointe, B.E., and Matzie, W.R. (1996) Effects of Stormwater Discharges on Eutrophication Processes in Nearshore Waters of the Florida Keys. *Estuaries*, **19**, 422-435.

Loya, Y. (1976) Effects of Water Turbidity and Sedimentation on the Community Structure of Puerto Rican Corals. *Bulletin of Marine Science*, **26**, 450-466.

Meesters, E.H., Bak, R.P.M., Westmacott, S., Ridgley, M., Dollar, S. (1998) A Fuzzy Logic Model to Predict Coral Reef Development Under Nutrient and Sediment Stress. *Conservation Biology*, **12**, 957-965.

Méndez-Lázaro, P., Hernández Delgado, E.A., Norat-Ramírez, J., Cordero-Rivera, L., and Santiago-Nieves, A. (2012) Técnicas de SIG Aplicadas al Estudio de Zonas Costaneras y Cuencas Hidrográficas en la Isla de Puerto Rico. *Revista Internacional de Ciencia y Tecnología de Información Geogfráfica, Geo-Focus*, **12**, 71-92.

Norat-Ramírez, J., Méndez-Lázaro, P., Hernández-Delgado, E.A., and Cordero-Rivera, L. (2013) El Impacto de Aguas Usadas de Fuentes Dispersas en el Litoral Costero de la Reserva Marina Tres Palmas (Rincón-Puerto Rico). *Revista de la Asociación Venezolana de Ingeniería Sanitaria y Ambiental*, **7**, 27-30.

Otero, E. (2009) Spatial and Temporal Patterns of Water Quality Indicators in Reef Systems of Southwestern Puerto Rico. *Caribbean Journal of Science*, **45**, 168-180.

Pastorok, R., and Bilyard, G. 1985. Effects of Sewage Pollution on Coral-Reef Communities. *Marine Ecology Progress Series*, **21**,175--189.

Schärer, M., Nemeth, M., Valdivia, A., Miller, M., Williams, D., and Diez, C. (2010) Elkhorn Coral Distribution and Condition Throughout the Puerto Rican Archipelago. *Proceedings of the 11th International Coral Reef* Symposium, 815-819.

Sekar, R., Kaczmarsky, L. and Richardson, L. (2008). Microbial Community Composition of Black Band Disease on the Coral Host *Siderastrea siderea* from Three Regions of the Wider Caribbean. *Marine Ecology Progress Series*, **362**, 85-98.

Szmant, A. (2002) Nutrient Enrichment on Coral Reefs: Is It a Major Cause of Coral Reef Decline?. *Estuaries*, **25**, 743-766.

Tomascik, T., and Sander, F. (1985) Effects of Eutrophication on Reef-Building Corals. I. Growth Rate of the Reef-Building Coral *Montastrea annularis*. *Marine Biology*, **87**, 143-155.

Tomascik, T., and Sander, F. (1987) Effects of Eutrophication on Reef-Building Corals. III. Reproduction of the Reef-Building Coral *Porites porites*. *Marine Biology*, **94**, 77-84.

Tomascik, T. (1991) Settlement Patterns of Caribbean Scleractinian Corals on Artificial Substrata Along a Eutrophication Gradient, Barbados, West Indies. *Marine Ecology Progress Series*, **77**, 261-269.

Torres, J.L., and Morelock, J. (2002) Effect of Terrigenous Sediment Influx on Coral Cover and Linear Extension Rates of Three Caribbean Massive Coral Species. *Caribbean Journal of Science*, **38**, 222-229.

Vega-Thurber, R., Burkepile, D., Fuchs, C., Shantz, A., McMinds, R., and Zaneveld, J. (2014) Chronic Nutrient Enrichment Increases Prevalence and Severity of Coral Disease and Bleaching. *Global Change Biology*, **20**, 544--554.

Walker, D., and Ormond, R. (1982) Coral Death from Sewage and Phosphate Pollution at Aqaba, Red Sea. *Marine Pollution Bulletin*, **13**, 21-25.

Weil, E., Hernández-Delgado, E., Bruckner, A., Ortiz, A., Nemeth, M., and Ruiz, H. (2002) Distribution and Status of Acroporid Coral (Scleractinia) Populations in Puerto Rico, 71-98. In, Bruckner, A.W. (ed.), Proceedings of the Caribbean *Acropora* Workshop: Potential Application of the U.S. Endangered Species Act as a Conservation Strategy. NOAA Tech. Memorandum NMFS-OPR-24, Silver Spring, MD, 199 pp.